THE ROLE OF INTERFERON STIMULATED GENES IN RESISTANCE AND IMMUNITY TO HEPATITIS C VIRUS INFECTION

APPROVED BY SUPERVISORY COMMITTEE

Michael J. Gale, Jr., Ph.D. (Supervisor)

Julie Pfeiffer, Ph.D.

Vanessa Sperandio, Ph.D.

Kim Orth, Ph.D

DEDICATION

I would like to dedicate this to my mom and dad, whose expectations and pride in me have been a constant push in my life to achieve my goals. Importantly, I would like to thank both my parents for their help with my twins, Miles and Mason, over the past two years. My mom practically raised the boys the first year of their life, and I truly do not think that without my parents help I would have been able to finish this endeavor! I would also like to acknowledge my sisters who are both wonderful women and each has characteristics that I try to emulate. I thank my husband, Trent, for being himself. He is a wonderful father; so I never have to worry about my sons, and as I know his love and support are constants, I do not have to worry about much of anything outside of work. My extended family, the Ericksons are extremely supportive and my mother in law is truly one of the sweetest and thoughtful women alive and has watched the boys each time I have gone out of town. I am blessed to have such a wonderful family and I thank you all!!

I would like to thank both past and present members of the Gale Lab. Especially Chunfu Wang, who trained me in my first few months in the lab and was a very useful source of information and technical support. The graduate students, Eileen Foy, Brian Keller, Rhea Sumpter, and Cindy Johnson, set the bar very high but were all extremely helpful in my initial years in the lab. Their love of science was infectious and produced a wonderful learning environment. I especially have to thank Cindy, as her scientific insight and grammar abilities have been a great help to me. Also, we have enjoyed a number of trips to meetings together and she is definitely missed. The post-doctoral researchers Ming Loo and Brenda Fredericksen also provided help with experimental techniques and proofreading documents for me. The addition of Takeshi Saito and Nanette lightened up the lab

atmosphere, as they both enjoy joking around. I would also like to thank Takeshi and Imran, a MSTP rotation student, for generously cloning the viperin expression plasmids for me while I was on maternity leave. Nanette continues to be an extreme help to me, sending me reagents the moment I ask for them, and without her my studies would probably not be nearing finish. David Owen was very helpful if you needed anything done in the lab in the middle of the night.

I cannot adequately express my gratitude to Julie Pfeiffer and her lab members for taking me in over the past year. Despite my use of valuable space and tissue culture hood time, they have always made me feel welcome. I would especially like to thank Karen Lancaster, Sharon Kuss and Kristie Ibarra for proofreading sections of this document for me. These girls are a great source of fun in and outside the lab. Julie has been a tremendous source of help for scientific insight, editing my manuscripts and forcing her lab to listen to my practice talks. She is a wonderful mentor and has helped keep me on track with Mike being gone. Also, Julie is great at keeping the atmosphere in the lab upbeat as you can usually hear her laughing about something a throughout the day.

Additionally I have to thank Julie and the other women on my thesis committee, Dr. Kim Orth and Dr. Vanessa Sperandio who have been valuable role models as well as sources of encouragement. Talking with Kim and Vanessa has reassured me that it is possible to achieve one's scientific goals without sacrificing the ability to be an attentive mother. Importantly, all of my committee members have provided tremendous scientific insight into the studies discussed in chapter four.

Last but of course not least I would like to thank my mentor Michael Gale. I would like to thank Mike for giving me the opportunity to work on these studies and for the funding

to support them. Also, I would like to thank you for your approach in mentoring me, in that I was never made to feel scientifically naïve, thus allowing my scientific confidence to build bit by bit. Also, I have thoroughly enjoyed discussing experiments with you, as you always have an interesting addition or alteration to my interpretations teaching me to look at experiments from different perspectives. Furthermore, thank you for all your support when I got pregnant with the boys. This was a difficult time for me and I was not confident that I would be able to finish my studies; however your support was a great relief to me. Also, thank you for the opportunity to travel to numerous scientific meetings which allowed me to meet some important virologists, like Grant McFadden, as well as staying patient with me over the last five years, I have greatly enjoyed every minute of it!

THE ROLE OF INTERFERON STIMULATED GENES IN RESISTANCE AND IMMUNITY TO HEPATITIS C VIRUS INFECTION

by

ANDREA KAUP ERICKSON

DISSERTATION

Presented to the Faculty of the Graduate School of Biomedical Sciences

The University of Texas Southwestern Medical Center at Dallas

In Partial Fulfillment of the Requirements

For the Degree of

DOCTOR OF PHILOSOPHY

The University of Texas Southwestern Medical Center at Dallas

Dallas, Texas

August, 2008

THE ROLE OF INTERFERON STIMULATED GENES IN RESISTANCE AND IMMUNITY TO HEPATITIS C VIRUS INFECTION

Publication No. _____

Andrea Kaup Erickson, Ph.D.

The University of Texas Southwestern Medical Center at Dallas, 2008

Supervising Professor: Michael Gale, Jr., Ph.D.

Hepatitis C Virus (HCV) is a global public health issue with 170 million people chronically infected. The only approved treatment for HCV infection is interferon-α-based therapy, resulting in viral clearance in approximately fifty percent of patients treated. Interferon therapy mimics endogenous type I interferon signaling, which plays a crucial role in the innate antiviral response through the regulation of interferon stimulated genes (ISGs). ISGs encode antiviral effector proteins that limit viral replication and spread. Hundreds of ISGs have been identified in the liver of HCV patients who respond to IFN therapy; however the functions of most these genes are not known.

In order to better understand the molecular mechanisms of the IFN antiviral response, studies were initiated to identify and characterize the functions of novel ISGs involved in controlling HCV infection. To determine the most effective IFN for these studies, the antiviral activity and functional effects of three distinct type I IFN subtypes were evaluated. Consensus interferon demonstrated maximal suppression of HCV replication, correlating with enhanced IFN signaling and ISG induction. A functional genomics analysis of IFN treated primary hepatocytes resulted in the identification of eighty-six ISGs differentially induced by consensus interferon. Future evaluations of the role of these genes in HCV outcome, using integrated approaches as described here, will be invaluable in further defining the molecular mechanisms of the innate IFN antiviral response.

Although a number of ISGs have recently been reported to function as antiviral proteins *in vitro,* these studies did not validate the involvement of these genes in innate immunity or disease outcome. In order to evaluate the biological relevance of a genetic variant of the oligoadenylate synthetase 1 (OAS1) gene in resistance to HCV infection, an integrated approach of epidemiology, molecular genetics, and functional biology was used. Genetic and epidemiologic analyses identified a single-base mutation in OAS1 that associates with HCV resistance in individuals with a high-risk for HCV infection. Functional studies of the resulting OAS1 variant demonstrated altered biological activities of the protein, resulting in enhanced suppression of HCV genotype 1a and 2a infectious clones. Furthermore, a recombinant drug form of the OAS1 variant demonstrated broad antiviral activity, suggesting great promise for this protein as a therapeutic for HCV infection.

TABLE OF CONTENTS

PRIOR PUBLICATIONS

Erickson AK, Iadonato SP, Scherer CA, Keller BK, Pfeiffer JP, Gale M, Jr. A novel OAS1 variant has distinct antiviral functions that associate with resistance to HCV infection in vivo. (2008) Nature Biotechnology, In Preparation.

Erickson AK, Seiwert S, Gale M, Jr. Antiviral potency analysis and functional comparison of consensus interferon, interferon-alpha2a and pegylated interferon-alpha2b against hepatitis C virus infection. (2008) Antiviral Therapy, accepted July 4, 2008.

Erickson AK, Gale M, Jr. Regulation of interferon production and innate antiviral immunity through translational control of IRF-7. (2008) Cell Research,18:1-3.

Keller BC, Johnson CL, **Erickson AK**, Gale M, Jr. Innate immune evasion by hepatitis C virus and West Nile virus. (2007) Cytokine Growth Factor Rev., Oct-Dec;18(5-6):535-44.

Loo Y-M, Owen D, Li K, **Erickson AK**, Johnson CL, Mar-Fish P, Carney S, Wang T, Ishida H, Yoneyama M, Fujita T, Saito T, Lee WM, Hagedorn CH, Lau DT-Y, Weinman SA, Lemon SM, Gale M, Jr. (2006) Viral and therapeutic control of IFN-beta promoter stimulator 1 during hepatitis C virus infection. Proc. Natl. Acad. Sci. U.S.A.,11;103(15):6001-6.

Hiesberger T, Gourley E, **Erickson A**, Koulen P, Ward CJ, Masyuk TV, Larusso NF, Harris PC, Igarashi P. (2006) Proteolytic Cleavage and Nuclear Translocation of Fibrocystin Is Regulated by Intracellular Ca^{2+} and Activation of Protein Kinase C. J. Biol. Chem., **281:** 34357-34364.

TABLE OF FIGURES

LIST OF TABLES

LIST OF ABBREVIATIONS

1A1-OAS1 ancestral allele 1
1D1-OAS1 derived allele 1
aa – amino acid
ANOVA – one-way analysis of variance
CARD – caspase activation and recruitment domain
CIFN- consensus interferon
CIP – calf intestinal alkaline phosphatase
CPE-cyotpathic effects
cpm-counts per minute
dsRNA – double-stranded RNA
EMCV- encephalomyocarditis virus
EMSA – electrophoretic mobility shift assay
ER – endoplasmic reticulum
FBS-fetal bovine serum
FFA-Focus Forming Assay
GAPDH – glyceraldehyde 3-phosphate dehydrogenase
HCV – hepatitis C virus
HIV-human immunodeficiency virus
HRP – horse-radish peroxidase
Huh7- human hepatoma cells
IFI-interferon induced
IFN – interferon
IFNAR – interferon alpha/beta receptor
IVDU-intravenous drug user
IPS-1 – interferon-β promoter stimulator 1
IRF-3 – Interferon regulatory factor-3
ISG – interferon stimulated gene
ISRE – interferon stimulated response element
MDA5 – melanoma differentiation associated gene 5
MOI – multiplicity of infection
mRNA-messenger RNA
NF-κB – nuclear factor-κB
NOD27-nucleotide-binding oligomerization domains 27
NS – nonstructural
NTPase – nucleoside triphosphatase
NTR- non-translated region
OAS- oligoadenylate synthetase
PBS-phosphate buffered solution
PH5CH8- immortalized primary hepatocytes
PEG-IFN-pegylated interferon

PRR – pathogen recognition receptor
PAMP – pathogen associated molecular pattern
poly(I:C) – polyinosinic:polycytidylic acid
RIG-I – retinoic acid-inducible gene I
RSAD2- radical S-adenosyl methionine domain containing 2
RT – room temperature
SDS – sodium dodecyl sulfate
SFM – serum-free media
SNP-single-nucleotide polymorphism
ssRNA – single-stranded RNA
SVR-sustained viral response
TLR – toll-like receptor
TM – transmembrane domain
TNF-α – tumor necrosis factor-α
TRAF – tumor necrosis factor receptor-associate factor
VSV – vesicular stomatitis virus
WT – wild-type

CHAPTER ONE
Introduction

HEPATITIS C VIRUS INFECTION

Epidemiology

HCV was initially identified in 1989 by researchers at Chiron Corporation from the serum of a person who had non-A, non-B hepatitis. The identification and subsequent cloning of HCV signifies a scientific hallmark in that it marks the first time a virus was entirely identified using molecular cloning techniques (Choo et al., 1989). The discovery of HCV led to the development of blood screening procedures, virtually eliminating the incidence of post-transfusion hepatitis by 1992 (McHutchison and Bacon, 2005). Despite these successful efforts to decrease the incidence of infection, HCV remains the most common persistent blood-borne pathogen in the United States with approximately 2.2% of the global population infected (2002; 2004). Intravenous drug use (IVDU) is now the most common risk factor and mode of HCV transmission. Alarmingly, it has been reported that the prevalence of HCV infection in populations of IVDU ranges from 65-90% (Ting Zhang, 2006). Recent studies have reported that HCV is rapidly acquired after approximately one year of the onset of drug injection, with the rate of infection dramatically increasing with the number of years of drug use (Garten et al., 2004; Hagan et al., 2004). Risk factors associated with increased acquisition of HCV infection in IVD users include co-infection with HIV, sexual activity and sharing of injection materials. Other modes of HCV transmission including occupational

exposure, hemodialysis, perinatal and household exposure together account for about 10% of infections (Chen and Morgan, 2006).

Disease Manifestations

The progression of HCV infection is slow and characterized by variable outcomes. The majority of acutely HCV-infected individuals are asymptomatic thus the transition from acute to chronic infection is usually without notice and left untreated (Seeff, 2002). HCV infection is self-limiting in only 15-25% of patients, and does not lead to protective immunity against reinfection. Chronic HCV infection is usually associated with persistent inflammation leading to progressive hepatic disease. HCV-associated hepatic fibrosis progresses to cirrhosis in approximately 10-15% of infected individuals. Host factors that have been associated with affecting the rate of chronicity include increased age at time of infection, male gender, African American race, HIV co-infection and immunosuppression (2002; 2004). As the stage of fibrosis progresses, there is an increased risk of hepatocellular carcinoma, a fatal condition occurring in about 1-4% of cirrhotic patients a year. As a result of these sequelae, chronic HCV infection is now the leading indication for liver transplantation in many countries including the United States (Chen and Morgan, 2006). The public health impact of HCV infection is compounded by substantial current and future economic burden, costing the United States alone millions of dollars annually. To date, the only drug that can eradicate HCV and directly inhibit chronic liver disease is interferon (IFN).

Interferon therapy

In 1986, even before the discovery of HCV, Hoofnagle et al. reported that administration of recombinant IFNα in patients with non-A, non-B hepatitis resulted in normalization of serum aminotransferase (ALT) levels (Hoofnagle et al., 1986). These studies led to the discovery of the antiviral effects of IFNα and prompted approval of the clinical use of IFNα as a therapeutic for HCV infection in 1991. Initially, IFNα monotherapy had limited success resulting in a sustained viral response (SVR) or undetectable HCV RNA in the serum six months post-treatment in 16-20% of patients (Di Bisceglie and Hoofnagle, 2002). SVR rates improved to 35-40% in HCV-infected patients treated with the addition of ribavirin, a guanine nucleoside analog, to IFNα-based therapies (**Figure 1-1)** (McHutchison et al., 1998). Further improvements in response rates have been achieved in recent years with the development of pegylated interferons (PEG-IFN), which is a modification of the recombinant IFN by the addition of polyethylene glycol. The most beneficial effect of PEG-IFNs is the extended half life of the protein, allowing for once weekly administration instead of every couple of days for the un-pegylated versions. Currently, the established standard of treatment for HCV infection is a combination of pegylated IFN-α2a or 2b (PEG-IFN) and ribavirin, which achieves SVR in around 50% of all patients, with lower SVR rates attributable to genotype 1 and 4 patients (McHutchison and Bacon, 2005). The recommended doses and duration of combination PEG-IFN plus ribavirin treatment depend on viral load and HCV genotype, where patients with genotypes 2 and 3 are treated for 24 weeks with lower doses of ribavirin, while 48 weeks of treatment in genotype 1 and 4 patients is recommended (Di Bisceglie and Hoofnagle, 2002). Response to IFN based treatment can be put into three

groups: SVR, relapse (HCV positive 6 months post-treatment) or nonresponse (never achieve negative HCV RNA levels). Relapse occurs in about 10-25% and nonresponse in about one-third of PEG-IFN plus ribavirin treated patients (Feld and Hoofnagle, 2005). Treatment response after standard therapy is thought to be predominantly determined by viral load and genotype. Wherein, SVR are consistently higher in patients with low baseline viral RNA levels and in genotype 2 and 3 patients (76-80% versus 40-46% in genotype 1 patients) **(Figure 1-1)** (Fried et al., 2002). Another factor influencing IFN treatment response in HCV-infected individuals is the time at which treatment is initiated following HCV infection. Studies have demonstrated that if IFN therapy is administered during acute infection, chronicity is lowered to 10%, and patients rapidly become HCV RNA negative, regardless of viral genotype or load (Jaeckel et al., 2001; Santantonio et al., 2005). These results suggest that a failed response to IFN therapy might be acquired during the establishment of chronic infection, but thus far there are no clear explanations for this observation. The commercially available IFNs approved for clinical use in the United States include the first generation IFNs, IFN-α2a and IFN-α2b, pegylated versions of each and consensus interferon (CIFN) **(Appendix A)**. CIFN is a synthetic IFN produced from the consensus sequence of several of the naturally occurring type I IFNs. Ongoing clinical studies are revealing the differential antiviral effects and optimized clinical uses of PEG-IFN and CIFN. When compared overall, these IFN-based therapies have similar outcomes of response, however notable differences are seen depending on the cohort of patients and with optimization of treatment regimen (Miglioresi et al., 2003; Sjogren et al., 2007; Tong et al., 1997; Witthoeft et al., 2007; Yasuda and Miyata, 2002). Interestingly, CIFN treatment of genotype 1 patients, who had relapsed

after PEG-IFN therapy, had increased SVR rates (69 vs 44% in PEG-IFN retreatment) with daily dosing of CIFN **(Figure 1-1)** (Kaiser S, 2006). Overall, therapy with CIFN plus ribavirin seems to have promising results, and may be a favorable alternative to PEG-IFN in genotype 1 patients who have not responded to standard therapy. Host factors including sex, race, obesity and age have been associated with treatment response but seem to have less of an impact than viral genotype in affecting SVR rates; however for race, it has been consistently found that African Americans have higher rates of chronic HCV infection than Caucasians (86% vs 68%) and have SVR rates that are one-half to one-third of those in Caucasians after IFN-based therapy (Howell et al., 2000). The IFN-based therapies are expensive and have considerable contraindications often necessitating discontinuation of therapy, including flu-like symptoms, anemia (associated with ribavirin use), cardiovascular events and severe depression. Clearly more effective therapies for HCV are still needed.

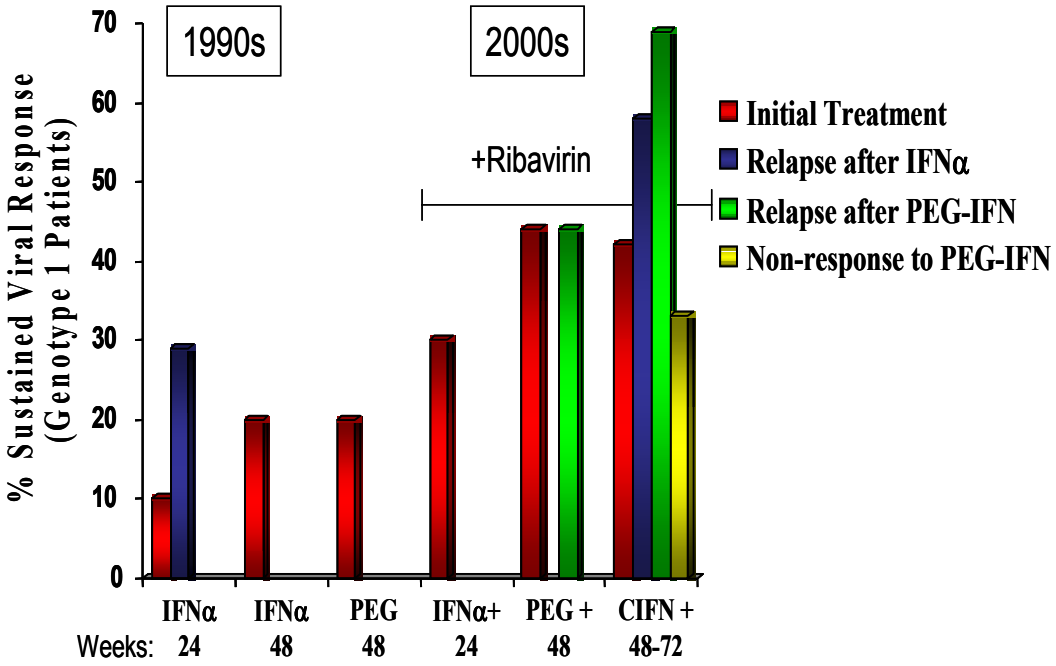

Figure 1-1. Developments in IFN-based therapy for chronic HCV

Progress in sustained viral response rates in "difficult to treat" HCV genotype 1 patients. IFNα was approved in 1991 for the treatment of HCV, resulting in SVR of ~10% when given for 24 weeks, 48 weeks of treatment increased SVR to 10-20% of patients. Initial therapy with PEG-IFN therapy had similar SVR of 10-20%. The addition of ribavirin increased SVR rates when given in combination with IFNα to 30-40% and with PEG-IFN to 40-50%. CIFN plus ribavirin has similar SVR rates as PEG-IFN plus ribavirin in treatment naïve patients (red bars) but has increased SVR rates in individuals who relapsed after previous IFN-based therapy (blue and green bars). CIFN was also effective in patients who have not responded to prior PEG-IFN therapy (yellow bars). PEG, pegylated IFNα-2b.

Emerging therapies

As there is a continual push for improved therapeutics to combat HCV infection, novel drugs and combinations of therapies are continuously in development and testing. New IFNs being

tested include Albuferon, which similar to PEG-IFN has a long half-life allowing dosing every two weeks or longer (Osborn et al., 2002). Initial results from clinical trials suggest there is no increased effectiveness of Albuferon as compared to PEG-IFN. Drug targets currently under study that specifically target essential steps in the viral life cycle include inhibitors of the HCV IRES (antisense oligonucleotides and ribozymes), NS3/4A protease inhibitors (peptidomimetic active site inhibitors) and NS5B polymerase inhibitors (nucleoside analogues). While some of these drugs offer promising results, specific targeting of the virus often results in drug-resistant variants due to the ability of the virus to quickly evolve under selective pressure. Therefore, these drugs will likely be given in a combination with IFN. Immunomodulatory agents are also under development for the treatment of HCV infection. Perhaps the most promising of these include agonists for the Toll-like receptors (TLR9), for which ongoing clinical trials have had initial successful results (reviewed in Deutsch and Hadziyannis, 2008) (McHutchison et al., 2007). Of course, a concern with these drugs is toxicology from over stimulating the immune response. Therefore, the identification of novel therapeutic strategies remains of importance.

MOLECULAR BIOLOGY OF HCV

HCV genome structure and viral proteins

HCV is the sole member of the *hepaciviridae* genus and is a member of the Flaviviridae family, which includes important human pathogens such as West Nile virus, Dengue virus and Yellow Fever virus (Robertson et al., 1998). Isolates of HCV have revealed a

remarkable degree of sequence heterogeneity, and based on analysis of sequences of the core, E1 and NS5 regions, 6 major HCV genotypes (designated 1-6) have been identified, with more than 50 subtypes (Simmonds, 1995). In a patient, HCV exists as a mixture of closely related but distinct genomes, or viral quasispecies. Quasispecies are produced due to low fidelity of the viral polymerase and selective pressure by the host immune response providing a selective advantage to variants through increased replication fitness and immune evasion (Gale and Foy, 2005; Martell et al., 1992).

HCV is a small, enveloped virion containing a 9.6 kilobase, positive-sense, single-stranded (ss) RNA genome encoding a single polyprotein that is co- and post-translationally cleaved into at least 10 mature viral proteins by cellular and virally encoded proteases (Penin et al., 2004). The HCV virion contains three structural proteins, including the highly basic core protein, the envelope glycoproteins E1 and E2, and the small integral membrane protein p7 (**Figure 1-2**). The core protein is the major structural component of the viral nucleocapsid, and has been proposed to regulate a wide variety of viral and host processes (Irshad and Dhar, 2006; Miyanari et al., 2007). E1 and E2 are glycoproteins embedded in the envelope lipid bilayer and are involved in receptor mediated entry of the virus into cells. The nonstructural (NS) p7 protein has been shown to function as an ion channel, and along with NS2 has been recently shown to be necessary for HCV replication in cell culture (Jones et al., 2007). The remaining NS proteins NS3, NS4A, NS4B, NS5A, and NS5B are required for the assembly of viral replicase complexes and are sufficient to support HCV RNA replication in the replicon systems (Lohmann et al., 1999). NS2 is a cysteine protease that cleaves at the NS2-3 site and is required for virus production. NS3 is a bifunctional molecule that carries a

serine-type protease activity, responsible for cleavage of virtually all of the NS proteins, and NTPase/helicase activity. NS4A is a co-factor of the NS3 protease (Johnson et al., 2007) whereas NS4B is required for the formation of the membrane-associated replication complex (discussed below). NS5A is an RNA binding protein thought to be involved in some step of viral RNA replication, and has been shown to interact with and inhibit the dsRNA-dependent protein kinase (PKR), an important cellular antiviral molecule (Gale et al., 1997). NS5B is the RNA-dependent RNA polymerase **(Figure 1-2)**.

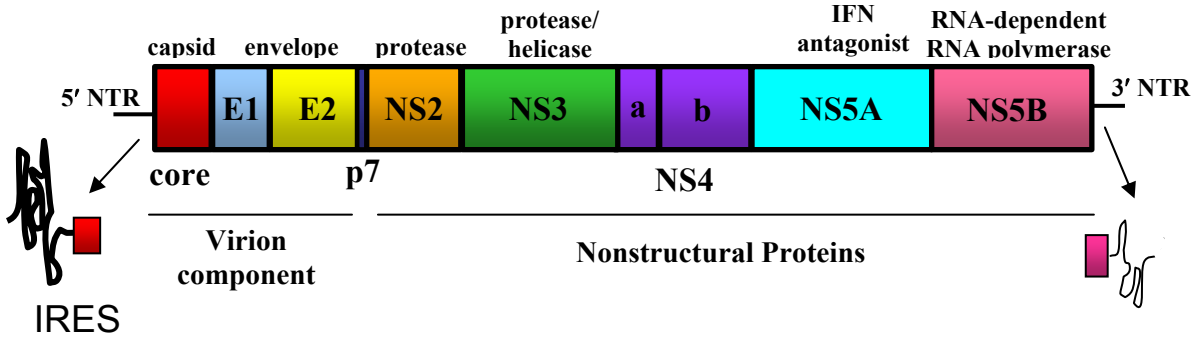

Figure 1-2. The Hepatitis C Virus (HCV) genome and viral proteins.
HCV has a 9.6 kilobase, single-stranded, positive-sense RNA genome that encodes one single polypeptide that is processed co- and post-translationally into the structural (virion components) and nonstructural proteins. IRES- Internal Ribosome Entry Site, NTR-non-translated region

HCV LIFE CYCLE

HCV entry and IRES-directed translation

HCV entry into the target host cell is a complex, multi-step process that requires numerous cellular factors including glycosaminoglycans, scavenger receptor class B member I (SR-BI),

the tetraspanin CD81 and claudin-1 (CLDN1) (reviewed in Barth et al., 2006; Bartosch and Cosset, 2006; Cocquerel et al., 2006; Evans et al., 2007; Pawlotsky et al., 2007). HCV entry is clathrin-dependent and requires a low pH compartment (Blanchard et al., 2006; Tscherne et al., 2006). Upon viral entry, the positive-strand genomic RNA is released into the cell cytoplasm, where it serves as messenger RNA (mRNA) for synthesis of the HCV polyprotein **(Figure 1-3)**. Both the primary sequence and secondary structure of the 5' nontranslated region (NTR) are highly conserved (Honda et al., 1996; Laporte et al., 2000). The 5′NTR is around 341 nucleotides containing four dsRNA domains, numbered I to IV, that are highly structured composed of stem loops and a pseudoknot (Wang et al., 1995). Domains II, III, and IV, together with the first 12-30 nucleotides of the core-coding region, constitute the internal ribosome entry site (IRES), while domain I modulates IRES-dependent translation (Honda et al., 1999; Tsukiyama-Kohara et al., 1992). The IRES directs cap-independent translation initiation of HCV RNA by binding the 40S ribosomal subunit directly, bypassing the need for ribosome scanning to the initiation codon and pre-initiation factors. The cellular proteins, eukaryotic initiation factors (eIF) 2 and 3 are then recruited to the surface of the 40S ribosomal subunit and subsequent joining of the 60S ribosomal subunit results in formation of the translationally competent 80S ribosome **(Figure 1-3)**. In contrast to the HCV IRES, the encephalomyocarditis virus (EMCV) IRES (~450nt) uses nearly all of the known cellular translation initiation factors, including eIF4G and eIF4A for binding of the 40S ribosomal subunit. Also, unlike the HCV IRES, association of the 40S ribosomal subunit to the EMCV IRES is ATP dependent (reviewed in Fraser and Doudna, 2007).

HCV replication complex

Infection with HCV leads to rearrangements of the rough endoplasmic reticulum (ER) membrane structures (membranous web) necessary for the formation of the replication complex that associates viral proteins, cellular components, and nascent RNA strands **(Figure 1-3)** (El-Hage and Luo, 2003). Compartmentalization of the viral replication complex offers numerous advantages to the virus including increased local concentrations of the necessary components for replication and protection from cellular antiviral molecules. The HCV NS4B protein seems to be sufficient to induce the formation of the membranous web, but the mechanism used for vesicle formation is unknown (Egger et al., 2002). These altered membranes are rich in cholesterol and fatty acids. The formation appears to be dependent on the degree of saturation of fatty acids which influences membrane fluidity and is important for replicase function (Kapadia and Chisari, 2005). Immunogold electron microscopy images have shown that the membranous web consists of small vesicles embedded in a membranous matrix that contains all of the nonstructural HCV proteins (Egger et al., 2002). Similar structures have been observed in the liver of HCV infected chimpanzees, suggesting the formation of the membranous web is not a cell culture artifact (Pfeifer et al., 1980).

Geranylgeranylation and HCV

The cellular proteins and membrane constituents required for the assembly and maintenance of the viral replication complex remain largely unknown. However we have previously shown that geranylgeranylation of the host protein FBL2 is critical for its interaction with the

HCV NS5A protein, and this association is required for HCV RNA replication (Wang et al., 2005; Ye et al., 2003). Geranylgeranylation of proteins occurs through geranylgeranyl transferase I (GGTase-1) attachment of the lipid substrate, geranylgeranyl, to cysteine residues in cellular proteins containing a carboxy-terminal Cys-A-A-X sequence (CAAX box), where C is cysteine, A is an aliphatic residue and X is typically leucine (Reid et al., 2004). Geranylgeranyl modification of proteins has been shown to facilitate membrane association (Zhang and Casey, 1996). The function of FBL2 in HCV RNA replication remains unknown, but its identification presents another avenue of research for the discovery of novel therapies to inhibit HCV infection.

HCV replication

Replication of the positive-strand RNA genome by the HCV NS5B RNA dependent RNA polymerase occurs via a negative-strand intermediate, estimated to represent only 10% of the entire viral RNA present within the infected cell. The negative-strand RNA serves as a template to produce numerous strands of positive polarity that will subsequently be used for polyprotein translation, synthesis of new intermediates of replication, or packaging into new virus particles. NS5B has inherently low fidelity, resulting in a mutation rate of around 10^{-3} base substitutions per genome site per year, promoting the generation of a quasispecies population within an infected individual (Martell et al., 1992).

HCV assembly and release

Due to the recent discovery of a HCV-infectious cell culture model, characterization of HCV assembly and release is actively being pursued. What is currently known suggests that the viral core protein recruits viral RNA, the replication complex and NS proteins to ER membranes associated in close proximity with lipid droplets in order to trigger particle formation. The HCV NS5A protein has been proposed to mediate the recruitment of the replication complexes to these lipid droplets. The lipid droplets are in close proximity to the ER lumen where the maturation and budding of virus particles probably occur (Appel et al., 2008; Miyanari et al., 2007). However, some evidence suggests that budding may traffic through the Golgi apparatus **(Figure 1-3)**. The detailed mechanisms underlying maturation and egress of HCV virions have yet to be completely understood.

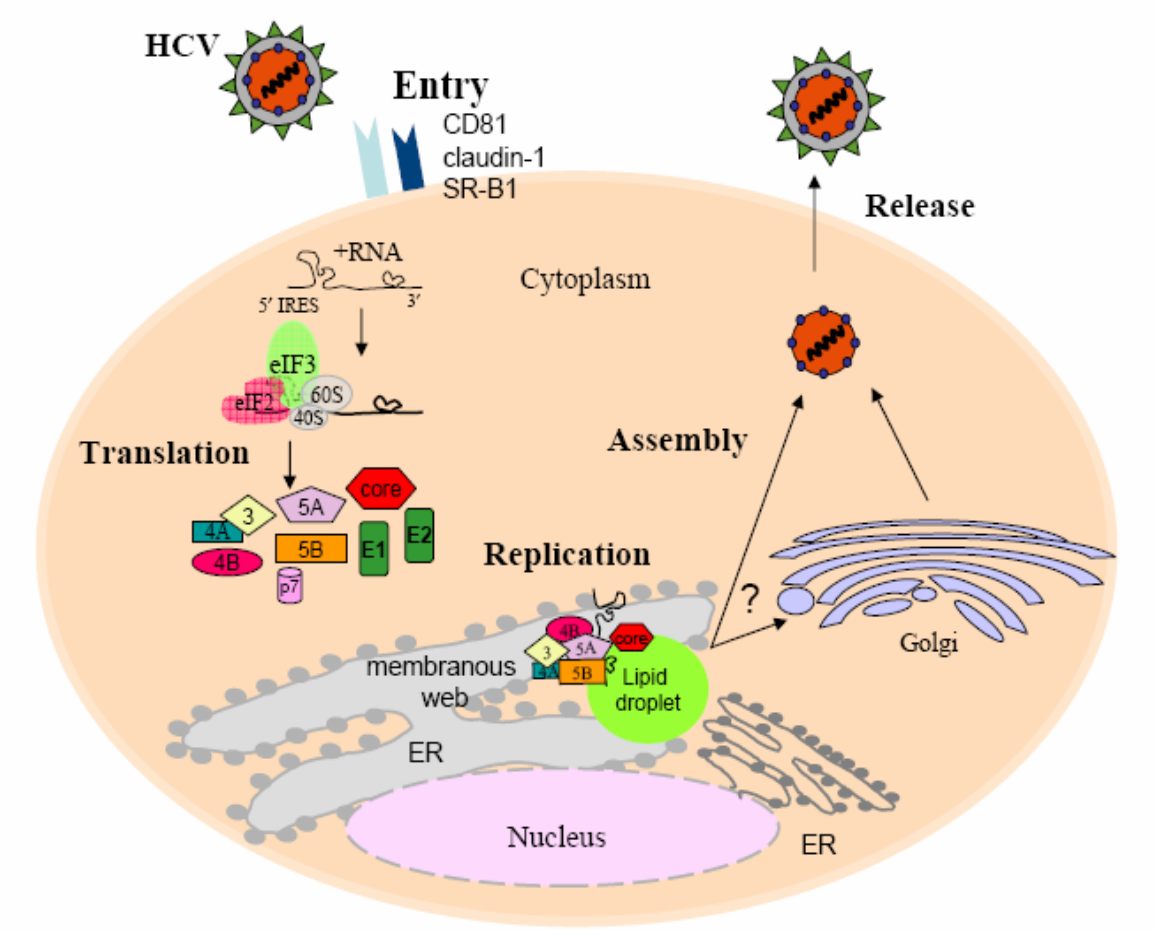

Figure 1-3. HCV Life Cycle. Upon entry into the host cell the viral positive-sense RNA genome is released into the cytoplasm. The HCV IRES then recruits the cellular translational machinery to begin synthesis of viral proteins. The viral proteins, cellular components and nascent RNA associate with the virally induced membranous web forming the replication complex. Assembly and release of viral progeny is thought to occur through the cellular secretory pathway in close association with lipid droplets. ER-endoplasmic reticulum, ?-budding may occur via trafficking through the Golgi Apparatus

MODEL SYSTEMS TO STUDY HCV INFECTION

Animal Models

Currently the only small animal model capable of supporting hepatitis C virus (HCV) infection is the human-mouse chimeric liver model consisting of the severe combined immunodeficiency disorder (SCID) mouse overexpressing the urokinase plasminogen activator (uPA) transgene. Expression of uPA is highly toxic and results in hepatocellular atrophy of mouse hepatocytes, which can be repopulated with human hepatocytes. Subsequent infection with HCV results in persistent infection and the production of infectious progeny virus in the human hepatocytes (Mercer et al., 2001). The utilization of these mice has been demonstrated in recent studies using gene expression analysis to characterize the contribution of the host response to HCV infection and in studies evaluating the efficacy and toxicity of novel antiviral agents (Vanwolleghem et al., 2007; Walters et al., 2006). Limitations to the mouse model include availability due to technical difficulties in breeding and transplantation. Also, these mice are immunodeficient, limiting applicability of this in vivo model to questions related to pathogenesis.

Chimpanzees are the only primate species shown to be susceptible to HCV infection, and have been instrumental in determining viral determinants that are critical for HCV infectivity such as the viral protease/helicase/polymerase, p7 protein and the 3' NTR (Kolykhalov et al., 2000; Sakai et al., 2003; Yanagi et al., 1999). Also, the chimpanzee model has been invaluable for examining the events that occur during acute infection, as most acute human infections are subclinical. Important observations from these studies

include the robust IFN induction in animals that clear HCV, confirming the importance of the IFN antiviral response in suppressing HCV infection (Bigger et al., 2001). In contrast to HCV infection in humans, around 60-70% of acutely infected chimpanzees spontaneously clear the virus, suggesting this is not a suitable model for studying persistent HCV infection (Bassett et al., 1998; Bassett et al., 1999). Despite the obvious advantages of a primate model for HCV infection, the high cost and limited availability reduce the utility of this animal model.

HCV RNA replicon system

Until recently, cell culture propagation of HCV in tissue culture was not possible and HCV replicons were the choice for investigation of virus-host interactions. In this system, human hepatoma cell lines (Huh7 or derivatives) are transduced with a bicistronic RNA encoding the authentic HCV 5' and 3' NTR and either the entire open reading frame or the NS genes from HCV. The HCV IRES directs translation of the selectable marker neomycin phosphotransferase II (NPT II) which confers resistance to G418, and the heterologous EMCV IRES drives expression of the viral proteins **(Figure 1-4)**. When introduced into cells the HCV replicon RNA can replicate autonomously to high levels, but does not produce infectious virus (Ikeda et al., 1998). The observation that the replicons acquired adaptive cell culture mutations resulting in enhanced viral fitness has facilitated the dissection of virus-host interactions (Krieger et al., 2001). Seminal studies from our lab demonstrated that HCV evolves to resist the antiviral actions of IFN when replicating under selective pressure

(Sumpter et al., 2004), demonstrating the importance for the replicon systems in advancing the field of HCV research.

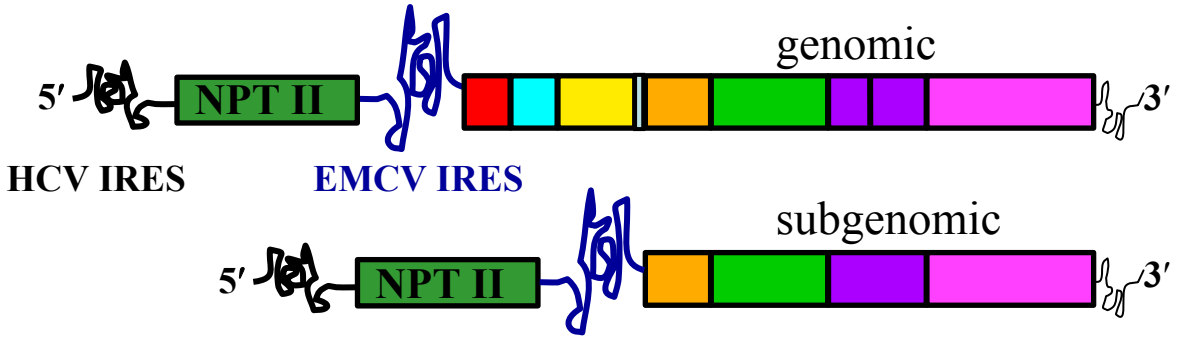

Figure 1-4. HCV RNA replicon system. The HCV replicon consists of a bicistronic RNA molecule which has the HCV internal ribosome entry site (IRES) controlling synthesis of the neomycin phosphotransferase II gene (NPT II), allowing for selection of replicon containing Huh7 cells with G418. The encephalomyocarditis (EMCV) viral IRES directs translation of the HCV proteins. The genomic replicons contain the entire HCV genotype 1b coding sequence, while the subgenomic replicons encode only the nonstructural proteins, which are sufficient to support high levels of replication.

Cell culture infectious clones

In 2005 the first robust cell culture infectious clone was discovered. This HCV genotype 2a strain was isolated from a Japanese patient with fulminant hepatitis (JFH-1). For as of yet undetermined reasons, full-length JFH-1 RNA produces high titer infectious HCV particles in cell culture, and JFH-1 derived subgenomic replicons do not require adaptive mutations for cell culture propagation (Wakita et al., 2005). In our hands, viral titers of 7 x 10^5 can be obtained. A number of groups have subsequently produced genotype 1/JFH-1 chimeric viruses that reach high titer in cell culture (Lindenbach et al., 2005; Zhong et al., 2005). The production of infectious genotype 1a HCV in cultured human hepatoma cells occurred in 2006 using the cell culture adapted Hutchinson strain (H77-S) (Yi et al., 2006). We were

graciously given a plasmid encoding this 1a strain from which RNA (HCV 1a) was produced and used to transduce Huh7.5 cells. Huh7.5 cells transfected with the HCV 1a RNA produced infectious virus albeit at much lower levels (10x) than cells transduced with JFH-1 RNA. The low amount of infectious virus produced prevented us from doing antiviral assays on directly infected cells. Instead, all HCV 1a experiments were done with cells that were transfected with HCV 1a RNA for 48-72 hours, trypsinized, and after recovery, treated appropriately for each experiment. This method resulted in reliable results with infectious RNA replicating and spreading in quantifiable amounts.

THE INTERFERON ANTIVIRAL RESPONSE

Interferons

2007 marked the 50th anniversary of the discovery of agents that interfered with viral replication, termed interferons by Alick Isaacs and Jean Lindenmann (Isaacs and Lindenmann, 1957). Characterization of the IFNs over the intervening years has revealed a large family of multifunctional secreted proteins involved in antiviral defense, cell growth regulation and immune activation. There are now three types of IFNs, designated as type I-III. The type I IFN includes IFNα/β/ω/τ/δ/κ/ε; type II IFN is IFNγ; type III IFN includes IFNλ or interleukin-28/29. IFNλ, which was discovered recently, is induced by virus infection, displays antiviral activities and uses a distinct receptor complex from the type I and II IFNs but similarly to type I and II IFNs, signals through the Janus kinase-signal transducers and activators of transcription (Jak-STAT) pathway (Kotenko et al., 2003). IFNγ is synthesized by immune cells (natural killer cells and activated T cells) in response to

recognition of infected cells. Of the type I IFNs, IFNα/β, are the best characterized and are produced in direct response to virus infection by most types of cells. There are 14 IFNα genes encoding 12 subtypes and 1 IFNβ gene (Katze et al., 2002; Stark et al., 1998). Once IFN is induced, it is secreted from the cell and acts in an autocrine and paracrine loop to stimulate an 'antiviral state' within the infected cell and of those cells neighboring it.

Viral recognition and signaling

IFN production is dependent on host recognition of invading pathogens. All pathogens possess conserved pathogen associated molecular patterns (PAMPs) that are unique and essential for survival of the microbe. These PAMPs are detected by cellular pathogen recognition receptor (PRR) proteins which initiate intracellular signaling cascades culminating in activation of immune defenses including IFN production. The two main groups of PRR proteins involved in viral recognition include the Toll-like receptors (TLRs) and a family of DExD/H box RNA helicases including retinoic acid inducible gene I (RIG-I) and melanoma differentiation-associated gene 5 (MDA5) (Alexopoulou et al., 2001; Li et al., 2005a; Sumpter et al., 2005; Yoneyama et al., 2004). These PRRs exhibit differential tissue distribution and expression, distinct cellular localization, as well as specificity for PAMP ligands (Meylan et al., 2006; Saito and Gale, 2007), allowing the host to mount an appropriate and specific immune response to the invading pathogen. In the case of HCV, RNA PAMP recognition is mediated by the cytosolic PRR, RIG-I **(Figure 1-5)** (Sumpter et al., 2005). Recent studies by our lab have shown that RIG-1 preferentially recognizes ssRNA containing a terminal 5' triphosphate (Saito et al., 2008). Binding to the viral RNA

ligand causes a conformational change in RIG-I that activates signaling through the caspase activation and recruitment domain (CARD) by binding to the adaptor protein interferon beta promoter stimulator 1 (IPS-1), which is localized at the cellular mitochondria (**Figure 1-5)** (Kawai et al., 2005; Saito et al., 2007; Saito et al., 2008). IPS-1 then recruits a large macromolecular signaling complex to activate the latent transcription factors, interferon regulatory factor (IRF) -3 and nuclear factor-kappa B (NF-κB). Activated IRF-3 and NF-κB translocate to the nucleus where they bind to the IFNβ promoter. Maximal IFNβ production occurs when all four of the positive regulatory domains (PRD) of the promoter are bound by their respective transcription factors forming the IFNβ enhanceosome. The enhanceosome consists of the following transcription factors; IRF-1 binds to PRDI, NF-κB binds PRDII, IRF-3 and IRF-7 bind PRDIII and c-Jun and activating transcription factor-2 (ATF-2) bind to PRDIV (Honda et al., 2006). Production and secretion of IFNβ marks the immediate-early phase of the innate antiviral response (Malmgaard, 2004). (**Figure 1-5)**

Jak-STAT signaling pathway

Activation of the antiviral response leads to the production and secretion of IFNβ, which can then bind to the type I IFN receptor (IFNAR). IFNα, different subtypes of IFNα, IFNβ as well as CIFN have varying affinities for the IFNAR and elicit differential cellular responses, suggesting that receptor-ligand interactions help modulate the activation of downstream signaling pathways (Blatt et al., 1996; Platanias et al., 1994; Platis and Foster, 2003) (reviewed in van Boxel-Dezaire et al., 2006). IFNAR has two chains which dimerize upon ligand binding, inducing the phosphorylation of the receptor-associated Janus kinase 1 (Jak1)

and tyrosine kinase 2 (tyk2) as well as phosphorylation of tyrosine residues on the receptor chains (Darnell et al., 1994) (**Figure 1-5)**. These phosphorylation events lead to the recruitment and activation of the signal transducers and activators of transcription (STAT) proteins. STAT2 is associated with IRF-9 basally within the cell, and upon phosphorylation by tyk2, STAT2/IRF-9 binds to phosphorylated STAT-1(tyrosine 701) forming the interferon stimulated gene factor 3 (ISGF3) transcription factor complex (Stark et al., 1998). Maximal transcriptional activation requires a further phosphorylation on serine 727 of STAT-1 (Wen et al., 1995) (**Figure 1-5)**. ISGF-3 binds to the IFN-stimulated response element (ISRE) present within the promoter of ISGs, resulting in the production of IFNα and IRF-7 which serve as important signals to amplify this overall response, effectively mounting the antiviral state within the infected and neighboring cells(**Figure 1-5)**.

Interferon Regulatory Factors

The first interferon regulatory factor, IRF-1, was identified as a transcription factor binding to the IFNβ promoter (Fujita et al., 1989). Subsequently 9 mammalian IRF members have been identified, all having significant homology in their amino-terminal DNA-binding domains. The IRFs can bind to PRD elements in the IFNβ promoter and ISRE of ISGs allowing dual action of these molecules to regulate IFN production and ISG induction. IRFs 1,5,7 and 9 are all expressed at low levels and are highly induced by IFN, while IRF-3 is basally expressed at high levels within the cytoplasm of uninfected cells. IRF-3 and IRF-7 are currently the most important players in the context of virally induced IFNs and ISGs. As stated above, upon RIG-I/IPS-1 mediated signaling, IRF-3 is hyperphosphorylated by the I

kappa B (IκB) homologs TANK-binding kinase 1 or IκB kinase ε, resulting in its dimerization and translocation into the nucleus (**Figure 1-5)**. Upon entry into the nucleus IRF-3 interacts with either of two nuclear histone acetyltransferases, CREB binding protein (CBP) or p300 to promote transcription of IRF-3 target genes including IFNα/β and ISGs including ISG56 and ISG15.

IRF-7

IRF-7 plays a pivotal role in regulating the IFN response by inducing a second wave of IFN production from infected cells, effectively amplifying the antiviral response. IRF-7 is expressed at low to undetectable levels in all cells except for B cells and dendritic cells where it is constitutively expressed, and is highly induced by IFN in all cell types (Sato et al., 2000; Servant et al., 2002; Taniguchi et al., 2001). IRF-7 is regulated at multiple levels: transcriptional, translational and activation. IRF-7 is transcriptionally induced in response to IFN induced Jak-STAT signaling, however the protein, similar to IRF-3, requires phosphorylation by a virally activated kinase in order to induce IFN expression (Taniguchi et al., 2001). Recently, translation of IRF-7 mRNA was shown to be regulated through the 4E-BP translational repressors, which until hyperphosphorylated by an as yet undetermined virally activated kinase, suppress translation of select mRNAs including IRF-7. This control mechanism would allow for the rapid production of IRF-7 without the need for the rate limiting steps of transcription, allowing the cell to mount a rapid IFN response upon viral infection (Colina et al., 2008). Notably, IRF-7 has a short half life, allowing the cell to quickly turn off the IFN response once the virus is cleared (Sato et al., 2000).

Non-canonical interferon signaling pathways

The Phosphoinositide 3 kinases (PI3K) and p38 mitogen-activated protein kinase (MAPK) pathways have emerged as critical regulators of the cellular response to IFN (reviewed in (Katsoulidis et al., 2005; Kaur et al., 2005). It is well established that IFNs activate PI3K, which has been found associated with the IFNAR through its p85 subunit (**Figure 1-5)**. It has been demonstrated that IFN results in PI3K mediated activation of downstream effectors including NF-κB and AKT to promote cell survival in healthy B cells, suggesting a role for this pathway in immune modulation (**Figure 1-5)**(Ruuth et al., 2001). The p38 MAPK pathway is activated in response to stress signals, proinflammatory cytokines, growth factors, dsRNA or LPS (through TLR signaling), and importantly IFN (Johnson and Lapadat, 2002; Katsoulidis et al., 2005). Previous studies have demonstrated that IFNα activation of p38 is required for ISRE-dependent gene expression and is involved in the anti-HCV activity of IFNα (**Figure 1-5)**. This was shown using inhibitors of p38 phosphorylation and similar experiments using PI3K, PKC-δ or ERK inhibitors did not have an effect on HCV replication. While it was shown that the p38 mediated antiviral effects were independent of Jak-STAT signaling, the downstream mechanisms of antiviral action is not understood (Ishida et al., 2004). Depending on the cell type, either p38 or PKC-δ can phosphorylate STAT-1 on serine 727 which is required for its maximal activation (**Figure 1-5)** (van Boxel-Dezaire et al., 2006). Following IFN treatment, numerous Jak-STAT dependent and independent pathways are activated. Delineating the functions of these pathways in modulating the host antiviral response is an area of active research.

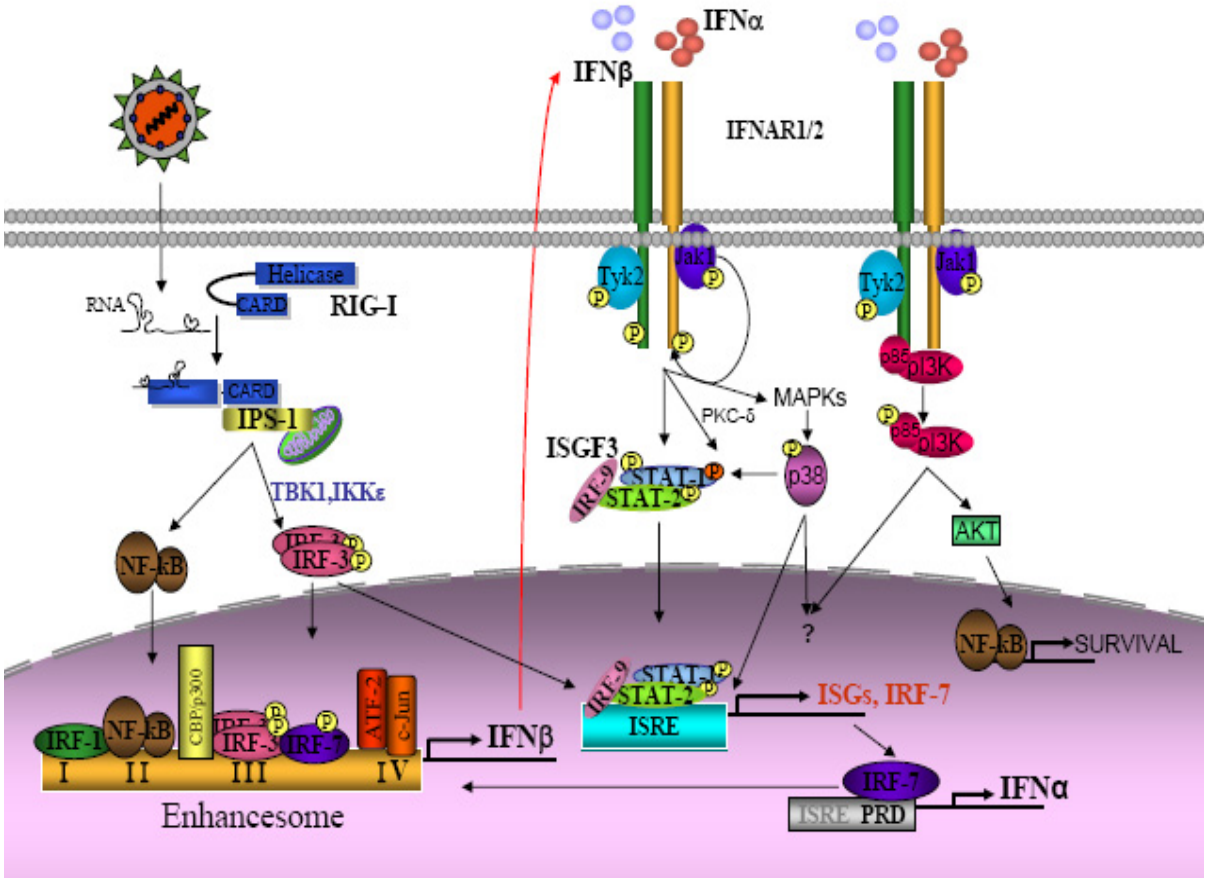

Figure 1-5. The Innate Interferon Antiviral Response. Upon virus infection, viral PAMPs such as dsRNA are recognized by the host PRRs, RIG-I for HCV. This drives a conformation change in RIG-I that promotes interaction with IPS-1, a downstream adapter protein anchored on the mitochondria outer membrane, and results activation of the latent transcription factors IRF-3 and NF-κB and binding to the IFN-β promoter. Maximal expression of the IFN-β promoter requires binding of a number of transcription factors to form the enhanceosome. Secreted IFN-β binds to the type I IFN receptor, triggering a downstream Jak-STAT signaling pathway as well as the p38 MAPK and PI3K pathways leading to the expression of interferon stimulated genes (ISGs), IRFs, and regulating a number of cellular processes including survival. The induction and subsequent virally mediated activation of IRF-7, results in IFNα production, further signaling ISG expression, resulting in amplification of the IFN antiviral response. P, tyrosine phosphorylation; orange P, serine 727 phosphorylation

INTERFERON STIMULATED GENES

Interferons are naturally produced during virus infection and are a main component in activation and amplification of the innate antiviral response through the induction of numerous antiviral genes. These molecules impart their antiviral actions through cellular mechanisms that act to limit virus replication and spread. Both in vitro and in vivo analyses using functional genomics and biochemical approaches have been utilized to characterize the spectrum of ISGs associated with viral infections and IFN therapy. These analyses have identified hundreds of ISGs involved in the interferon antiviral response, however the mechanism of action of only a few are currently known (Der et al., 1998; Sarasin-Filipowicz et al., 2008; Smith et al., 2003). Below is a summary of the current literature on ISGs that are indicated in the intracellular interferon response to HCV infection.

Components of the intracellular signaling pathways

Many of the ISGs are components of the intracellular antiviral signaling pathways including the PRRs (RIG-I) and transcription factors (IRF-1,5,7,9) involved in the IFN amplification loop **(Appendix A)**. These signaling components are basally expressed at low levels in uninfected cells to mediate surveillance, and induction by IFN may provide the infected cell and surrounding tissues with enhanced sensitivity to signaling.

PKR

One of the most extensively studied ISGs is the dsRNA-activated serine/threonine protein kinase, PKR (Meurs et al., 1990). PKR is activated by binding to dsRNA leading to its autophosphorylation. Activated PKR can then phosphorylate eIF2α preventing its association with the cellular translational machinery, thus inhibiting both viral and cellular protein synthesis **(Figure 1-6)**. In addition to its role in translational control, PKR activates a number of transcription factors, NF-κB and IRF-1, involved in the IFN, dsRNA and stress signaling pathways (Kumar et al., 1997). The importance of PKR in virus-host interactions is highlighted by the observation that nearly all viruses have evolved a mechanism to block its activity (Gale and Katze, 1998).

ISG56

The ISG56 encoded protein, p56, and the closely related p54, p60 and p58 proteins all contain a tetratricopeptide repeat motif that mediates specific protein-protein interactions (Wathelet et al., 1998). P56 binds to the p48 subunit of the translation initiation factor, eIF-3, blocking its function in protein synthesis **(Figure 1-6)** (Guo et al., 2000). We have found that p56 dominantly suppresses HCV IRES-mediated translation, demonstrating the role of this protein in host defense (Wang et al., 2003).

ISGylation

ISG15 encodes a small ubiquitin like protein that functions as a protein modifier, resulting in 'ISGylation' of numerous target proteins including PKR, MxA, Stat1, Jak1, ERK and RIG-I **(Figure 1-6)** (Sadler and Williams, 2008). It is currently unknown how ISGylation of these proteins affects their function. However, ISG15 conjugation seems to promote the antiviral state by subverting proteasome-mediated degradation of activated IRF-3 in infected cells, thus prolonging IRF-3-mediated induction of IFNβ **(Figure 1-6)** (Lu et al., 2006). ISG15 conjugation in vitro is accomplished by the concerted action of three enzymes; the activating or E1 enzyme E1-like ubiquitin-activating enzyme (UBE1L), the conjugating enzyme E2 ubiquitin-conjugating enzyme (Ubch8), and the ligating or E3 enzyme homologous to the E6-associated protein C terminus (HECT) domain and RCC1-like domain containing protein 5 (HerC5)(Kim et al., 2004; Wong et al., 2006; Yuan and Krug, 2001; Zhao et al., 2004). To note, other E2 and E3 enzymes have also been implicated in ISGylation (Sadler and Williams, 2008; Zhao et al., 2004). The deconjugating enzyme, Usp18, is a negative regulator of the IFN signaling pathway both by decreasing ISGylation and blocking Jak-STAT signaling (Malakhova et al., 2006). Importantly, ISG15, Herc5 and USP18 are all highly induced by IFN **(Appendix B)**. The consistent observations that ISG15 is released from cells and found in the serum of IFN-treated patients, has led to investigations of the cytokine activity of this molecule as has been suggested for ubiquitin (D'Cunha et al., 1996; Majetschak et al., 2003). It was found that ISG15 can induce IFNγ from immune cells and activate natural killer cells, however the mechanism by which extracellular ISG15 mediates these immunomodulatory functions is not understood (D'Cunha et al., 1996). While

considerable work still needs to be done to define the function of ISGylation, mounting evidence suggests an important role for this protein in the IFN-mediated antiviral response.

Viperin

Viperin (*v*irus *i*nhibitory *p*rotein, *e*ndoplasmic *r*eticulum-associated, *in*terferon-inducible) was identified as an IFN-stimulated antiviral protein that is directly induced by human cytomegalovirus (Chin and Cresswell, 2001). Viperin has been shown to inhibit a number of viruses including, influenza A virus, dengue virus, alphaviruses and HCV (Wang et al., 2007) (Fink et al., 2007; Jiang et al., 2008a; Karla J. Helbig, 2005; Zhang et al., 2007). Structure/function analysis demonstrated that viperin is a putative radical *S*-adenosyl-$_{L}$-methionine enzyme whose functional enzymatic activities are necessary for the inhibition of HCV infection (Jiang et al., 2008a). In the case of influenza A virus infection, viperin expression disrupts the formation of lipid rafts (which are important in the budding process) on the plasma membrane by binding to and inhibiting an enzyme involved in the biosynthesis of isoprenoid-derived lipids **(Figure 1-6)** (Wang et al., 2007).

ISG20

ISG20 has also been recently identified as an ISG that confers resistance to various RNA viruses including VSV, HIV and HCV. These studies have shown that the antiviral activity of ISG20 depends on its 3'-5' exonuclease activity, but direct degradation of HCV viral RNA has not been conclusively demonstrated **(Figure 1-6)** (Espert et al., 2003; Espert et al., 2006; Jiang et al., 2008a).

OAS

OAS Structure and Isoforms

The OAS proteins are encoded by a highly conserved family composed of four genes, OAS1-3, and OASL located on chromosome 12. The OAS proteins each contain at least one conserved OAS unit where OAS1-3 contain one, two or three active catalytic domains, respectively. The OAS like gene, OASL, encodes one OAS unit that lacks enzymatic activity and a C-terminal domain of two ubiquitin-like repeats. (Hovnanian et al., 1998) (Rebouillat et al., 1998). Expression of OASL is highly induced by IFN in primary hepatocytes, however the function of this protein is unknown **(Appendix B)**. Alternative splicing events lead to the expression of multiple OAS isoforms including OAS1 (p42/44/46/48), OAS2 (p69/71) and OAS3 (p100) (Justesen et al., 2000). The functional OAS variants all contain the three conserved aspartic acids in their N-terminal catalytic domains thought to be necessary for enzymatic activity. While the OAS proteins do not possess any known RNA binding domains, the crystal structure of the porcine OAS1 protein and deletion studies suggest a large putative RNA activation site spanning much of the protein (Hartmann et al., 2003). Despite their conserved N-terminal regions, the OAS isoforms have differential subcellular localization, cell type expression and OAS enzymatic activity (Bonnevie-Nielsen et al., 2005; Rebouillat and Hovanessian, 1999). All of the OAS variants produce 2'-5' linked

oligoadenylate chains (2-5As) from ATP, so the reason for multiple variants is unclear, but suggests that they might have multiple functions.

OAS/RNase L Pathway

The oligoadenylate synthetases (OAS) are a family of interferon induced proteins that are activated in the presence of dsRNA resulting in the synthesis of 2'-5' linked oligoadenylate chains (2-5As) from ATP. In turn, 2-5As can bind to the latent ribonuclease L (RNase L) leading to its dimerization and activation. Activated RNase L degrades viral and cellular RNA inhibiting protein synthesis and viral growth. RNase L preferentially cleaves single-stranded RNA at UA and UU dinucleotides, leaving small cleavage products that signal through the RIG-I antiviral pathway to amplify IFN-α/β production (Floyd-Smith et al., 1981; Malathi et al., 2007; Wreschner et al., 1981). The importance for the RNase L and OAS systems in controlling viral infections has been demonstrated for a number of RNA viruses including members of the picornaviridae and flaviviridae **(Figure 1-6)** (reviewed in (Silverman, 2007). OAS and RNase L have also been implicated in the regulation of cellular events including apoptosis and cell growth (Castelli et al., 1998; Ghosh et al., 2001).

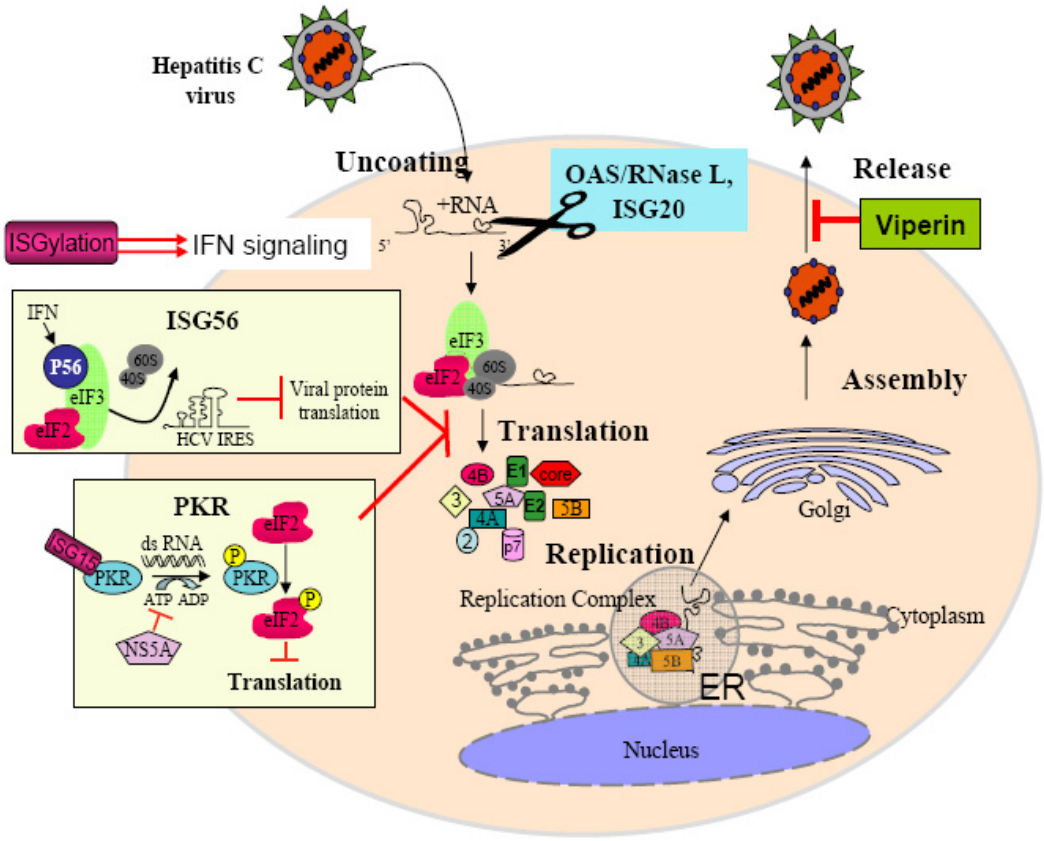

Figure 1-6. ISGs, the effector proteins of the IFN antiviral response. The proteins encoded by ISGs suppress viral infections by blocking various steps within the virus life cycle. PKR, ISG56, ISG20 and OAS/RNase L block protein translation through distinct mechanisms. ISG20 has been proposed to directly cleave viral RNA, while OAS and PKR are activated in the presence of viral RNA intermediates, illustrating a dual role for these molecules in sensing viral infections as well having direct antiviral functions. PKR and ISG56 both inhibit the functions of eukaryotic translation initiation factors which are essential for HCV IRES-mediated viral protein synthesis. Upon binding dsRNA, OAS gains functional synthetase ability leading to activation of RNAse L, which cleaves viral and cellular RNA, directly inhibiting the virus while also inducing apoptosis of the infected cell. Viperin has been shown to inhibit a protein essential for lipid synthesis at the plasma membrane which leads to disruption of the budding of progeny virions. ISGylation occurs when ISG15 is conjugated to its target proteins, many of which are involved in the intracellular antiviral response. ISGylation is proposed to prevent degradation of antiviral proteins, thus amplifying the overall IFN antiviral response.

HCV EVASION OF INTERFERON ANTIVIRAL RESPONSE

In order for a virus to efficiently propagate within a host it must evade the host immune defenses. Viruses employ a variety of strategies to block the IFN response often blocking more than one step of the IFN regulatory pathway, including disruption of IFN production, IFN signaling and inhibition of the protein functions of ISGs.

HCV has evolved countermeasures to deal with multiple steps of the IFN response **(Table 1-1).** Perhaps the most effective method HCV uses to block the intracellular antiviral response is through disruption of IRF-3 and NF-κB activation (Foy et al., 2003). This is mediated through the HCV NS3/4A cleavage of IPS-1, the adaptor molecule downstream of RIG-I. Cleavage of IPS-1 disrupts its localization in the mitochondria, thus preventing the downstream events necessary for phosphorylation and activation of IRF-3 and NF-κB, effectively shutting down the intracellular antiviral response (Li et al., 2005c; Loo et al., 2006; Meylan et al., 2005). HCV has also been shown to block the Jak-STAT signaling pathway through the disruption of STAT1 function and induction of the suppressor of cytokine proteins (SOCS), which are negative regulators of the Jak-STAT pathway (Bode et al., 2003; Heim et al., 1999). Additionally, the HCV NS3/4A protease has been found to disrupt TLR3 mediated IFN signaling by cleavage of the Toll-interleukin-1 receptor-domain-containing adaptor inducing IFNβ (TRIF) protein (Li et al., 2005b). It has also been found that HCV regulates the non-canonical IFN signaling pathways, suggesting the importance of these pathways in host intracellular antiviral response. For example, HCV stimulates the prosurvival PI3K-Akt pathway and mTOR to inhibit apoptosis, preventing elimination of

infected cells. Interestingly, Akt and mTOR kinases phosphorylate NS5A in vitro, leading to reduced HCV replication, perhaps contributing to the establishment of persistent infection by regulating HCV levels (Mannova and Beretta, 2005).

The HCV E2 envelope and NS5A proteins have both been found to bind to PKR and inhibit its catalytic activity (Gale et al., 1998; Taylor et al., 1999). This allows the virus to evade the translational-suppressive effects of PKR on both viral protein synthesis as well as prevents PKR-dependent activation of transcription factors involved in IFN signaling (Kumar et al., 1997). OAS activation and subsequent RNase L mediated degradation of HCV viral RNA has been demonstrated in vitro. The susceptibility of HCV mRNA cleavage by RNase L was correlated with viral genotype, wherein the IFN-resistant HCV genotype 1 sequences contain fewer UU and UA dinucleotides as compared to the IFN sensitive genotypes 2 and 3 (Han and Barton, 2002; Han et al., 2004). Therefore, HCV has evolved to have a paucity of RNase L cleavage sites, thus evading the antiviral affects of the IFN-induced OAS/RNase L pathway.

TABLE 1-1. HCV EVASION OF THE INNATE IFN RESPONSE.

HCV protein	**Blocks**	**Mechanism of action**
NS3/4A protease	RIG-I signaling pathway	Cleaves adaptor protein, IPS-1
NS3/4A protease	TLR3 signaling pathway	Cleaves TRIF
Core	Jak-STAT signaling	Disrupts STAT1 function, induces SOCS
E2/NS5A	PKR activation of NF-κB and IRF-1, translational control	Binds PKR blocking activation
Genome (genotype 1)	Evades OAS/RNase L pathway	Paucity of RNase L cleavage sites within RNA genome

CHAPTER TWO
Methodology

In Vitro Transcription

HCV 2a RNA was produced from pJFH-1, a plasmid encoding the infectious clone of HCV genotype 2a which has been described (Loo et al., 2006; Zhong et al., 2005). HCV 1a RNA was produced from pH77-S, an infectious clone of HCV genotype 1a (kindly provided by S. Lemon). RNA for the in vitro translation assays was generated from the bicistronic luciferase reporter plasmid, pRL-HL (a gift from S. Lemon, (Honda et al., 2000)). Linearization of plasmid DNA was carried out by digesting 10μg of the pJFH-1 or pH77-S with 3μL *Xba*I and 10μg of pRL-HL with *Apa*I overnight at 37°C, followed by incubation for 30 minutes with 2μL Mung Bean Nuclease (New England Biolabs, Ipswich, MA) to degrade single-stranded extensions from the end of the DNA molecules. Enzyme reactions were terminated by adding $1/20^{th}$ the reaction volume of 0.5M EDTA, 5M NaOAC at $1/10^{th}$ the volume and 2x 100% ethanol. Digested DNA was precipitated by incubation at -20°C overnight, washed 2x with ice-cold ethanol and resuspended in 10μL H_20. In vitro transcription reactions were performed overnight at 37°C using the Ambion T7 MEGAscript Kit following the recommended manufacturer's protocol. Template DNA was removed by incubating the reactions with TurboDNAse at 37°C for 30 minutes. In vitro transcribed RNA was then recovered using phenol:chloroform extraction and isopropanol precipitation, resuspended in 10μL H_20, quantitated and stored at -80°C until use.

In Vitro Translation

In vitro translation assays were performed using the rabbit reticulocyte lysates translation system according to the manufacturer's protocol (Promega). 1μg of in vitro transcribed RNA from pRL-HL was incubated with buffer or the indicated concentration of IB657 for 30 minutes at 30°C then immediately added to translation reactions containing 35μL rabbit reticulocyte lysates, 1μL [^{35}S]methionine, 1μL amino-acid mixture lacking methionine, 1μL RNase inhibitor and H20 to a final volume of 50μL. The reactions were incubated at 30°C for 90 minutes and 5μL of each added to 20μL of SDS sample buffer, boiled and ^{35}S-labeled proteins analyzed by separation on a 12% SDS-polyacrylamide gel. Gels were fixed (50% methanol, 10% acetic acid) for 30 minutes, dried for 90 min at 80°C on a vacuum dryer, and then analyzed by phosphorimaging. Also, dual-luciferase reporter assay was performed as described below, using 2.5μL of each translation reaction in quadruplicate.

Plasmids

Expression plasmids for ISG15, Usp18, UbcH8 and Herc5 as well as duplex siRNAs targeting human Usp18 and UbcH8 were generously provided by Dr. Bob Krug, UT Austin, Austin, TX (Zhao et al., 2004). Expression constructs encoding the OAS1 variants; p40, p42, p46, p40+CTIL p42+CTIL, and p46 with the CTIL mutated to STIL by site-directed mutagenesis were generously provided by Kineta, Inc. and were subcloned into the 5'XhoI and 3'XbaI multiple cloning sites in the pCMVT$_N$T (Promega) expression vector. pEFBos-N-RIG was a gift from T. Fujita (Yoneyama et al., 2004). IMAGE clones of the full cDNA sequences of Viperin, ISG20, NOD27 and ISG44 were used as template in high fidelity PCR

reactions with primers to engineer the *Not*I and *Pme*I restriction enzyme sites at the 5' and 3' ends. PCR products were digested and subcloned into the respective sites of pEFTak (encoding a N-terminal FLAG tag) as previously described (Saito et al., 2007).

Cell Culture

Huh7 and Huh7.5 cells are human hepatoma cells that have been previously described (Blight et al., 2002; Sumpter et al., 2005). PH5CH8 cells are immortalized primary human hepatocytes, a kind gift from Dr. N. Kato (Okayama University Graduate School of Medicine, Dentistry, and Pharmaceutical Sciences, Okayama, Japan)(Ikeda et al., 1998). Cells were propagated in culture media consisting of Dulbecco's Modified Eagle's Medium (Fisher) supplemented with 10% fetal bovine serum (FBS, Hyclone), 25mM HEPES (Cellgro), 1x minimal essential amino acids and antibiotic-antimycotic solution (Sigma). Huh7-L2198S, Huh7-K2040, Huh7-A7 and Huh7-HP cells are clonal Huh7 cell lines harboring genetic variants of an HCV genotype 1b subgenomic RNA replicon described previously(Foy et al., 2003; Pflugheber et al., 2002; Sumpter et al., 2004). Huh7-JFH-1 is a clonal Huh7 cell line harboring the HCV genotype 1b subgenomic RNA replicon. The HCV replicon cell lines were maintained in culture medium supplemented with 200 μg G418/mL. For IFN or IB657 treatment of HCV-replicon cells, G418 containing media was removed, cells washed once with PBS and replaced with culture medium containing the indicated concentrations of each IFN and/or IB657. All cells were grown at 37°C under 5% CO_2 in water-jacketed incubators.

IFNs

IFN-α2a was obtained from PBL Interferon Source (Piscataway, NJ), PEG-Intron™ (PEG-IFN) from Schering-Plough Corp. (Kenilworth, NJ), and CIFN (INFERGEN®; Interferon alfacon-1) from InterMune Inc. (Brisbane, CA). The pharmacologic C_{max} concentration of IFN-α2a and Peg-IFN-α2b was determined from the product sheet provided by the manufacturer. The pharmacologic C_{max} concentration of CIFN was obtained following FDA-approved clinical dosing schedules, which corresponded to 80 pg/mL (Tan et al., 2005).

HCV Assays

HCV 2a was produced from 10^6 Huh7.5 cells transduced with 4μg of in vitro transcribed RNA from the JFH-1 infectious clone using the TransMessenger RNA transfection reagent (Qiagen). Infected cell cultures were serially passaged into 15cm dishes. Virus stocks were prepared from supernatants of infected cells cultured in medium containing 2% FBS and virus concentrated 100 fold using Centricon Plus-70 filters (Millipore, Lowell, MA). HCV 2a titers were determined by focus forming assay. Concentrated virus stocks or cell supernatants were serially diluted 10-fold in complete DMEM and used to infect 10^4 naïve Huh7.5 cells per well in 48-well plates. The inoculum was incubated with cells for 1-3 h at 37°C and then supplemented with fresh culture medium. The level of HCV infection was determined 2 days post-infection by immunohistochemical staining for HCV proteins using human antiserum specific to HCV (patient serum obtained with informed consent and Institutional Review Board Approval through Dr. W. Lee at UT Southwestern Medical Center, Dallas, TX) that detects both HCV genotypes 1 and 2, and has been described (Loo et al., 2006). Infected

cells were visualized after incubation with anti-human horseradish peroxidase-conjugated (HRP) secondary antibody for 30 minutes, and cells stained brown using the Vector® VIP substrate kit for peroxidase detection according to manufacturer's recommendations (Vector Laboratories Burlingame, CA). The viral titer (ffu/mL) was determined by limiting dilution as described by Reed and Munch, by quantifying the average number of HCV-positive foci (ffu/mL) detected at the highest dilutions. The HCV genotype 1a infectious virus does not replicate in cell culture to high enough levels for concentration of the virus. Therefore antiviral assays using the HCV 1a virus were done using a modified version of the above protocol for HCV 2a production. HCV 1a RNA was transcribed from pH77-S (kindly provided by S. Lemon) using the T7 Megascript kit (Ambion). HCV 1a RNA transfection was performed using 6 μg of RNA per 5×10^5 Huh7.5 cells with the *Trans*IT®-mRNA Transfection Kit (Mirus) for 48-72 hours. Cells were then trypsinized and plated in 4-chamber well slides or 48 well dishes at 2×10^4 cells per well. After recovery for 24 hours the cells were washed and cell culture media containing fresh media or the indicated drugs added. After 72 hours of treatment the levels of HCV 1a replication and spread was quantitated by determining the % of HCV positive cells by immunofluorescence assay IFA), where HCV positive cells (serum A) and the total number of cells (DAPI) were counted in 6 fields per treatment. Also, the average number of HCV 1a-positive foci was determined by focus forming assay as described above for HCV 2a.

Immunoblot Assay

For evaluation of protein expression, cell lysates were prepared by trypsinization or scraping of the cells into 1mL PBS and lysis of the cell pellets in modified radioimmunoprecipitation assay (RIPA) buffer (10mM Tris pH 7.5, 150mM NaCl, 0.02% NaN_3, 1% Na-deoxycholate, 1% Triton X-100, 0.1% SDS, 10μL/mL Sigma protease inhibitor cocktail, and 10μL/mL phosphatase inhibitor cocktail set II and 1μM okadaic acid (Calbiochem). Cell lysates were stored at -80°C, until use. Thawed lysates were spun at 4ºC for 15 minutes at ≥18,000x*g* to pellet membrane fractions and cellular debris. Supernatants were collected and protein concentrations measured by Bradford assay. Equivalent amounts of protein from 20-30μg were resolved by SDS-polyacrylamide gel electrophoresis (PAGE) on 10% or 12% polyacrylamide gels, and immediately transferred to NitroPure nitrocellulose membranes (Micron Separations, Inc.) using Towbin's transfer buffer at 120V for 1 hour at 4°C. Membranes were incubated in blocking solution (PBS containing 0.1% Tween-20 (TPBS) and 5% nonfat dehydrated milk (Carnation) for 30 minutes. Blots probed with antiserum specific to PKR, ISG56, ISG15, RIG-I or IPS-1 have been described previously (Foy et al., 2003; Loo et al., 2006; Pflugheber et al., 2002). Antibodies against GAPDH, actin, IRF-1, IRF-9, IRF-7, and total STAT2 were purchased from Santa Cruz (Santa Cruz, CA). Antibodies against total STAT1 or phosphorylated STAT1 were purchased from Cell Signaling (Danvers, MA). The neomycin phosphotransferase II rabbit polyclonal IgG was purchased from Cortex Biochem and used at 1:1000 dilution in TPBS. Two well-characterized anti-HCV patient serum were obtained with informed consent and Institutional Review Board approval through Dr. W. Lee, UT Southwestern Medical Center, Dallas, TX

and were used for detection of HCV proteins. Primary antibodies were prepared in TPBS supplemented with 10% FBS and 0.02% NaN_3. Between primary and secondary antibodies, and after secondary antibody, membranes were washed 3 x 5 min. in TPBS. Secondary antibodies were diluted 1:5000 (anti-goat antibody) or 1:10,000 (all other secondary antibodies) in blocking solution. Anti-human and anti-goat HRP-conjugated secondary antibodies were obtained from Jackson Laboratories; anti-rabbit and anti-mouse HRP conjugated secondary antibodies were obtained from Perkin Elmer. Protein bands were visualized by enhanced chemiluminescence, ECL-Plus reagent (Amersham Biosciences).

Electrophoretic Mobility Shift Assay (EMSA)

EMSA analysis of ISGF-3 DNA binding activity was conducted on IFN-treated Huh7 or PH5CH8 nuclear extracts as described (Fredericksen et al., 2002). Cells were harvested by scraping into ice-cold PBS and pelleted at 1850 x g for 10 min at 4°C. The supernatant was removed, 100µl lysis buffer (50mM Tris-HCl pH 8.0, 60mM KCl, 1mM EDTA, 2mM DTT and 0.15% NP40) added to each sample, and cells were incubated on ice for 15 minutes. Lysates were centrifuged at 3300 x g for 15 min to separate cytosolic and nuclei. The pelleted nuclei were lysed in 1 volume nuclear extract buffer (20mM Tris-Cl pH 8.0, 400mM NaCl, 1.5mM $MgCl_2$, 200µM EDTA and 25% glycerol) and incubated on ice for 2 min. NaCl was added to nuclear extracts to reach a final concentration of 400mM in order to strip proteins from DNA, and incubated on ice for 10 min. Samples were vortexed for 15 sec and centrifuged at maximum speed for 30-45 minutes to collect nuclear extract. For analysis of IB657 HCV-RNA binding, HCV 5'UTR RNA was synthesized from the 500 bp

*Sex*AI/*Eco*RI restriction fragment of pJFH-1 using the T7 Megascript kit (Ambion). Probes were labeled by incubating 5 pmol dsDNA template (ISRE from ISG15 sequence) or 5μmol HCV RNA, 35μg polyIC RNA or 5 μmol dsDNA template from pCDNA3.1 with ^{32}P-γATP, and T4 Kinase (GibcoBRL) for 30 min at 37°C. The probes were purified on a spin column to remove unincorporated nucleotide (BioRad). Binding reactions were carried out with 5 μg nuclear extract or the indicated concentrations of IB657 or 2μM of the IB657-DAD mutant protein and 50,000 cpm radiolabeled probe in EMSA binding buffer (60mM HEPES pH 7.9, 50mM NaCl, 1mM EDTA, 0.5mM DTT, 0.3 mg/ml BSA, 52μg/ml salmon sperm DNA and 10% glycerol) for 30 min at 30°C. For antibody supershift analysis and cold competitor control, nuclear extracts were incubated with 2μg anti-STAT1, anti-IRF-9 antibody or non-radiolabeled HCV 5'UTR RNA probe for 15 minutes at 30°C prior to addition of labeled probe. Bound complexes were separated via native 6% Tris-glycine-polyacrylamide gel electrophoresis for 90 min at 275V at 4°C. Gels were fixed (50% methanol, 10% acetic acid) for 30 minutes, soaked in Amplify buffer (Amersham) and dried at 80°C for 90 min on a vacuum dryer. Bands were visualized by autoradiography and quantitated using densitometry.

^{35}S-Methioning Labeling and Immunoprecipitation

Huh7.5 cells were infected with the HCV 2a at an MOI of 0.5 and passaged. At this point 100% of the cells were infected, as determined by parallel anti-HCV immunostaining. The cells were then plated at 10^5 cells per well of a 6-well dish and 24 hours later cells were washed. Culture media were then replaced with media containing the respective

pharmacologic C_{max} concentration of IFNs or the indicated concentrations of IB657. After a further 24-48 hours, media was removed and cells were starved of methionine for 2 hours. Cells were labeled by adding 100 μCi of [^{35}S] methionine to the starvation media for 1 hour. Cells were washed 3x and collected by scraping into 1mL ice-cold PBS. Cells were briefly spun at 2400xg for 5 minutes, then resuspended in 100μl Seize II immunoprecipitation (IP) lysis buffer (25mM Tris-HCL (pH 7.5), 150mM NaCl) plus 1%NP40, okadaic acid, protease and phosphatase inhibitors (lysis buffer) as described above for immunoblot analysis. Cell lysates were diluted in 300μl lysis buffer and centrifuged at ≥ 20,000xg for 15 minutes to pellet intact cells and membranes. Supernatants were collected and precleared with 40μL of protein-A agarose beads (Roche) for 3 hours at 4°C. Recovered lysates were subjected to immunoprecipitation using 1μL of anti-HCV serum plus 40μL of Protein-A agarose beads and incubated for 3 hours at 4°C. The immunecomplexes were recovered by centrifugation at 100xRCF for 5 minutes, washed 5 times with lysis buffer and 40□l of SDS-sample buffer were added. Samples were boiled for 5 minutes and proteins separated on a 10% SDS-polyacrylamide gel (SDS-PAGE). The gel was fixed, soaked in amplify buffer (Amersham, Piscataway, NJ) for 30 minutes, dried and exposed to phosphor screen for 3-6 days. The radiosignal was visualized and quantified by phosphorimager analysis.

Quantitative Real-Time Reverse Transcription-PCR (qRT-PCR)

Total RNA was isolated from cells with Trizol LS reagent (Invitrogen, Carlsbad, California) or Qiagen's RNeasy Mini Kit (Qiagen, Valencia, CA) as recommended by the manufacturer. Purified total cellular RNA was treated with Turbo DNAse (Ambion) to remove any

contaminating genomic DNA for 1hr at 37°C. Enzyme activity was neutralized with DNAse inactivation reagent for 2hr at room temperature (Ambion). HCV, human glyceraldehyde-3-phosphate dehydrogenase (GAPDH), Usp18 or firefly luciferase RNA levels were determined by one-step qRT-PCR using the ABI Prism 7500 sequence detection system in the presence of SYBR green with 100-250ng total RNA per reaction and each reaction done in triplicate. Reaction conditions were as follows: 48º for 30 min; 95ºC for 10 min; and 40 cycles of 95ºC for 15 s, 60ºC for 1 min. The primer pairs used for the detection of HCV were 5'-TGC GGA ACC GGT GAG TACA-3'(sense), 5'-CGG GTT GAT CCA AGA AAG GA-3'(antisense), Human GAPDH, 5'-CTGGGCTACACTG AGCACCAG- 3' (sense), 5'CCAGCGTCAAAGGTGGAG-3' (antisense), Usp18 5-TCATTTTCCATTTCCGTTCC-3(sense), 5'GCAAAATCTCTTAGAAGACTCCGTA-3' (antisense) and firefly luciferase 5'AGAGATACGCCCTGGTTCCT-3'(sense),5'CCAACACCGGCATAAAGAAT-3' (antisense) and were purchased from IDT (Integrated DNA Technologies). Relative mRNA expression levels were calculated using the comparative cycle threshold (CT) method with human GAPDH as the internal standard, and fold change values were calculated using the $\Delta\Delta C_t$ ($2^{-\Delta\Delta Ct}$) (Anonymous, 1997, updated 2001).

RNA silencing

Duplex siRNAs targeting a scrambled negative-control were obtained from Ambion and Usp18 and UbcH8 from Dharmacon using previously published sequences (Wong et al., 2006). siRNA was transfected into Huh7-HCV replicon cells using the TransMessenger transfection reagent (Qiagen) according to the manufacturer's protocol by using a ratio of 16

μL of Transmessenger per 400 pmol of siRNA duplexes for each 60 mm dish. Transfection was carried out for 4 hours at 37°C in 2 mL serum free media which was changed to complete media containing 50U/mL IFNα for 24-48 hours and cells harvested for total RNA or protein extraction.

Microarray Expression Analysis

PH5CH8 cells were plated at a density of 10^6 cells per 100 mm dish, allowed to recover for 48 hours, and medium then removed and replaced with media containing the respective pharmacologic C_{max} of the indicated IFN. Cells were harvested in a reverse time course following 20, 8, and 4 hr treatment with the various IFNs, or mock-treatment with media alone (control). Total RNA was extracted using Qiagen's RNeasy Mini Kit following the manufacturer's recommendations (Qiagen, Valencia, CA). Four independent samples were generated for each IFN and mock treatment at every time point. Expression analysis was performed using Affymetrix (Santa Clara, CA) Genechip® U133 plus 2.0 arrays in accordance with manufacturer-recommended protocols. Data were exported from Affymetrix MAS5 software and only those probe sets called "present" in all replicates of at least one condition were used for further analysis in order to purge the data set of unreliable information. Statistical analysis was performed in Partek Pro 5.1 (Partek, St. Paul, MN) or GeneSpring 6.1 (Silicon Genetics, Redwood City, CA). Statistical significance of expression differences was determined by 2-way ANOVA (time, IFN treatment, interaction of time and IFN treatment) with untreated samples excluded, and a Bonferonni $p < 0.05$ used as a multiple test correction. Principle Component Analysis (PCA) was used to visualize inter-

sample variability associated with the expression profiles of the genes deemed to have statistically significant differences in expression with the various IFN treatments. Probe sets identified in the 2-way ANOVA as significantly different in IFN treatment were used in a 1-way ANOVA with a Tukey post hoc test. In this second statistical test, $p < 0.05$ was considered significant and ANOVA were conducted for each time point.

Immunofluorescence Assay (IFA) and Microscopy

In four-chamber slides, 2 x 10^4 cells per well were plated. The next day media was replaced with culture media containing the indicated concentration of IB657 or transfected with 500ng DsRED, pCMV-p46, pCMV-IB657 or N-RIG. After a further 24 hours cells were infected with HCV 2a at an MOI=2. 48 hours later the cells were fixed in 4% paraformaldehyde, permeabilized with 0.2% Triton X-100 for 15 min and then blocked in PBS containing 10% FBS for 1 hour. Cells were incubated for 1 hr with 1/1000 dilution of HCV patient serum, 1/200 dilution of mouse anti-OAS1 monoclonal antibody (gift from S. Iadonato, Kineta, Inc) or rabbit anti-RIG-I pAb (generously provided by Dr. Takashi Fujita). Slides were washed three times followed by 30 minute incubation with 1/1000 dilution of Alexa 488-conjugated goat anti-human, Alexa 594-conjugated goat anti-mouse or anti-rabbit secondary antibodies (Invitrogen) plus 1/100 dilution of DAPI to stain nuclei. Cells were washed three times, the chamber removed and the slide allowed to dry. Slides were mounted with Vectashield solution (Vector Laboratories) and examined using a Zeiss Axiovert digital imaging microscope or a Zeiss Pascal laser scanning confocal microscope in the University of Texas

Southwestern Pathogen Imaging Facility. The images shown were taken with oil immersion at 63X and analyzed using Zeiss LSM software.

Dual-Luciferase Reporter Assays

Luciferase analysis for simultaneous assessment of cap- and HCV IRES-dependent (pRL-HL) or EMCV IRES-dependent (pCMVRluc-EFluc) translation has been previously described in detail (Wang et al., 2003). Briefly Huh7, Huh7.5 or 293 cells were cotransfected with 250ng of the bicistronic reporter plasmid pRL-HL or pCMVRluc-EFluc and the indicated amounts of p40 using the FuGENE 6 transfection reagent (Roche Molecular Biochemicals) as recommended by the manufacturer with a DNA:FuGENE 6 ratio of 1:4. For IFN treatment culture media was replaced with media containing 50U/mL of IFN-α2a four hours after transfection. 48 hours after transfection cellular extracts were prepared using the Dual-Luciferase^{R} Reporter Assay System (Promega) to simultaneously evaluate firefly and *Renilla* luciferase activity. Luciferase assays were performed as recommended by the manufacturer, except that 20 µl cell lysates and 50 µl of assay reagents were used. Firefly and *Renilla* luciferase activity was measured with a luminometer over a 10 second interval following an initial 2 second delay after the addition of the assay reagent to the cell lysates.

CHAPTER THREE
Antiviral potency analysis and functional comparison of consensus interferon, interferon-alpha2a and pegylated interferon-alpha2b against hepatitis C virus infection

INTRODUCTION

Hepatitis C virus (HCV) infection represents a serious global health problem wherein the World Health Organization estimates that approximately 2.2% of the world population is infected with HCV (2004). IFN-α2a or IFN-α2b, pegylated versions of each (PEG-IFN-α2a or Peg-IFN-α2b), and consensus IFN (CIFN) are each approved for HCV treatment in the United States in which the current standard of care consists of PEG-IFN-α2a or PEG-IFN-α2b with ribavirin **(Appendix A)** (Deutsch and Hadziyannis, 2008). Among these IFN preparations, CIFN a synthetic type I IFN produced from the consensus sequence of several naturally occurring IFN-α subtypes (Blatt et al., 1996). Previous *in vivo* studies have demonstrated the efficacy of CIFN in the treatment of chronic HCV infection (Miglioresi et al., 2003; Sjogren et al., 2007; Tong et al., 1997; Witthoeft et al., 2007; Yasuda and Miyata, 2002). When compared against IFN-α2b alone, administration of overall lower doses of CIFN resulted in greater reduction of serum HCV RNA levels in treated patients (Tong et al., 1997). However, the distinctions by which each IFN type mediates antiviral actions against HCV have not been evaluated. Problematically, only about 50% of treated individuals respond to IFN therapy overall (Fried et al., 2002; McHutchison, 2004; McHutchison et al., 1998). This low response rate necessitates a continual push to improve IFN therapy

application and treatment regimen. A number of studies have linked the poor response rate of HCV to IFN therapy with the ability of the virus to evade and antagonize the intracellular antiviral defenses that are triggered by infection and/or induced by IFN (Feld and Hoofnagle, 2005). However, the molecular mechanisms of IFN action against HCV are not well understood, thus impeding the development of improved therapeutic strategies to combat the HCV pandemic.

IFNs are potent cytokines and key players in stimulating the innate antiviral immune response. IFNs mediate antiviral effects through the transcriptional activation of IFN-stimulated genes (ISGs) (Der et al., 1998). ISGs are primarily induced by intracellular signaling triggered by IFN through the α/β IFN receptor, which activates the canonical Janus kinase-signal transducer and activator of transcription (Jak-STAT) pathway (Heim, 1999). IFN triggers the phosphorylation of STAT1 and STAT2 to mediate STAT activation and formation of the ISGF3 complex consisting of STAT1, STAT2, and IRF-9 (Sen, 2001; Stark et al., 1998). ISGF3 binds to the interferon stimulated response element (ISRE) within the promoter region of ISGs to induce gene expression. ISG products impart cellular actions that limit viral replication and cell to cell virus spread, and that indirectly modulate the maturation of the adaptive immune response (Guo et al., 2001; Kolumam et al., 2005; Prabhu et al., 2004; Shimazaki et al., 2002; Wang et al., 2003). IFNs are naturally produced during infection with HCV or other viruses. In the case of HCV, viral RNA recognition by the retinoic acid-inducible gene-I (RIG-I) protein triggers a signaling cascade through the essential interferon promoter simulator-1 (IPS-1) protein, leading to activation of the

interferon regulatory factor-3 (IRF-3) transcription factor and its induction of α/β IFN expression (Guo et al., 2001; Meylan et al., 2005; Prabhu et al., 2004; Shimazaki et al., 2002; Wang et al., 2003). HCV can antagonize RIG-I signaling of IRF-3 through the actions of the viral NS3/4A protease, which targets and cleaves IPS-1 disrupting IRF-3 activation (Foy et al., 2005; Johnson et al., 2007; Lau et al., 2008; Loo et al., 2006; Meylan et al., 2005). Thus, therapeutic application of IFN to mediate high, sustained ISG expression and concomitantly promote or restore RIG-I signaling in infected cells might provide increased antiviral potency against HCV.

Clinical studies indicate that IFN-α2a and IFN-α2b or PEG-IFN-α2a and PEG-IFN-α2b have similar efficacies in the treatment of HCV, with the pegylated-interferons achieving better antiviral responses than their non-pegylated counterparts when given in combination with ribavirin (reviewed in Hayashi and Takehara, 2006). *In vitro* studies found that CIFN had increased antiviral and immune modulation activity as compared to IFNα-2a and IFN-α2b, which had very similar activities (Ozes et al., 1992). The primary objective of this study was to define the signaling distinctions and antiviral properties of IFN-α2a, PEG-IFN-α2b and CIFN toward regulating ISG expression and controlling HCV infection in vitro. Our rationale for studying these IFNs is that each has been used for the treatment of HCV infection, and they comprise a representative set of the standard and pegylated IFNs that are currently approved for anti-HCV therapy applications. Our studies reveal unique properties of CIFN that confer potent and differential ISG expression that associates with enhanced suppression of HCV replication. Our results suggest that strategies aimed at modifying HCV

treatment protocols for maximal expression of specific ISGs should be considered for improving IFN therapy.

MATERIALS AND METHODS

Enzyme-Linked Immunosorbent Assay (ELISA)

In order to quantify neomycin phosphotransferase II (NPT II) protein levels in HCV subgenomic replicon cell lines a NPT II ELISA was performed as described by the kit manufacturer (Agdia, Elkhart, Indiana). Huh7-K2040 and Huh7-HP cells were respectively plated at $4.5x10^3$ or $6x10^3$ cells per well of a 96 well dish. Cells were cultured for 48 hours in media alone or with media containing serial dilutions of each IFN ranging from 4-2000 pg/mL. Cell extracts were prepared using the provided PEB1 extraction buffer and 20μL of total cell extract added to the provided NPT II antibody-coated 96-well microtiter plate in triplicate and ELISA performed exactly as instructed by the kit manufacturer. Bound NPT II protein in each well was measured using a plate reader with a 450nm absorbance filter. Standard curves were generated and used to quantify the NPT II concentration.

Electrophoretic mobility-shift assays (EMSA).

Nuclear proteins were extracted and subjected to EMSA as previously described (Fredericksen et al., 2002). Extracts were incubated for 30 minutes at room temperature with a ^{32}P-labeled double-stranded oligonucleotide probe corresponding to the ISRE from the ISG15 promoter. Bound complexes were analyzed via native 6% Tris-glycine-polyacrylamide gel electrophoresis. Gels were dried and bands visualized by autoradiography

and quantitated using densitometry. For control samples, demonstrating that the observed shifted band represents the ISGF-3/ISRE DNA complex, we performed antibody blocking experiments by incubating IFN-α2a treated PH5CH8 nuclear extracts with 2μg anti-STAT1 or anti-IRF-9 antibody for 15 minutes at room temperature prior to addition of labeled probe.

RESULTS

Differential ISG expression induced by therapeutic IFNs

To define the response of human hepatocytic cells to clinically-relevant IFNs, we examined the induction of ISGs and IRFs after IFN treatment in Huh7 and PH5CH8 cells. Immunoblot analysis of cell lysates after 24 hours of treatment with increasing doses of IFN-α2a, PEG-IFN and CIFN revealed that CIFN treatment comparatively induced the highest expression of ISG56, ISG15 and PKR, known ISGs that impart antiviral actions against HCV or other RNA viruses **(Figure 3-1A)** (Lenschow et al., 2007; Pflugheber et al., 2002; Wang et al., 2003). Pharmacological studies have determined that the maximum IFN serum levels obtained in patients occur 2 hours following clinical dosing schedules and correspond to 130 pg/mL IFN-α2a, 320 pg/mL PEG-IFN and 80 pg/mL CIFN (C_{max}) (Tan et al., 2005). We found that maximal induction of PKR and ISG15 expression occurred at 130 pg/mL IFN-α2a, 714 pg/mL PEG-IFN and 20 pg/mL CIFN in both cell lines. In Huh7 cells induction of ISG56 was only appreciably induced at 24 hours post treatment, with 80 pg/mL of CIFN **(Figure 3-1A)**. The Huh7 and PH5CH8 cell lines were also evaluated for expression of proteins which are involved in driving IFN signaling and ISG expression. As seen in **Figure**

3-1B, after 24 hours of treatment with IFN, we observed the induced expression and similar high abundance of IRF-1, IRF-9, total STAT1 and total STAT2 within the treated cells.

Effects of CIFN Treatment on the Jak-STAT Signaling Pathway

In order to determine the mechanism by which CIFN directed enhanced ISG expression in the Huh7 and PH5CH8 cell lines, we evaluated the Jak-STAT pathway in IFN-treated cells. STAT1 is activated by IFN signaling upon phosphorylation of tyrosine 701, wherein activated STAT-1 leads to increased STAT and IRF-9 abundance (Sen, 2001). As shown in **Figure 3-2A**, treatment of cells with the C_{max} of each IFN resulted in the accumulation of active STAT1 phosphorylated on tyr-701. Treatment with CIFN induced the highest abundance of phosphorylated STAT1, with maximum levels reached at approximately 60 minutes in Huh7 cells and 30 minutes after treatment in PH5CH8 cells. There were no appreciable differences in total STAT1 levels induced among the different IFNs. We also evaluated kinetics of induction of IRF-9, observing increased expression at 240 minutes post IFN treatment with the highest levels induced by CIFN **(Figure 3-2A)**.

We also assessed the affect of the different therapeutic IFNs on the formation of ISGF3 and its DNA binding activity to the ISRE. Cells were treated with the C_{max} of each IFN and nuclear proteins evaluated for their ability to bind to the ISRE from the ISG15 promoter in an EMSA. As shown in **Figure 3-2B**, IFN treatment induced the formation of a gel-shift complex. Complex formation was abrogated by prior incubation of the reaction with antibodies specific to STAT1 or IRF9, thus defining the complex as ISGF3 (Sen, 2001). CIFN treatment of PH5CH8 or Huh7 cells respectively resulted in an approximate 10 and 50-

fold increase in ISGF3/DNA complex formation compared to nontreated cells, wherein lower levels of ISGF3/DNA complex formation were observed in cells treated with IFN-α2a or PEG-IFN. Together these results indicate that CIFN has increased signaling potency over IFN-α2a or PEG-IFN.

Therapeutic IFNs have Differential Antiviral Effects Against HCV RNA Replication

The antiviral potency of IFN has been directly linked to the strength of Jak-STAT pathway signaling (Sen, 2001), suggesting that differential signaling actions by the IFNs could impart distinct properties to limit HCV replication. We therefore assessed the antiviral actions of each IFN for their ability to suppress the replication of genetically distinct HCV 1b subgenomic RNA replicons in Huh7 cells. For these analyses we compared IFN actions within cells harboring IFN-sensitive (Huh7-K2040 cells) or IFN-resistant (Huh7-HP cells) replicon variants (Foy et al., 2003; Sumpter et al., 2004). We treated each replicon cell line with the C_{max} of the respective IFN for 24, 48 or 96 hours and evaluated host and viral protein expression in the treated cells. HCV protein levels within the Huh7-K2040 cells decreased within 24 hours of treatment with each of the IFNs **(Figure 3-3A, left panel)**, consistent with the induction of ISGs and the IFN-sensitivity of this HCV replicon variant (Sumpter et al., 2004). By contrast, our analyses demonstrated that the HCV-HP replicon was relatively resistant to IFN but that CIFN treatment suppressed the abundance of the HCV NS5A protein within 96 hours of treatment of the Huh7-HP cells **(Figure 3-3)**. Compared to the rapid but transient activation of the Jak-STAT pathway that is mediated by IFN treatment

[10], ISG expression by CIFN was maintained throughout the 96 hr treatment in association with the suppression of HCV protein abundance.

The reduction of viral protein expression by CIFN was linked to enhanced levels of ISG56 and PKR **(Figure 3-3A)**, known antiviral proteins that suppress translation from the HCV internal ribosome entry site to suppress protein synthesis and viral RNA replication (Jiang et al., 2008b; Pflugheber et al., 2002; Wang et al., 2003). We therefore evaluated the relative potency of the different IFNs toward suppressing HCV RNA replication of the different replicon variants. In the replicon system the HCV IRES directs the synthesis of the NPT II gene conferring neomycin resistance (Lohmann et al., 1999; Pflugheber et al., 2002). We therefore measured the HCV IRES-driven NPT II protein levels in cells treated with increasing concentrations (4-2000 pg/ml) of each IFN. The effective concentration of each IFN required to reduce NPT II levels by 50% (EC_{50}) after 48 hour treatments was calculated. We found that CIFN had an EC_{50} of 18.7 pg/mL in Huh7-K2040 cells compared to 37.1 and 50.9 pg/ml for IFN-α2a and PEG-IFN, respectively. The EC_{50} of CIFN treatment of the IFN-resistant Huh7-HP cells was 54.6 pg/mL compared to 169.2 pg/mL for IFN-α2a and 360.2 pg/mL for PEG-IFN treatment **(Figure 3-3B)**. These results demonstrated that CIFN has potent antiviral activity against distinct HCV RNA replicon variants and induces antiviral activity at much lower doses than treatment with IFN-α2a or PEG-IFN.

Differential Restoration of IPS-1 by IFN treatment

The difference among the IFNs to suppress HCV protein abundance could be an important determinant modulating the status of the RIG-I pathway through viral protease cleavage of

IPS-1. We therefore examined the ability of the IFNs to impart reduced viral protein expression concomitant with restoration of IPS-1 to its noncleaved, full-length form that is competent to mediate RIG-I signaling and IFN amplification (Loo et al., 2006). For these analyses we compared IFN treatment among Huh7 cells harboring distinct HCV RNA replicons of low (Huh7-L2198S) or high replication fitness (Huh9-K2040 cells) due to the presence of different adaptive mutations within their viral protein-coding region (Foy et al., 2003; Pflugheber et al., 2002). The replication fitness of the HCV replicon variants corresponded with the partial or complete proteolysis of endogenous IPS-1, respectively **(Figure 3-4)**. Following CIFN treatment IPS-1 was protected from cleavage in both HCV replicon cell lines correlating with a marked reduction in viral protein abundance. However, cleavage of IPS-1 was only minimally protected by either IFN-α2a or PEG-IFN treatment.

CIFN Regulation of HCV Infection

In order to determine how IFN impacts actual HCV infection, we examined HCV 2A JFH1 infectious virus production and viral RNA levels Huh7 cell cultures treated with the different IFNs (Cai et al., 2005). Cells were infected with HCV 2A for 24 hours before media was replaced with C_{max} concentrations of each IFN. Supernatants were harvested 24 hours after treatment and viral titer determined by focus forming assay. Total RNA from infected cells was also harvested 24 hours post-IFN treatment and HCV RNA levels quantitated using real-time RT-PCR. As shown in **Figure 3-5 (left panel)**, IFN treatment for 24 hours resulted in a significant decrease in infectious virus production that was greatest in cells treated with CIFN. In contrast, viral RNA levels remained relatively unchanged from mock-treated cells

and among the IFN treated cells after 24 hrs of treatment **(Figure 3-5, left panel)**. We determined that after 24 hours CIFN treatment resulted in an acute decrease of 94% reduction of infectious HCV 2A released into the culture supernatant as compared to parallel cultures of untreated infected cells, while viral RNA levels remained relatively unchanged at this time point.

Previous studies have shown that IFN treatment of cells induces cellular translational control programs which dominantly suppress translation from the HCV IRES (Sumpter et al., 2004; Wang et al., 2003), consistent with our observation of an acute reduction in HCV production over viral RNA abundance in the IFN-treated cells. To determine the impact of the different IFNs on HCV protein synthesis, we conducted metabolic labeling studies and anti-HCV protein immunoprecipitation analyses of infected cells cultured alone or with the different IFNs. As shown in **Figure 3-6**, 24 hours of IFN treatment rendered a specific reduction in HCV protein synthesis but had little overall effect on total cellular protein synthesis (input). The greatest suppression of viral protein synthesis was observed in cells treated with CIFN, which mediated greater than 90% decrease in the synthesis of the HCV-polyprotein and the fully processed NS5B protein as compared to their approximate reduction of 60% for IFN-α2a or PEG-IFN treatment. While HCV RNA levels decreased only modestly after 24 hours of treatment with either IFN **(see Figure 3-5)** prolonged IFN treatment through 96 hours resulted in a significant reduction of HCV RNA **(Figure 3-6, lower panel)**. These observations support previous studies indicating that IFN mediates a translational blockade of HCV replication, and suggest that prolonged suppression of viral protein abundance during IFN treatment results in an overall suppression viral RNA levels.

These results demonstrate enhanced HCV translational-suppressive properties of CIFN compared to IFN-α2a or PEG-IFN.

Gene Expression Differences between the various IFNs

To determine if CIFN conferred differential gene expression that might associate with its enhanced antiviral actions against HCV compared to IFN-α2a and PEG-IFN, genome-wide microarray analysis of the cellular transcriptome was performed following treatment of PH5CH8 cells with the different IFNs. We identified 8251 unique or redundant probe sets whose expression profile exhibited time dependent regulation by one or more of the IFNs. Using a 2-way ANOVA analysis, 86 probe sets were detected with significantly different expression levels at one or more time point following treatment with CIFN compared to IFN-α2a or PEG-IFN-α2b **(Appendix B)**. Principle Component Analysis (PCA) was used to visualize inter-sample variability associated with the expression profiles of the ISGs detected by these 86 probe sets. PCA represents an orthogonal linear transformation of expression data to a new coordinate system, reducing variance dimensionality by retaining those characteristics of the data set that contribute most to its variance. Post hoc analysis of expression at each time point was used to associate expression differences identified by the 2-way ANOVA with differences between CIFN and IFN-α2a, CIFN and PEG-IFN-α2b, or IFN-α2a and PEG-IFN. Together PCA and post hoc analysis clearly demonstrated that, at all time points examined, the transcriptional responses of human hepatocytes to CIFN is radically different from the responses to IFN-α2a or PEG-IFN treatments, which clustered similarly to each other **(Figure 3-7)**. In general, the genes observed to be differentially

regulated by microarray analysis confirm and extend the IFN-dependent expression differences characterized by immunoblot analyses. Differentially regulated genes identified by microarray analysis include products known to participate in antiviral cell signaling (JAK2, MYD88, RIG-I, IRF-7), in elaborating direct antiviral responses (OAS proteins, Mx, ISG20, RIG-I, IFIT proteins, IFI proteins) and in the adaptive immune responses (IL15RA, WARS). Additionally, many proteins of unknown function are also observed **(Appendix B)**. These observations represent the seminal analysis of IFN-induced gene expression over a time course in primary hepatocytes, thus providing insights into the hepatocyte response to different IFNs. Our results demonstrate that CIFN induces a distinct transcriptional response in hepatocytes compared to IFN-α2a and PEG-IFN.

DISCUSSION

The overall low response rate of HCV to IFN-based therapy suggests that HCV can evade or resist the antiviral actions of IFN, and that variable host responses to IFN may underlie treatment efficacy. The failure of IFN treatment has been associated with large quasi-species diversity and high viral load, suggesting that continual pressure from the host immune response may drive the outgrowth of highly fit HCV variants able to evade or resist IFN actions (Farci et al., 2002). Thus, aggressive initial treatment may be a means of increasing success of therapy by limiting the emergence of HCV 'evasion variants'. CIFN treatment of patients with relapsing HCV infection after previous standard of care treatment demonstrated that CIFN was faster than IFN-α2b plus ribavirin in the time taken to reach maximal

response rate and had a lower prevalence of relapse of infection (Miglioresi et al., 2003). In accordance with this our study provides evidence that CIFN has enhanced ability over IFN-α2a or PEG-IFN to rapidly induce the expression of ISGs known to govern HCV infection, enhance immunity, and to direct the cellular antiviral response. CIFN treatment of hepatocytic cell lines led to robust activation of the Jak-STAT signaling pathway characterized by increased levels of STAT1 phosphorylation, ISGF-3 DNA binding and ISG expression. We also observed that despite inducing robust ISG expression **(Figure 3-1)**, PEG-IFN treatment of cells rendered reduced levels of STAT1 tyr-701 and ISGF3 activation compared to CIFN **(Figure 3-2)**. These data suggest that pegylation may alter the signaling properties of IFN, and/or that other, non-canonical pathways of IFN signaling can contribute to ISG expression. Indeed, IFN treatment can trigger signaling through STAT-independent cellular pathways, including MAP kinase and PKC pathways. We speculate that signaling differences among the IFNs tested could include noncanonical IFN signaling pathways whose differential actions by CIFN might enhance the overall response to treatment.

Our study also demonstrates that CIFN has superior ability to suppress the replication of genotype 1b HCV RNA replicon variants, including the HCV-HP replicon that evolved under selective pressure from endogenous IFN to resist the antiviral actions of IFN-α2a (Sumpter et al., 2004). We showed that when all three IFNs were used at C_{max} concentrations CIFN effectively reduced viral protein levels of the highly fit HCV-K2040 and the HCV-HP replicons to an extent better than the other IFNs tested. Importantly, our data show that CIFN has increased potency compared to IFN-α2a and PEG-IFN against the HCV 2a JFH1 cell culture-infectious virus, and that overall, IFN imposes its antiviral actions against HCV by

directing a dominant blockade to viral IRES function and RNA translation. This blockade of viral RNA translation imposes limitations to HCV protein production that impart subsequent reduction of intracellular viral RNA and infectious virus production. Moreover, we found that CIFN treatment resulted in protection of IPS-1 from proteolysis by HCV through reduced levels of the viral NS3/4A protease. Therefore CIFN may provide a therapeutic benefit by restoring the function of the RIG-I pathway to amplify endogenous IFN production and direct a diverse repertoire of ISG expression, further limiting virus replication and spread (Yoneyama et al., 2004). The anti-HCV actions of CIFN occurred at lower concentrations than of IFN-α2a or PEG-IFN, suggesting that CIFN might be amenable to lower dose administration in patients to obtain similar antiviral effects.

Mathematical models derived from analyzing viral kinetics in HCV-infected patients during IFN-α therapy have shown that viral decline follows a bi-phasic pattern where the initial phase of rapid viral decline in the serum is attributed to acute blockade of de novo virus production (Neumann et al., 1998). The present study provides further support that IFN treatment mediates an acute suppression of viral RNA translation, possibly explaining the molecular mechanism of the first-phase of viral decline in treated patients. Our data show that CIFN imposed a more potent blockade of HCV protein synthesis, reducing viral protein levels to a greater extent than IFN-α2a or PEG-IFN, and ultimately suppressing viral RNA levels. Overall, our results support a model in which CIFN mediates its enhanced antiviral actions, in part, by acute induction of cellular translational control programs that disrupt viral protein synthesis, imposing limitations on viral RNA replication and infectious virus production.

CIFN binds the α/β IFN receptor with higher affinity and avidity that IFN-α2a, supporting the idea that it might trigger the intracellular signaling pathways, including the JAK-STAT pathway and other IFN-responsive pathways to mediate its distinct biological effects (Blatt et al., 1996). Our microarray analysis support these results demonstrating that while IFN-α2a or PEG-IFN induced a similar set of genes in immortalized primary human hepatocytes, the gene expression profile after CIFN treatment is quantitatively distinct. These results suggest that CIFN may impart multiple and distinct biological activities, against HCV, including the suppression of viral protein synthesis and general immune enhancement. Our findings correlate with published results from clinical studies evaluating the antiviral response of CIFN therapy in HCV infected patients. Collectively, these studies indicate that CIFN may be a useful therapeutic alternative for the effective treatment of HCV patients infected with high viral load, HCV genotype 1 or for non-responders and relapsers after standard PEG-IFN therapy (Miglioresi et al., 2003; Sjogren et al., 2007; Tong et al., 1997; Witthoeft et al., 2007; Yasuda and Miyata, 2002).

In conclusion, we have shown that CIFN exerts anti-HCV efficacy *in vitro* with higher potency compared to IFN-α2a or PEG-IFN-α2b, and that the antiviral actions of IFN against HCV are attributed in part to a dominant suppression of HCV IRES function. Our study provides evidence of the complex nature of the IFN response, wherein the induction of specific ISGs may impart differential outcome of therapy and infection. Modification of IFN therapy regimens to impart the rapid and high level expression of ISGs known to suppress HCV replication could offer therapeutic benefits to improve treatment outcome.

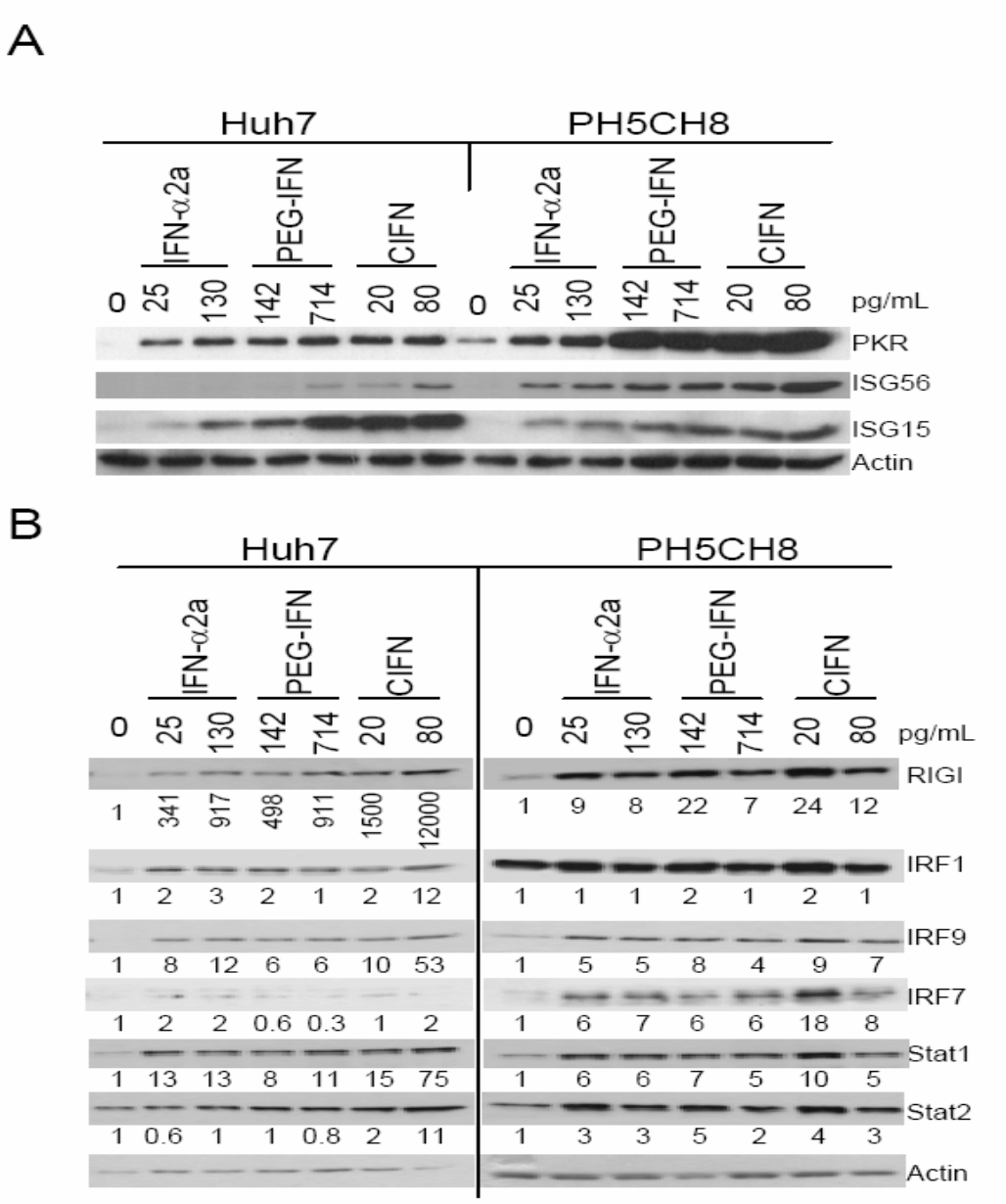

Figure 3-1. CIFN induces enhanced ISG expression. Huh7 or PH5CH8 cells were cultured for 24 hours in media alone (0) or with the indicated concentrations of each IFN (shown above each lane in pg/ml). Immunoblot analysis was conducted to evaluate the expression of ISGs, including select antiviral ISGs **(A)** or ISGs and signaling proteins involved in the IFN response **(B).** Protein expression levels were determined by densitometry analysis in which the protein levels in each lane were normalized to their respective actin control band. The fold change in protein abundance compared to the untreated control is shown under each respective lane.

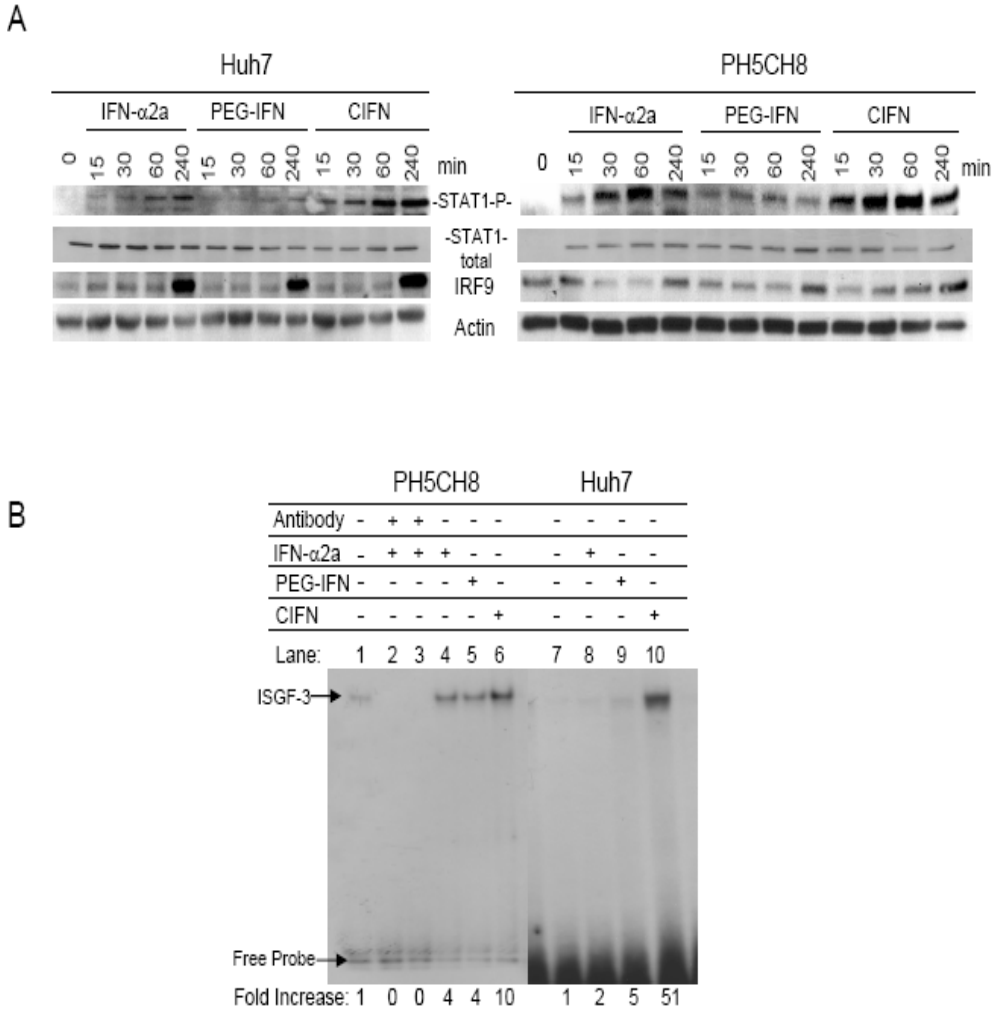

Figure 3-2. CIFN maximally activates the Jak-STAT pathway. **(A)** The abundance of phosphotyrosine 701 STAT-1 (activated STAT-1), total STAT-1 and IRF-9 was measured by immunoblot analysis after treatment with the different IFNs at the C_{max} dose for the time in minutes above each lane. Treatment of Huh7 (left panel set) and PH5CH8 (right panel set) is shown. **(B)** EMSA of the ISGF-3 transcription factor complex in PH5CH8 (lanes1-6) and Huh7 (lanes 7-10) cells treated with the C_{max} of each IFN for 30 minutes. Arrows indicate the positions of the unbound probe and ISGF-3 complex, as shown by IRF-9 and Stat1 antibody blocking analysis. Densitometry analysis was used to quantitate bands corresponding to the ISGF-3 complex, displayed as fold-increase relative to the untreated controls which were set to 1 (lanes 1 and 7). Results shown are representative of three independent experiments.

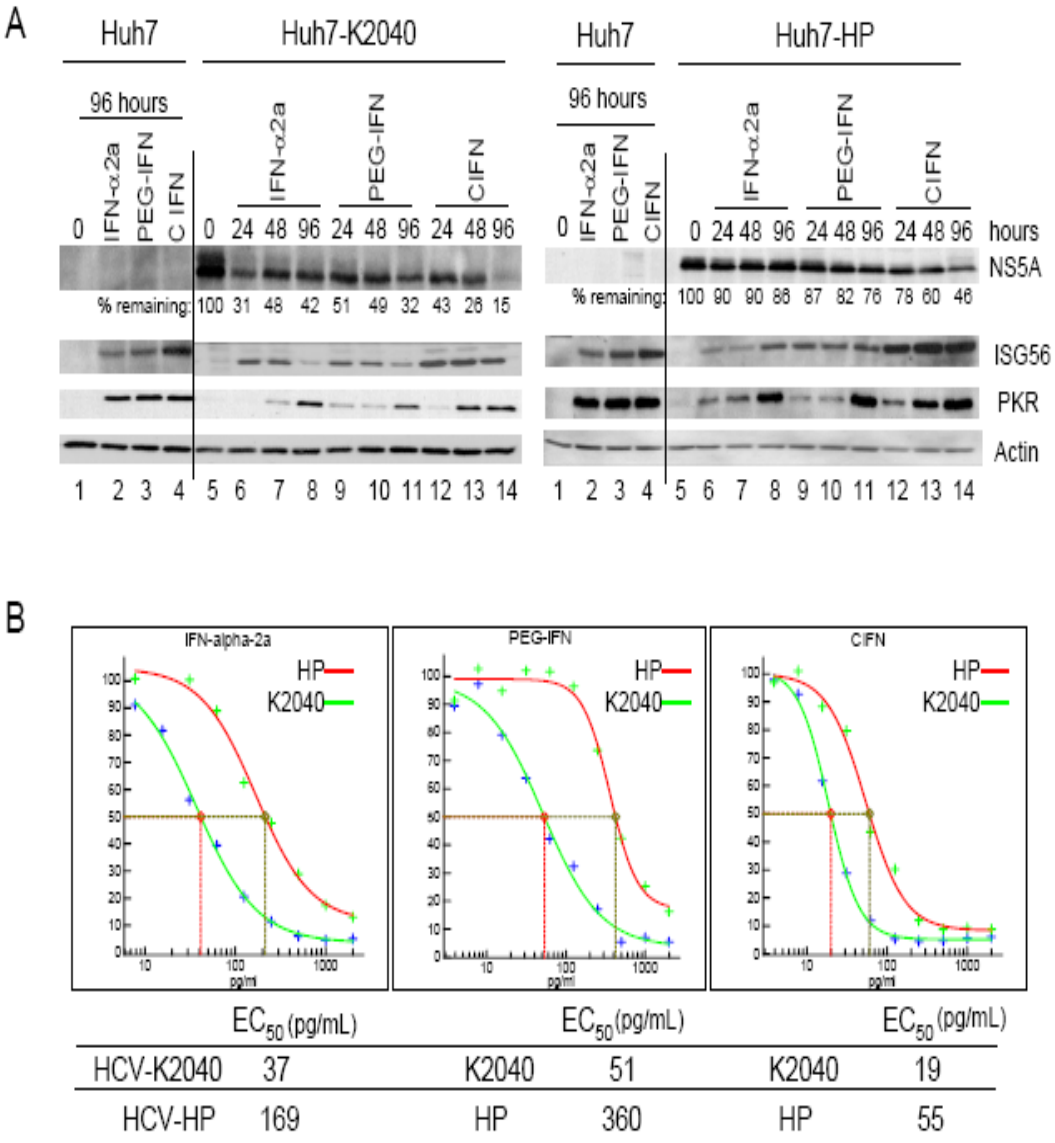

Figure 3-3. Comparison of the antiviral effects rendered by the IFNs on HCV RNA replicon containing cells. **(A)** Immunoblot analysis of Huh7 cells (lanes 1-4 on both panels) and Huh7 cells harboring the HCV RNA replicons after incubation with the C_{max} of each IFN for the indicated times. HCV NS5A protein levels were quantified by densitometry analysis and the values are displayed below the corresponding lane as a percentage of the protein within matched control cells cultured with media alone. Control values from nontreated cells were set at 100%. **(B)** ELISA of NPT II protein levels from HCV-K2040 (green) and HCV-HP (red) IFN treated cells. The calculated EC_{50} of each IFN is displayed under the corresponding graph. Data are representative of three independent experiments.

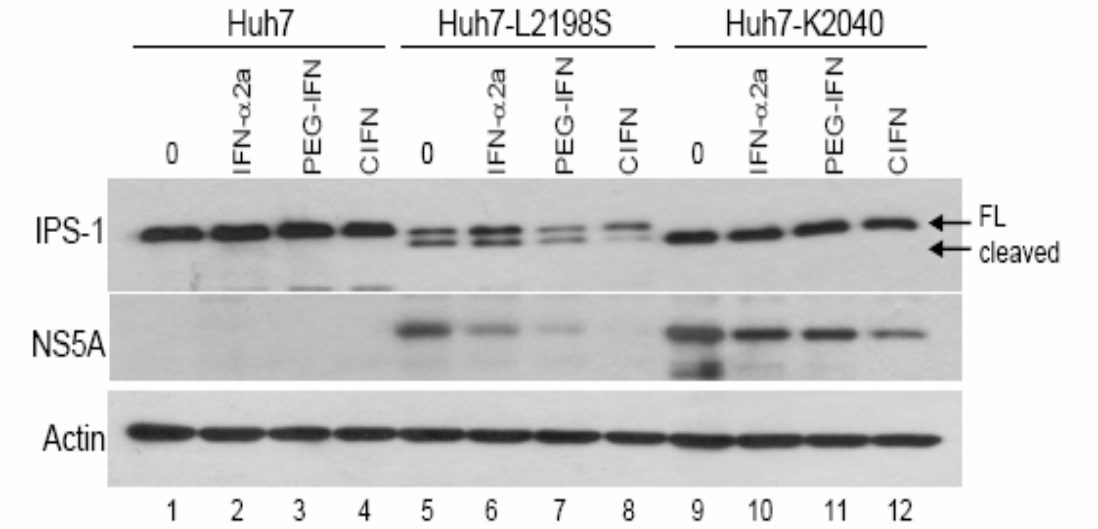

Figure 3-4. CIFN treatment protects IPS-1 from cleavage by the HCV-NS3/4A protease. Immunoblot analysis of endogenous IPS-1, NS5A and actin expression in control Huh7 cells (lanes1-4), Huh7-L2198S cells (lanes 5-8) and Huh7-K2040 cells (lanes 9-12) cultured with media alone (0) or C_{max} of each IFN for 72 hours. Arrows denote the full length (FL) and cleaved forms of IPS-1.

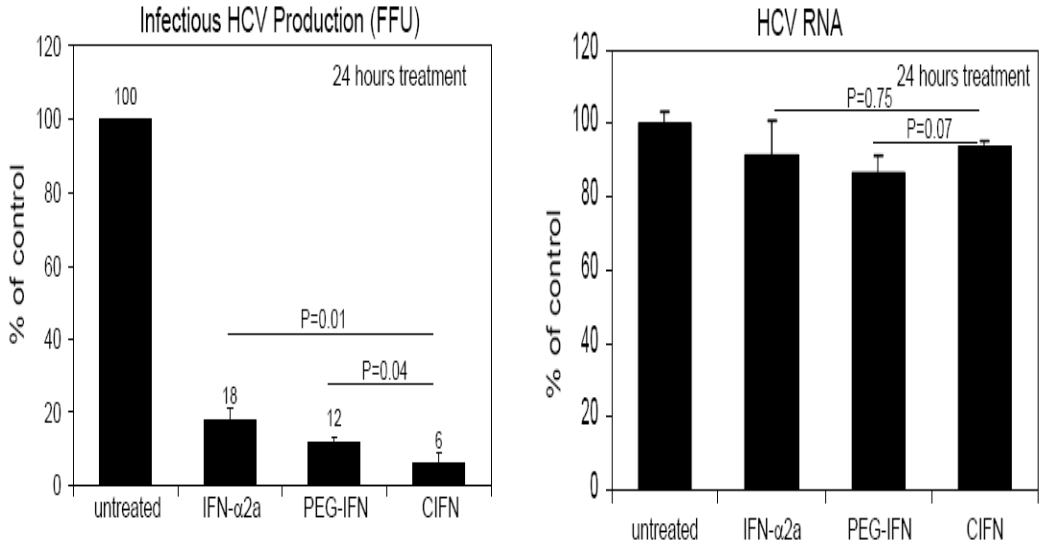

Figure 3-5. CIFN exhibits enhanced antiviral efficacy against the HCV 2a infectious clone. Huh7 cells were infected with HCV 2a at an MOI of 1. 24 hours later media was replaced with fresh media alone (nontreated) or with fresh media containing the C_{max} of each IFN. After a further 24 hours the viral titer was assessed by focus forming assay. Results are the mean number of infected foci (ffu) ±SD expressed as a percent of the untreated control **(left panel)**. The right panel shows % decrease of HCV RNA, 24 hours post-treatment, as compared to untreated samples with GAPDH mRNA levels used as an internal standard. Results are representative of two independent experiments conducted in triplicate.

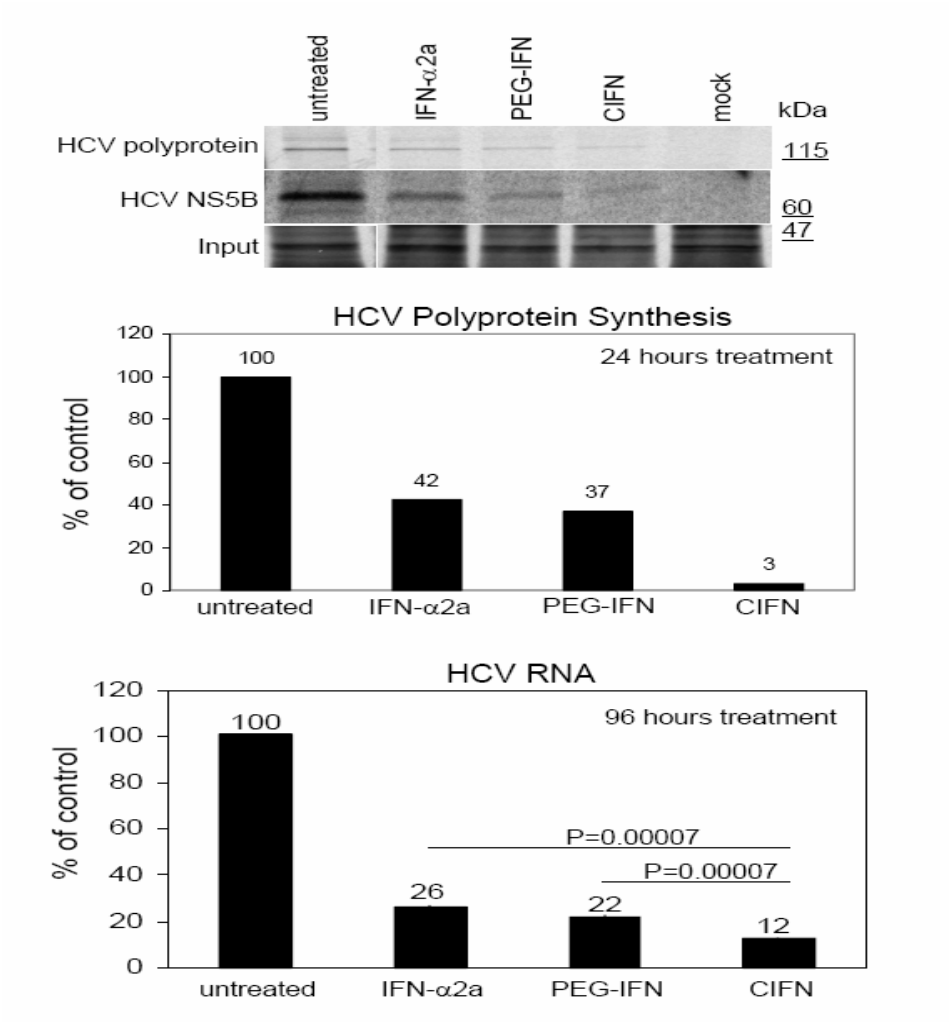

Figure 3-6. Cellular and viral protein synthesis. Huh7.5 cells (mock) and HCV 2a-infected Huh7.5 cells were cultured for 24 hours in the presence of the C_{max} of each IFN followed by [^{35}S]methionine pulse-labeling for 1 hour. The bands shown were selected from the autoradiogram from SDS-PAGE analyses of the total cellular proteins (input) and HCV proteins (polyprotein and NS5B) recovered from cell extracts by immunoprecipitation. The incorporation of radiolabel into the HCV-polyprotein was quantified and values displayed as a percentage of the untreated sample, set to 100%. Molecular masses, in kDa, are indicated on the right side of the autoradiogram. HCV RNA levels were assessed after a continued IFN treatment of 96 hours by quantitative real-time RT-PCR and are presented as the percentage HCV RNA remaining relative to the untreated control **(lower panel**). The error bars represent the standard deviation of the means of HCV RNA levels from triplicate samples. P values denote significant reductions in CIFN treated samples compared to IFN-α2a or PEG-IFN treated samples (Student's t-test). Results are representative of two independent experiments.

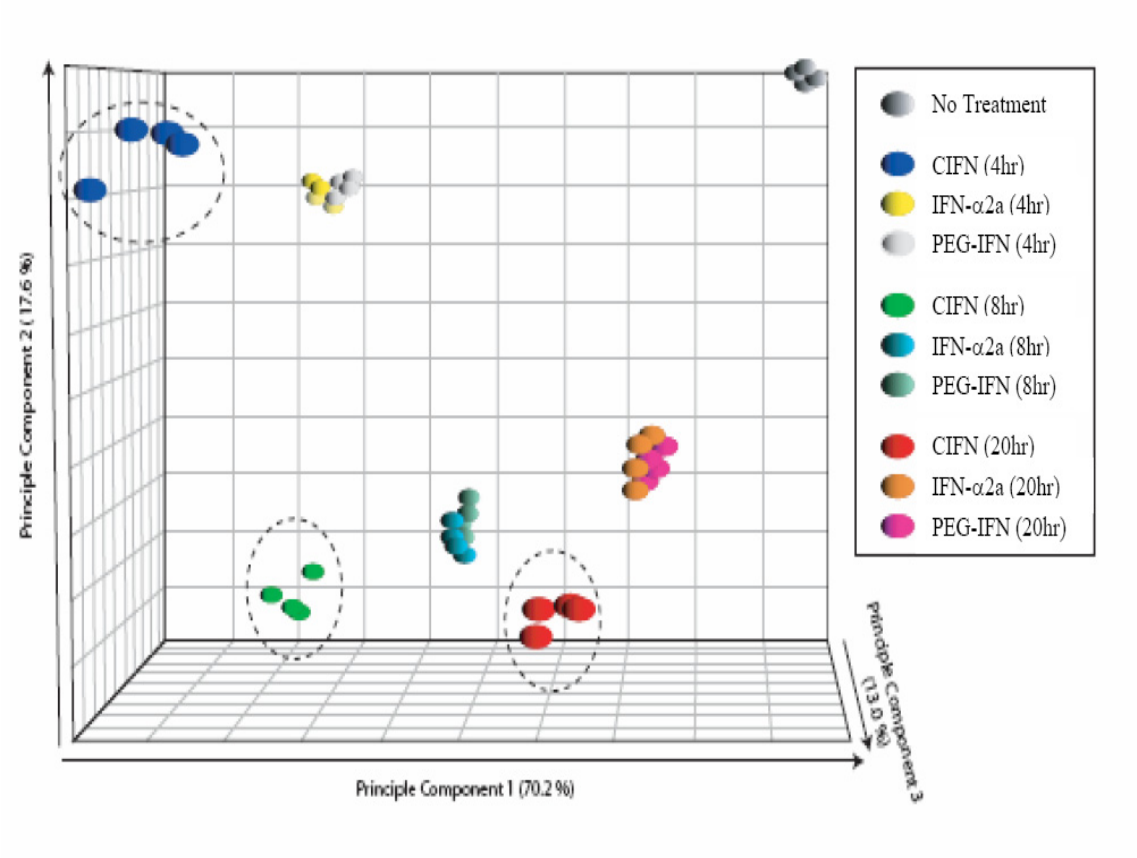

Figure 3-7. ISG expression induced by CIFN in human hepatocytes is distinct from IFN-α2a and PEG-IFN. The figure shows Principle Component Analysis (PCA) of the IFN-regulated transcriptome from PH5CH8 cells that were cultured in the presence of media alone (CTRL) or media containing the C_{max} of each IFN for 4, 8 or 20 hours as indicated. The greatest determinant of inter-sample variance lies on the X coordinate (the first principal component), the second greatest variance on the Y coordinate (the second principal component), and the third greatest principle component on the Z coordinate. Higher-order principal components contributing less to intersample variability are ignored.

CHAPTER FOUR
A novel OAS1 variant has distinct antiviral functions associating with resistance to HCV infection in vivo

INTRODUCTION

Hepatitis C virus (HCV) establishes a chronic infection in the majority of infected individuals and is a major cause of liver disease worldwide (Shepard et al., 2005). HCV persistence occurs in about one-half of all patients treated with the current IFN-based regimens. Although viral and host determinants have been implicated in treatment failure, there are no definitive predictors of response outcome (reviewed in Yee, 2004))(Muir et al., 2004). Injection drug use is currently the most common risk factor and mode of HCV transmission. Rates of HCV infection among intravenous drug users (IVDUs) has been reported to be as high as 90% with infection rapidly acquired after initial drug use (Ting Zhang, 2006). In order to identify host factors that protect against HCV infection we used a genetic-based screen of IVDUs who were at a high-risk for HCV exposure, yet remained HCV-seronegative. We identified polymorphisms in the oligoadenylate synthetase gene 1 (OAS1) derived allele, 1D1, that associate with resistance to HCV infection in a recessive genetic manner (Magness, CL et al., in preparation).

The oligoadenylate synthetases (OAS) are a highly conserved family of interferon induced proteins encoded by four genes, OAS1-3 and OAS-like (OASL), located on chromosome 12. Alternative splicing events lead to the expression of multiple OAS isoforms including OAS1 (p42/44/46/48/52), OAS2 (p69/71) and OAS3 (p100) (Justesen et al., 2000).

These OAS variants have differential subcellular localization, cell type expression, and OAS enzymatic activity (Bonnevie-Nielsen et al., 2005; Rebouillat and Hovanessian, 1999). In the presence of dsRNA, the OAS proteins become enzymatically active resulting in the synthesis of 2'-5' linked oligoadenylate chains (2-5As) from ATP (Kerr and Brown, 1978). In turn, 2-5As can bind to the latent ribonuclease L (RNase L) leading to its dimerization and activation. Activated RNase L degrades viral and cellular RNA, directly inhibiting protein synthesis and viral growth, while also amplifying IFN-α/β production through signaling of the retinoic acid inducible gene-I (RIG-I) antiviral pathway (Floyd-Smith et al., 1981; Malathi et al., 2007; Wreschner et al., 1981). Antiviral actions of the OAS1 isoforms independent of OAS activity and RNase L activation have been demonstrated. For example, in mice, OAS1b confers resistance to West Nile virus and other flaviviruses by an undetermined mechanism (Scherbik et al., 2006). Expression of OASL is highly induced by IFN in primary hepatocytes however, the protein lacks enzymatic activity and the function of OASL is unknown **(Appendix B)** (Hovnanian et al., 1998) (Rebouillat et al., 1998).

HCV is an enveloped virus containing a single-stranded positive sense RNA genome of approximately 9.6 kb. The HCV 5'-nontranslated region encodes an internal ribosome entry site (IRES) which directs cap-independent translation of a single polyprotein that is posttranslationally processed to the mature structural and functional viral proteins. The HCV IRES and 5' NTR consist of regions of extensive double-stranded RNA structure that are required for viral protein synthesis(Honda et al., 1999). HCV RNA replication is thought to occur with the assembly of viral RNA and nonstructural proteins into a replication complex on modified cellular membranes(Egger et al., 2002; El-Hage and Luo, 2003). We previously

reported that HCV RNA replication requires geranylgeranylation of the host protein FBL2 and its subsequent binding to the HCV NS5A protein (Ye et al., 2003). Furthermore, we found that the p46 variant of OAS1 which contains a putative geranylgeranyl site (CTIL), also binds NS5A, albeit at lower levels than FBL2 (Wang et al., 2005).

The present study was undertaken to assess the biological and functional relevance of the OAS1 1D1 allele in resistance to HCV infection. A single-base mutation in the OAS 1D1 allele leads to the expression of a truncated OAS1 variant (p42) that lacks the carboxy-terminal CTIL sequence. Using molecular assays and our HCV cell-culture infectious systems we demonstrated that the absence of the geranylgeranyl site in the OAS1 p40/42 isoform results in distinct molecular functions of the protein that act to inhibit HCV replication and spread through dominant suppression of HCV-IRES mediated viral translation. Herein, we supply evidence for the potential applicability of a recombinant drug form of OAS1 p40 as a novel therapeutic to combat HCV infection.

MATERIALS AND METHODS

Cell Culture and Drug Treatments

Huh7, Huh7.5 (gift from C. Rice) and Huh7-HCV RNA replicon containing cells are human hepatoma derived cell lines and were propagated as previously described (Blight et al., 2002; Sumpter et al., 2005). HeLa cells were purchased from ATCC. Purified recombinant protein drug forms of IB657 were produced using an E. coli directed expression of human OAS1 essentially as described in provisional patent application No. 20080038753. For treatments with IB657 and mutant IB657 drugs, cells were cultured for the indicated times with medium

containing either buffer alone (at μL amounts equal to highest μL of IB657 in each experiment), the indicated concentrations of IB657 or the mutant IB657 proteins and IFN-α2a (PBL Laboratories). For geranylgeranyl inhibitor experiments 10^6 lymphoblast cells were seeded in 5mL of media and treated with 10 U/mL IFN-α alone or in addition to 10 μM GGTI-286 (Lerner et al., 1995) for 24 hours. Cells were pelleted, washed with PBS, and fractionated into cytosolic (0.2% spooning soluble) and membrane (PBS/1% Triton X-100 soluble) fractions. $3x10^5$ cell equivalents were loaded on a 12.5% Tris-Lysine gel and separated by electrophoresis for 50 minutes at 200V. The proteins were transferred and subjected to immunoblot analysis for OAS1 expression.

Plasmids and Transfections

Expression constructs encoding the OAS1 variants; p40, p42, p46, p40+CTIL, p42+CTIL, and p46 with the CTIL mutated to STIL by site-directed mutagenesis were generously provided by Kineta, Inc. and were subcloned into the 5'XhoI and 3'XbaI multiple cloning sites in the $pCMVT_NT$ (Promega) expression vector. Huh7.5 cells were plated at $2x10^4$ cells per well of 4-chamber slides and 24 hours later cells were transfected with 500 ng of the indicated expression plasmids using FuGENE 6 (Roche Applied Science). After an additional 24 hours, cells were infected with HCV 2a (MOI of 2) for 48 hours when cells were fixed, permeabilized, and IFA performed exactly as described in Chapter 2.

HCV Assays

Quantitative RT-PCR (qRT-PCR), ^{35}S metabolic labeling studies, and anti-HCV protein immunoprecipitation analyses were performed exactly as described in Chapter 2. For determination of IC_{50} values $2x10^4$ naïve Huh7.5 cells were infected with HCV 2a at an MOI of 0.5 and 4 hours later, cells washed and cultured with media containing the indicated concentrations of IB657 or buffer in triplicate for 48 hours and the number of infected foci determined by FFA. In HCV 1a experiments, Huh7.5 cells were transfected with in vitro transcribed HCV 1a RNA for 72 hours prior to drug treatments. For IB657 and IFN cotreatments, $6x10^4$ cells/4-chamber well of HCV 2a-infected cells (MOI of 2 for 24 hours) or HCV 1a-transduced cells were cultured with media containing buffer, 2 μM IB657, 25 U/mL IFN-α2a or 2 μM IB657 and 25 U/mL IFN-α2a for 72 hours. The percentage of HCV 2a-infected cells was determined by IFA, in which the total number of cells were determined by DAPI staining and the number of HCV infected cells was counted in six representative fields. The number of HCV 1a infected cells was determined by counting the total number of infected cells per 4 chamber well in triplicate wells.

Antibodies

Dilutions for primary antibodies were, 1:1000 for anti-HCV (from Dr. W Lee), 1:500 for N-RIG, gift from T. Fujita (Yoneyama et al., 2004), 1:200 for anti-OAS (a gift from Kineta, Inc.), 1:1000 for anti-neomycin phosphotransferase II (NPT II) (Cortex Biochem) and 1:500 for anti-GAPDH (Santa Cruz Biotechnology). Primary antibodies were used in combination with 4'-6-Diamidino-2-phenylindole (DAPI) and the appropriate Alexa 488- or Alexa 594-conjugated secondary antibodies (1:500) (Invitrogen) for IFA, and anti-human, anti-goat

(Jackson Laboratories) or anti-mouse (PerkinElmer Life Sciences) horseradish peroxidase-conjugated secondary antibodies (1:1000) for immunoblot analysis.

Gel Mobility Shift Analysis

HCV 5'UTR RNA was synthesized from the ~500bp SexAI/EcoRI restriction fragment of pJFH-1 using the T7 Megascript kit (Ambion). Probes were labeled by incubating 5 μmol HCV RNA, 35 μg polyIC RNA or 5 μmol dsDNA template from pCDNA3.1 with 32P-γATP, and T4 Kinase (GibcoBRL) for 30 min at 37°C. Binding reactions containing purified, labeled probes and the indicated concentrations of IB657 or 2 μM IB657-DAD or Triple cysteine mutant proteins were performed as described (Fredericksen et al., 2002). For competition experiments cold HCV 5'NTR RNA was pre-incubated with IB657 for 15 minutes at 30°C prior to addition of the probe. Protein-RNA complexes were resolved via native 6% Tris-glycine-PAGE. Gels were dried and bound complexes visualized by phosphorimaging.

OAS/RNase L assays

Purified OAS proteins, IB657 and the IB657-DAD mutant were used in OAS high performance liquid chromatography (HPLC) activity assays as previously described (Sarkar and Sen, 1998). For RNase L assays 10^6 HeLa cells were cultured with DMEM alone or with DMEM containing 2 μM IB657 for 4-16 hours. The cells were washed and transfected with 2 μg/well of HCV 2a RNA transcribed in vitro or polyIC using the Transmessenger RNA transfection reagent (Qiagen). Cells were harvested 4 hours after transfection and total

RNA extracted using Qiagen's RNeasy Mini kit following the manufacturer's protocol. RNA was separated by electrophoresis in 1% agarose gels containing 0.1 μg/mL ethidium bromide and visualized using UV light.

Dual-luciferase assay

Luciferase analysis for simultaneous assessment of cap- and HCV IRES-dependent translation was performed as described previously (Wang et al., 2003). Briefly, Huh7.5 cells were cotransfected with 250ng of the bicistronic reporter plasmid pRL-HL (Honda et al., 1999) and the indicated amounts of pCMV-p40. For drug treatments, 24 hours after transfection, culture media was replaced with media containing 50 U/mL of IFN-α2a or the indicated concentrations of IB657. After a further 48 hours, cells were harvested and total RNA extracted for quantitative real-time PCR (qRT-PCR) or extracts prepared for dual luciferase assay (Promega). The primer pairs used for detection of firefly luciferase and GAPDH RNA are available upon request. Relative mRNA expression levels were determined by one-step qRT-PCR calculated using the comparative cycle threshold (CT) method with human GAPDH as the internal standard exactly as described in Chapter 2.

G418 Killing Assay

Huh7-K2040 replicon cells were plated at 10^5 cells per 6 well. After a 24 hour recovery, cells were cultured with medium containing buffer, IB657 or IFN with or without 5μg/mL G418 (Sigma) was added. After 72 hours of treatment, 250 μl of trypsin was added to each well to release the cells from the plate, followed by addition of 750 μl of culture media to stop

trypsinization. Trypan blue was added to 100 µl of each sample and the number of living cells in 10 µl from each sample was counted using a hemacytometer, repeated four times for each sample. The remaining 900 µl of cells was pelleted and used for immunoblot analysis evaluating NPT II, HCV and GAPDH protein levels in equivalent cell numbers.

Viruses

For West Nile Virus (WNV) infections Huh7 cells were pretreated with increasing concentrations of IB657 for six-eight hours, followed by infection with WNV strains, Madagascar 78 (MAD78) or Texas-02 at an MOI of one for 24-40 hours. Infectious virus production in MAD78 infected cells was measured using plaque assay on Vero cells as previously described (Keller et al., 2006). Viral protein levels after treatment were assessed using immunoblot analysis for WNV viral proteins. Similar viral assays were performed to evaluate the affect of IB657 on Influenza A Virus, Respiratory Syncytial Virus (RSV) and Encephalomyocarditis Virus (EMCV) replication and spread, infectious virus production, viral protein expression and cellular cytopathic effects (CPE) (Iadonato, personal communication).

RESULTS

Patient Study

Case subjects were enrolled with the criteria that they were HCV antibody negative, had injected drugs for ten years or more, and had increased risk for HCV exposure due to behavioral factors such as needle sharing. Control subjects who were either HCV antibody

or RNA positive were gender- and ethnically-matched to the HCV seronegative case subjects. A total of 86 control and 33 case subjects were enrolled. Case subjects were monitored for an average of 15.5 months after enrollment for subsequent HCV seroconversion, with three of 26 becoming HCV antibody positive and reclassified as control subjects. HCV viral genotype and load was assessed on 61 of the control subjects. It was found that around 75% of the control subjects were infected with HCV genotype 1. Approximately 20% of the control subjects had no detectable serum HCV RNA, suggesting spontaneous viral clearance. Results from the patient study indicated that the case subjects remained HCV seronegative despite having at least as great of risk for contracting HCV as the HCV antibody positive control subjects **(Table 4-1)**. Genomic DNA from each of the case and control subjects was used for sequencing of the OAS genes on human chromosome 12. The locations of the polymorphisms identified in the OAS1 gene are shown in **Figure 4-1a**. Genetic analyses of these mutations in the Caucasian reference panel revealed that the OAS1 derived allele 1D1 occurs more frequently in case subjects than controls as a result of significantly more homozygote carriers in the case subjects (26% vs 5%, Fisher exact test, p=0.015) **(Table 4-1)**. To note, the Caucasian reference panel was the only ethnically distinct population of sufficient size to perform these genetic analyses. Together these results demonstrated that the OAS1 allele 1D1 is associated with persistently HCV-negative serostatus in a recessive genetic fashion (Magness, CL et al., in preparation).

A single nucleotide polymorphism in OAS1 associates with HCV resistance

Of the mutations identified in the OAS1 1D1 allele the single-base mutation rs10774671 (G/A) **(Figure 4-1a-highlighted in red)** has the most compelling functional effects, where it was previously shown to control splicing events leading to the expression of either the p42 or p46 OAS1 variants (Bonnevie-Nielsen et al., 2005). To verify this differential expression OAS1 expression in IFN-α (100 U/mL) treated lymphoblasts from subjects homozygous and heterozygous for the 1D1 or the ancestral, 1A1, alleles was examined. It was found that expression of p42 is directly correlated with genotype for rs10774671 (**Figure 4-1b**). **Figure 4-2** depicts the OAS1 isoforms p46 and p42; with the terminal translated amino acid sequences shown below. The underlined CTIL peptide sequence in p46 is a putative signal for geranylgeranylation (Reid et al., 2004). The absence of the CTIL site in the OAS1 isoform p42 was of particular interest due to our previous findings that inhibition of geranylgeranylation of host proteins disrupts HCV RNA replication (Wang et al., 2005; Ye et al., 2003). It has been demonstrated that the attachment of geranylgeranyl groups to cellular proteins anchors them to membranes (Goldstein and Brown, 1990). Therefore we evaluated the subcellular localization of the OAS1 variants, p42 (lacks CTIL sequence) and p46 (contains CTIL sequence). Lymphoblasts from individuals homozygous for the 1D1 (p42) or 1A1 (p46) OAS1 alleles were treated with IFN-α alone **(Figure 4-3a)** or IFNα and the geranylgeranyl transferase I inhibitor (GGTI-286) **(Figure 4-3b)**. The cells were harvested and fractionated into cytosolic (soluble) and membrane fractions. Cellular fractions were then subjected to electrophoresis and immunoblot analysis using a monoclonal antibody specific to OAS1. As shown in **Figure 4-3**, p46 is mainly localized to the membrane-bound cellular

fractions and inhibitor treatment resulted in re-localization of p46 primarily to the cytosolic fractions, similar to the distribution of the p42 isoform which is localized to the soluble fractions with or without GGTI treatment. Therefore the rs10774671 mutation controls both OAS1 isoform p42 production and cellular localization.

To determine if altered subcellular localization of the p42 OAS1 isoform resulted in distinct antiviral actions, the HCV-infectious cell culture system was utilized. Using Immunofluorescence microscopy (IFA), human hepatoma derived cells (Huh7.5) were monitored for HCV 2a infection of cells expressing plasmids encoding the OAS1 isoform p46, p46 with the geranylgeranylation site mutated (p46-STIL), p42, the truncated p42 sequence lacking the intron 5 nucleotides **(p40, Figure 4-2)**, and p40 or p42 with the CTIL sequence engineered into the carboxy-terminus (p40+CTIL, p42+CTIL). As with fractionation studies presented in **Figure 4-3**, we found differential cellular distribution of the OAS1 variants. Proteins containing the CTIL motif (p46 and p40/42 + CTIL) were localized to the perinuclear regions with punctate staining patterns throughout the cell **(arrows in Figure 4-4a, top panel)**. However, mutation of the CTIL sequence or its absence resulted in a more diffuse localization, often with the formation of large vacuoles within the cell cytoplasm **(arrows Figure 4-4a, lower panel)**. Nuclear OAS staining was observed in many transfected cells with no correlation to the presence of the CTIL motif, consistent with previous reports identifying both p40/46 isoforms in the nuclei of fibroblasts (Chebath et al., 1987). When expressed in Huh7.5 cells, the OAS1 variants, p40, p42 and p46-STIL, or constitutively active RIG-I (N-RIG) inhibited HCV 2a infection as demonstrated by a dramatic decrease in the percentage of infected cells as compared to dsRED transfected

control cells **(Figure 4-4c)**. Also, we observed exclusion or decreased expression of HCV proteins (green) in transfected cells (red) **(Figure 4-4b, p42 and p40 panels)**. However, OAS1 variants containing the CTIL peptide sequence had decreased ability to inhibit HCV 2a infection with an increased percentage of infected cells as compared to the wild-type counterparts **(Figure 4-4b and c)**. We also observed apparent co-localization of p46 with HCV proteins, consistent with its ability to bind NS5A **(Figure 4-4b, p46 and p42+CTIL panels)** (Wang et al., 2005). Collectively, these results demonstrate that the single-base mutation in the human OAS1 derived allele 1D1 has functional biological effects that restrict HCV infection.

IB657, a recombinant OAS1 protein

In order to more fully evaluate the biological activity of the human OAS1 ID1 allele, recombinant proteins were produced from the p40 sequence (IB657), the p40 sequence harboring mutations in the OAS enzymatic active site, D74A and D76A, (DAD-mutant) as well as a triple cysteine mutant that abolishes cell entry (C24S, C37S, C53S) as a negative control **(Figure 4-2)**. Coomassie staining of the purified IB657 protein showed a single band with apparent molecular mass of 40 kDa **(Figure 4-5a)**. Previous studies demonstrating cellular uptake of large polybasic proteins in vivo and the consistent detection of OAS in the serum of IFN-treated patients (Murashima et al., 2000; Solinas et al., 1993) prompted us to determine the ability of IB657 to be taken up by human hepatoma cells (Schwarze et al., 1999). To detect intracellular IB657, we performed IFA on Huh7 cells that were cultured in media containing buffer or IB657 for 24 hours, trypsinized to remove any surface associated

protein, replated in 4-chamber well slides and 24 hours later immunostained with a monoclonal antibody raised against the p40 sequence (anti-OAS) and Alexa-594 conjugated anti-mouse secondary **(red staining, Figure 4-5b)**. Immunoblot analysis of extracts from IB657 treated HCV 2a infected Huh7 cells for 72 hours confirmed the presence of IB657 in human hepatoma cells **(Figure 4-6c)**. Furthermore, we found that IB657 treatment of HCV 2a infected-Huh7.5 cells for 24 hours suppressed HCV infection as demonstrated by reduced viral spread and complete exclusion of viral protein expression (green) in cells containing IB657 (red) **(Figure 4-5C)**. In order to ensure that IB657 treatment does not result in cellular cytotoxic effects or apoptosis, numerous human cell lines were treated with 0-15 μM IB657 for 24 hours and MTS or caspase 3/7 activation evaluated. No evidence of cytotoxicity or apoptosis was found **(Table 4-2)**. These results illustrate the potential utilization of IB657 as a novel antiviral therapeutic agent.

Antiviral activity of IB657 against HCV

To assess the ability of IB657 to inhibit HCV 2a replication and spread, HCV 2a-infected Huh7.5 cells were cultured with media containing buffer or increasing concentrations of IB657, and the number of HCV infected foci determined after 48 hours. As shown in **Figure 4-6a,** IB657 treatment suppressed HCV 2a infection in a dose dependent manner, with 50% inhibitory concentrations (IC_{50}) ranging from 1.3-2.4 μM, depending on lot of recombinant protein used. Pretreatment of cells with IB657 for 24 hours prior to infection had a similar inhibitory effect on HCV 2a infection (data not shown). In order to determine the ability of IB657 to inhibit infectious virus production, Huh7.5 cells were infected with HCV 2a at

various multiplicities of infection (MOIs). Infection was allowed to proceed for 24 hours, then fresh media containing buffer or 4 μM of IB657 was added to the cell cultures. After an additional 24 hours, cultures were washed and fresh media without drug was added. Viral titers in the drug-free supernatants were assessed 24 hours later. IB657 treatment resulted in approximately a 5-fold decrease in infectious virus production as compared to buffer treated control samples **(Figure 4-6b)**. To further characterize the antiviral effects of IB657 on HCV infection, we evaluated viral protein levels after 72 hours of treatment using immunoblot analysis. As shown in **Figure 4-6c**, IB657 treatment of HCV2a-infected Huh7.5 cells resulted in a dose-dependent decrease of HCV NS5A protein levels.

HCV genotype 1 is the predominant HCV genotype circulating in the western hemisphere, which is problematic due to its ability to resist the antiviral actions of IFN (Fried et al., 2002). Therefore we evaluated the ability of IB657 to suppress replication and spread of an infectious genotype 1a clone. Huh7.5 cells were transfected with RNA corresponding to the HCV 1a sequence, and 72 hours later, the cells were treated with increasing concentrations of IB657. We found that IB657 treatment inhibited HCV 1a replication and spread in a dose dependent manner **(Figure 4-7)**. The current standard of care for HCV infection is IFNα-based therapy, therefore, we evaluated the ability of IB657 to augment the anti-HCV actions of IFNα against the IFN-sensitive genotype 2a virus or the IFNα-resistant HCV 1a virus. We found that IB657 and IFNα co-treatment of HCV 2a-infected Huh7.5 cells resulted in around a 90% decrease in the number of HCV infected cells as compared to around a 60% decrease with IB657 or IFNα treatment alone **(Figure 4-8, left panel)**. Furthermore, the combination of IB657 and IFNα treatment of HCV 1a-infected cells lead to

an 80% decrease in the percentage of infected cells, substantially increasing the antiviral effects of IFNα which alone only decreased HCV 1a replication and spread by about 30% as compared to buffer treated control cells **(Figure 4-8, right panel).**

IB657 and the OAS/RNase L antiviral pathway

As described above, IB657 was produced from the sequence of a naturally occurring truncated OAS1 isoform. Although all the OAS genes encode the antiviral effector enzyme 2',5'-oligoadenylate synthetase, not all OAS isoforms are enzymatically active (Justesen et al., 2000). Therefore we assessed the synthetase activity of IB657 in the presence of polyIC and HCV RNA. We demonstrated that IB657 has functional, dsRNA dose-dependent, OAS enzymatic activity **(Figure 4-9a)**. To determine if the OAS synthetase activity of IB657 is necessary for the observed anti-HCV actions, we utilized the IB657-DAD mutant protein, which lacks synthetase activity upon polyIC stimulation **(Figure 4-9a)**. HCV 2a-infected cells were treated with buffer, 4 μM IB657, the IB657-DAD mutant, or the IB657-triple cysteine mutant for 48 hours and HCV infection levels were quantified by focus forming assay. As shown in **Figure 4-9b**, the IB657-DAD mutant protein efficiently suppressed HCV replication and spread by ~50% as compared to buffer treated control cells. These results demonstrated that the OAS enzymatic activity of IB657 is dispensable for its antiviral actions against HCV. To determine if the altered biological functions of IB657 result in direct activation of endogenous RNase L, we treated HeLa cells with IB657 alone or in the presence of HCV and polyIC RNA. We found that IB657 alone does not lead to cleavage of rRNA bands and does not increase the amount of rRNA cleavage after transfection with

polyIC or HCV RNA **(Figure 4-9c)**. Together these results suggest that IB657 inhibits HCV infection independent of the OAS/RNase L antiviral pathway.

IB657 suppresses HCV protein translation

The ability of IB657 to inhibit HCV replication and spread, independently of its OAS enzymatic activity, led us to determine at which step in the viral life cycle the drug is acting. The HCV genome consists of a positive-sense RNA molecule that, upon entry into the host cell, is directly translated by a cap-independent mechanism involving the HCV IRES (Tsukiyama-Kohara et al., 1992). Translation of the viral proteins is essential for replication of the viral genome and for inhibition of the cellular immune response. Therefore we assessed de novo viral protein synthesis using metabolic labeling studies and anti-HCV protein immunoprecipitation analyses of HCV 2a infected-Huh7.5 cells after treatment with buffer (48 hours), IB657(24 and 48 hours) or 50U/mL IFNα (24 hours). As shown in **Figure 4-10**, IB657 treatment rendered a pronounced reduction in total HCV protein synthesis, with a greater than 60% decrease in the HCV-polyprotein levels as compared to the buffer treated control cells **(Figure 4-10b),** a similar reduction was found in the levels of NS3, NS5A, NS5B and core HCV proteins. Total RNA from parallel cultures of infected/treated cells was harvested and HCV RNA levels quantified using real-time reverse transcription-polymerase chain reaction (qRT-PCR). We found no significant changes in viral RNA levels in cells cultured with IB657 as compared to buffer-treated control cells **(Figure 4-10c)**. These results indicate that IB657 reduces HCV protein synthesis without affecting RNA levels.

IB657 suppresses HCV IRES directed translation

Due to our findings that IB657 suppresses de novo viral protein synthesis and is enzymatically activated in the presence of HCV RNA and polyIC, we evaluated the ability of IB657 to bind to dsRNA regions containing the HCV IRES. Gel-shift assay was performed with ^{32}P end labeled-polyIC or HCV RNA corresponding to the 5' NTR of HCV. As shown in **Figure 4-11**, IB657 efficiently binds to polyIC (lane 8) and HCV 5' NTR RNA in a dose-dependent manner (lanes 10-14) but is not able to bind to dsDNA (lane 6). We also found that the IB657 active site and triple cysteine mutants can efficiently bind polyIC and HCV RNA in a cell free system **(Figure 4-11, lanes 1-4)**. These results suggested that IB657 may directly inhibit HCV IRES function. Therefore, we performed cell free translation reactions using RNA generated from the bicistronic pRL-HL construct directing 5' cap-dependent Renilla luciferase translation and HCV IRES-dependent firefly luciferase (ff-luc) translation in the presence of buffer or IB657 and ^{35}S methionine. Translation products were analyzed by SDS-PAGE and dual-luciferase activity assay. As shown in **Figure 4-12**, addition of IB657 to the translation reactions resulted in a dose-dependent decrease in luciferase levels, with significantly increased suppression of HCV IRES-directed ff-luc translation as compared to cap-dependent Renilla luciferase translation (ren-luc) **(Figure 4-12b)**. To determine if IB657 inhibits HCV IRES-directed translation within human hepatoma cells, we performed luciferase activity analyses on extracts from Huh7 cells cotransfected with increasing amounts of p40 and the bicistronic luciferase reporter, pRL-HL. As shown in **Figure 4-13 (top panel)**, p40 expression rendered a dominant suppression of HCV-IRES directed firefly luciferase translation (black bars). We also tested the recombinant IB657

protein in this assay by culturing pRL-HL transfected cells with buffer, 10 U/mL IFNα or the indicated concentrations of IB657 for 48 hours. Similar to expression of p40 from a plasmid, IB657 treatment suppressed HCV IRES-directed ff-luc translation in a dose dependent manner **(Figure 4-13, top panel)**. Quantification of ff-luc RNA levels by qRT-PCR confirmed that IB657 was not inhibiting transcription of the reporter plasmid **(Figure 4-13, lower panel)**. We also evaluated the ability of IB657 to target other virally encoded IRES elements. Huh7 cells were cotransfected with the pCMV-renilla and the EMCV IRES-firefly luciferase reporter constructs, which has the IRES from encephalomyocarditis virus (EMCV) controlling firefly luciferase translation. Using dual-luciferase activity assays as described above, we found that p40 expression or IB657 treatment did not suppress EMCV IRES-directed translation from a luciferase reporter plasmid **(Figure 4-14)**.

To definitively demonstrate that IB657 is selectively targeting the HCV IRES, the HCV RNA replicon system was utilized. The replicon system consists of Huh7 cells harboring distinct, autonomously replicating, bicistronic RNA molecules that have the HCV IRES directing translation of neomycin phosphotransferase II (NPT II), which prevents cell death upon G418 treatment, and the EMCV IRES directing translation of the HCV subgenomic or genomic protein coding region **(Figure 1-4)**. We cultured 10^5 Huh7 or Huh7-K2040 (genotype 1b subgenomic replicon) cells with media containing buffer, 2 μM IB657 or 50 U/mL IFNα in the presence or absence of G418 for 72 hours and assessed cell viability and HCV, NPT II and GAPDH protein levels. We found that only IB657 + G418 treatment of the HCV replicon cells resulted in significantly ($p<0.01$) enhanced cell death **(Figure 4-15, top panel)**, correlating with decreased levels of HCV IRES directed NPT II protein levels

in IB657 treated cells with or without G418 treatment **(Figure 4-15, see fold expression)**. However, in IB657 treated cells, HCV protein levels were increased in comparison to buffer treated K2040 cells from **(Figure 4-15, see fold expression)**, consistent with luciferase data that IB657 does not inhibit EMCV IRES-directed translation **(Figure 4-14)**. The reason for the apparent increase in EMCV IRES-directed translation is unknown. IFNα treatment of replicon cells resulted in decreased cell numbers as well as viral protein levels, confirming previous studies demonstrating that IFNα acts to suppress HCV translation through more global cellular mechanisms (Wang et al., 2003). Moreover, IB657 treatment in the absence of G418 did not result in reduced HCV protein or RNA levels of a genotype 2a subgenomic or a genome length 1b replicon **(Figure 4-16)**. Together these results demonstrated that IB657 selectively inhibits HCV IRES function, resulting in decreased viral protein synthesis and subsequent suppression of HCV replication and spread.

IB657 has broad antiviral activity

Using standard antiviral assays we found that IB657 has antiviral potency against a number of distinct RNA viruses **(Table 4-3)**. We determined that IB657 pretreatment of Huh7 cells resulted in a dose dependent inhibition of WNV (Madagascar strain78-MAD78) infectious virus production, with a calculated IC_{50} of 1.7 μM (data not shown) (Keller et al., 2006). In addition, we found that increasing concentrations of IB657 reduced Respiratory Syncytial Virus (RSV A-2) induced cytopathic effects (CPE), replication and spread (IC_{50} of 1.01 μM), and RSV as well as influenza A viral protein production (S. Iadonato, unpublished observations). The Encephalomyocarditis Virus (EMCV) was also found to be sensitive to

IB657 treatment with reduced infectious virus production (IC_{50} of 0.78 μM) as well as decreased EMCV-induced CPE in infected-Huh7 cells (S. Iadonato, unpublished observations). Considering the RSV and Influenza viral genomes do not encode IRES elements and IB657 does not suppress EMCV infection through inhibition of IRES-directed translation, it is apparent that IB657 employs multiple modes of antiviral action. Further investigations into the molecular mechanisms for the broad antiviral activity of IB657 are currently being explored.

DISCUSSION

While a number of host genetic factors have been potentially associated with susceptibility or resistance to HCV infection, the data is often conflicting and lacking in conclusive evidence of the functional effects of these variants in disease outcome (reviewed in Yee, 2004). The purpose of the current study was to determine if the genotypic variant encoded by the HCV resistance-associated OAS1 1D1 allele has functional significance in controlling HCV infection. We found that the single-base mutation, rs10774671, encoded by the OAS1 1D1 allele controls alternative splicing events leading to the expression of isoform p42. The OAS1 p42 isoform lacks the geranylgeranylation motif (CTIL) found in p46, encoded by the OAS1 1A1 ancestral allele. We demonstrated that mutation or absence of the CTIL site resulted in altered subcellular localization of the OAS1 isoforms leading to suppression of HCV infection. Furthermore, we found that the CTIL motif is necessary for co-localization of the OAS1 variants with HCV proteins. The function of this co-localization is unknown and while we did not find a significant increase in HCV infection in p46 overexpressing cells

we cannot rule out a role for p46 in HCV replication, as was demonstrated for the host protein, FBL2 (Wang et al., 2005). Although p40 has been previously shown to interact with NS5A in coimmunoprecipitation experiments using overexpressed proteins (Taguchi et al., 2004), we did not detect co-localization of viral proteins with p40, p42 or p46-STIL in our studies. Instead, in the few transfected cells that were productively HCV-infected, we found viral protein expression in cellular compartments separate from the OAS1 proteins. Also, we did not find decreased HCV RNA levels at early time points after IB657 treatment as would be expected if IB657 was disrupting viral replication through targeting NS5A.

The importance of genetic variation at the OAS1 locus in modulating the host antiviral response is further suggested by recent findings that individuals expressing the ancestral OAS1 p46 variant have increased susceptibility to autoimmune type I diabetes, which is thought to have a viral etiology (Field et al., 2005). Also, this OAS1 polymorphism has been associated with increased susceptibility to multiple sclerosis (Fedetz et al., 2006) and persistent HCV infection (Knapp et al., 2003). Seminal studies by Bonnevie-Nelson et al. demonstrated that this polymorphism, rs10774671, alters the splice acceptor site at the seventh exon in OAS1. The genotype at this site controls expression of the OAS1 variants, p42/46/48/52. Furthermore it was found that these variants have differential basal OAS activity in vivo. Wherein, genotype GG at this OAS1 splice-site results in p46 production which was found to have higher OAS activity as compared to genotype GA (p46 + p42/p48/p52) or AA (p42/p48/p52) (Bonnevie-Nielsen et al., 2005). The apparent inconsistency of enhanced OAS enzymatic activity of the p46 variant and increased susceptibility to virus infections could be due to a number of factors. For example, the

increased basal activity of p46 could lead to a desensitized IFN response, wherein the effects of endogenous and exogenous IFN are dampened. This dampened IFN response in individuals could help to explain observations that HCV infected African Americans do not respond well to IFN-based therapy (Howell et al., 2000), due to the increased frequency of the GG-allele in this population (Bonnevie-Nielsen et al., 2005). Bonnevie-Nelson et al. also found that individuals homozygous for the GG sequence at the splice-site do not make the OAS1 isoform p48, which has been shown to have proapoptotic activity independently of its synthetase and RNase L activities (Ghosh et al., 2001). Similarly, we found that individuals homozygous for the OAS1 1A1 allele, p46, do not produce the p42 isoform, which was found to have direct anti-HCV activity. Therefore individuals who are homozygous for the OAS 1A1 allele do not produce the antiviral OAS1 isoforms p42 and p48 and therefore are at a potential disadvantage depending on their virus exposure. These findings suggest that the increased frequency of the OAS 1D1 allele in Caucasian and Asian populations may have occurred due to evolutionary pressure to increase host antiviral fitness.

In this study we have demonstrated that a soluble recombinant purified form of the OAS1 isoform p40 (IB657) efficiently entered human hepatoma cells, suppressing the replication and spread of two distinct HCV genotypes. We found that IB657 restricts HCV infection through dominant suppression of viral protein translation, most likely as a result of binding to the HCV IRES. IB657 inhibition of HCV IRES function is specific as it does not dramatically suppress 5' cap-dependent or EMCV IRES-directed translation. This ability of IB657 to target the HCV IRES could be advantageous in the clinical setting. The IRES is essential for the viral life cycle and its primary and secondary structure are highly conserved

among viral isolates(Honda et al., 1996; Laporte et al., 2000), suggesting that the emergence of drug-resistant viral variants would be limited. The ability of IB657 to bind to the HCV IRES might also have a dual function in blocking viral assembly and budding by tethering the viral genomic RNA in the cytoplasm, thus preventing its incorporation into new virions. Future experiments will address this possibility, possibly providing insight into the antiviral mechanism of IB657 against other RNA viruses. Herein, we provide in vivo and in vitro evidence that p40 (IB657) has potent anti-HCV activity. Furthermore, we illustrate the potential for IB657 as a novel therapeutic agent for the treatment of HCV infection and possibly as a broad antiviral agent to combat RNA viruses.

TABLE 4-1. HCV RISK FACTORS AND OAS1 ALLELE DISTRIBUTION IN THE CASE (HCV-) AND CONTROL (HCV+) SUBJECTS

	Caucasians		All Subjects			
	Cases (N 23)	Controls (N 57)	Cases (N 33)	Controls (N 86)	**HCV Genotype**	N (%)
Risk Factor					1a	29 (60)
Male Gender	91%	84%	79%	80%	1b	7 (15)
Age (years)	41	38	40	38	2b	3 (6)
IDU (years)	20	15	20	16	3	9 (19)
Behavior Risk					PCR negative	13 (21)
Needle sharing	81%	89%	86%	86%		
Needle sharing(<6mo prior)	57%	64%	58%	65%		
Equipment sharing	96%	98%	97%	95%		
Sex with IVDU	86%	77%	83%	75%		
OAS1 Allele Distribution			**Homozygous (p=0.015)**			
1D1	46%	33%	**26%**	**5%**		
1D2	15%	20%				
1D3	4%	7%				
1A1	15%	15%				
1A2	20%	22%				
other	0%	3.5%				

N, number of subjects; IDU, intravenous drug use; IVDU, intravenous drug user
1D1, derived allele 1; 1A1, ancestral allele

a

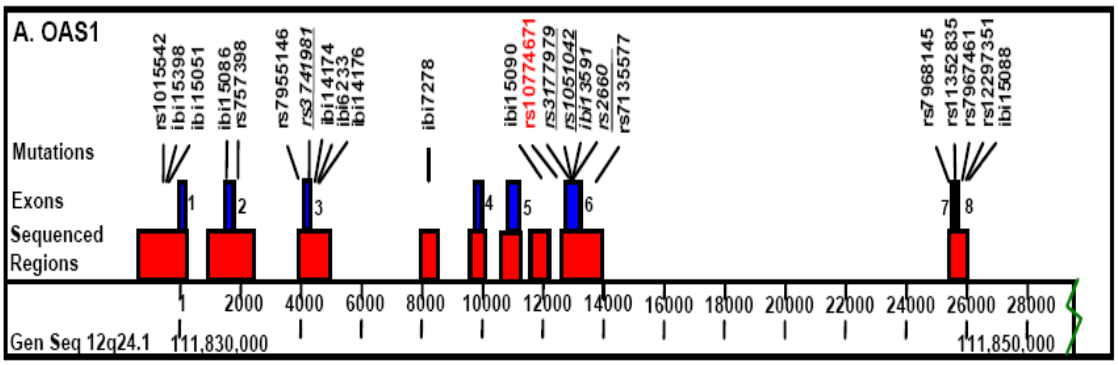

b

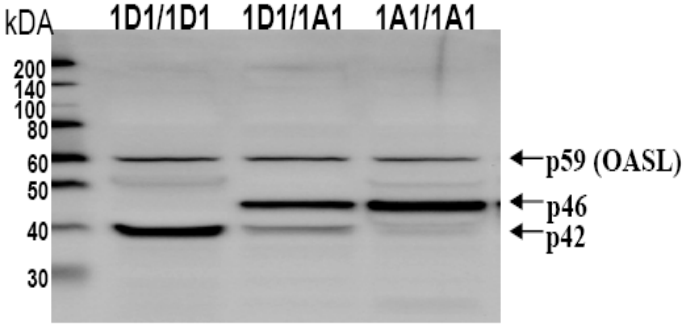

Figure 4-1. The OAS1 1D1 allele controls expression of the OAS1 variant, p42.

(a) Schematic of the intron/exon sequence of the OAS1 gene where the regions sequenced are represented by red boxes and the exons in blue. The mutations identified in the OAS1 derived allele, 1D1, as associating with HCV resistance, are listed on top of their respective location within the gene. The single-base mutation that controls expression of the OAS1 isoforms p42 or p46, rs10774671, is highlighted in red. **(b)** Immunoblot of OAS expression in IFNα treated lymphoblasts from individuals homozygous or heterozygous for the OAS1 1D1 allele or the ancestral allele, 1A1. Arrows mark the positions of the p42, 46 and 59 OAS isoforms.

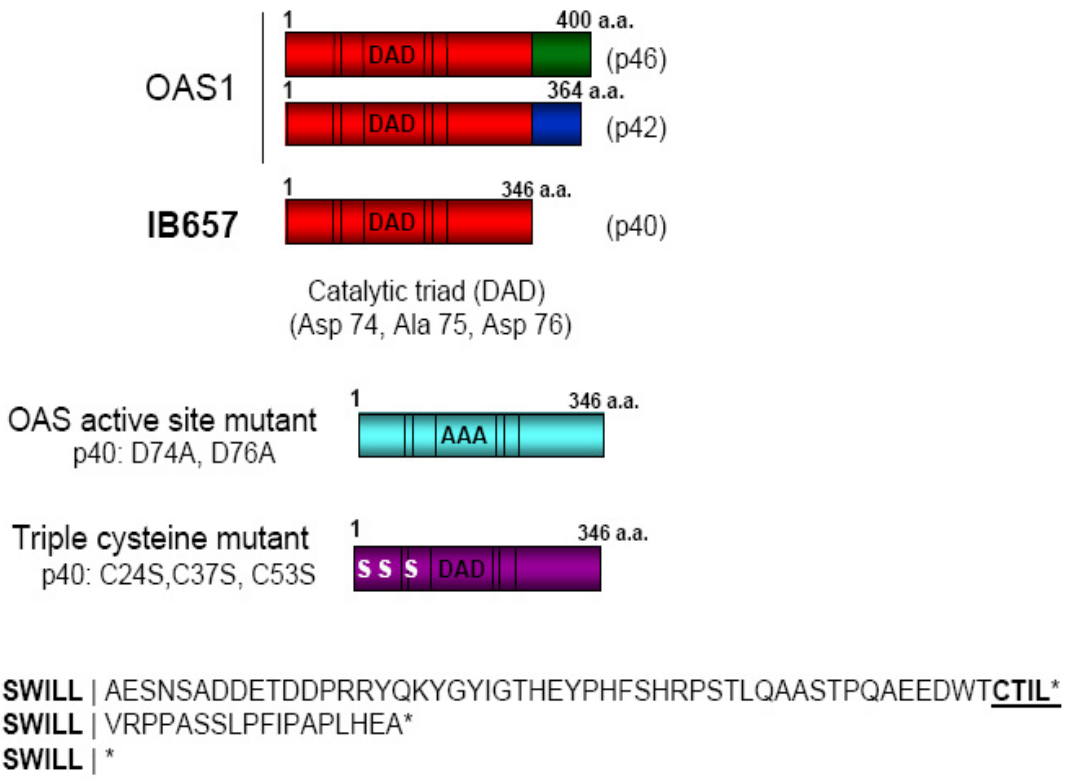

Figure 4-2. Structural features of the natural OAS1 isoforms, p46 and p42, and the recombinant drug form of p42, termed IB657/p40. The black lines indicate positions of putative dsRNA binding regions. DAD represents the approximate position of the catalytic triad, which was mutated to alanines (AAA) to ablate OAS activity (OAS active site mutant). The triple cysteine mutant (purple) has amino acid changes at the positions listed, abolishing cellular entry of the protein. Differential splicing results in production of p42 (includes exon 6) or p46 (excludes exon 6 and includes exon 7), which are identical in the first 346 amino acids (red) but have different carboxyl-terminal amino acid sequences (blue and green, respectively) as listed. Recombinant OAS1 p40 lacks the terminal amino acid sequence encoded by intron 5. The underlined CTIL sequence is a putative site for geranylgeranylation. Asterisks denote the stop codon.

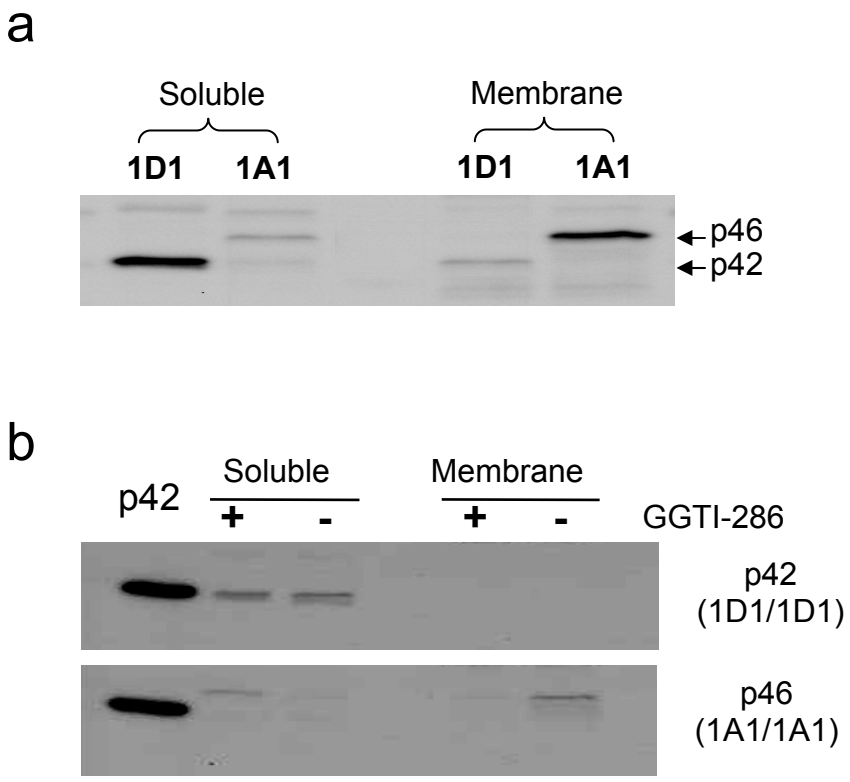

Figure 4-3. Geranylgeranylation is important for the subcellular localization of human OAS1 proteins. Lymphocytic cells from individuals homozygous for the OAS1 1D1 (p42) or 1A1 (p46) alleles were treated with 100 U/mL of IFNα alone **(a)** or in combination with 10 μM of the geranylgeranyl transferase 1 inhibitor GGTI-286, for 24 hours **(b)**. The cells were harvested, separated into soluble (0.2% saponin) or membrane (1% Triton-X 100) fractions, and subjected to immunoblot analysis for OAS expression in the different cellular fractions. The monoclonal OAS1 antibody recognizes the N-terminal of OAS1, allowing it to recognize all isoforms of OAS1. Purified p42 protein (5ng) was run in parallel with endogenous proteins as a control to distinguish between the p42 and p46 bands.

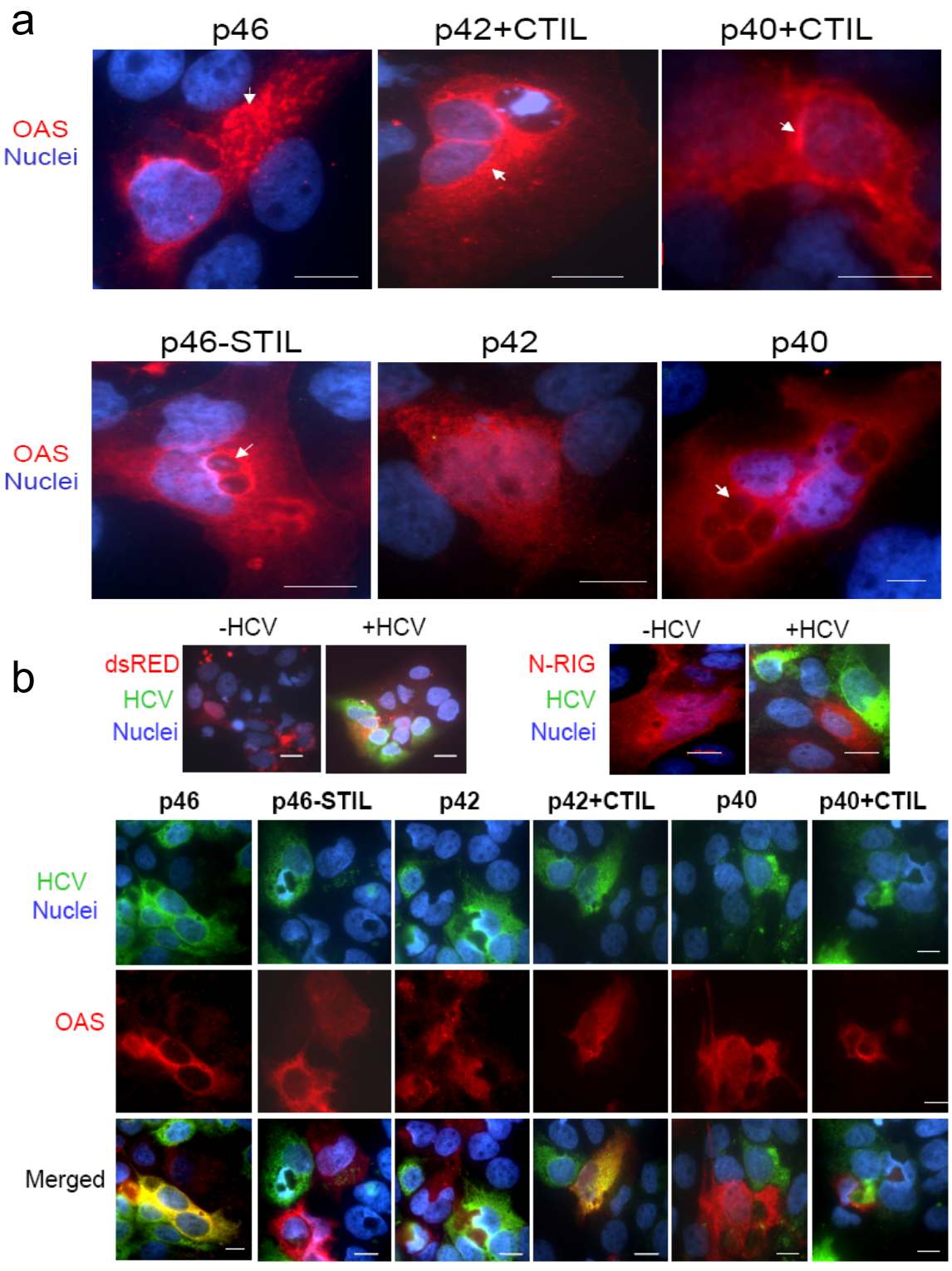
a
p46
p42+CTIL
p40+CTIL
OAS
Nuclei
p46-STIL
p42
p40
OAS
Nuclei
b
-HCV
+HCV
dsRED
HCV
Nuclei
-HCV
+HCV
N-RIG
HCV
Nuclei
p46
p46-STIL
p42
p42+CTIL
p40
p40+CTIL
HCV
Nuclei
OAS
Merged

c

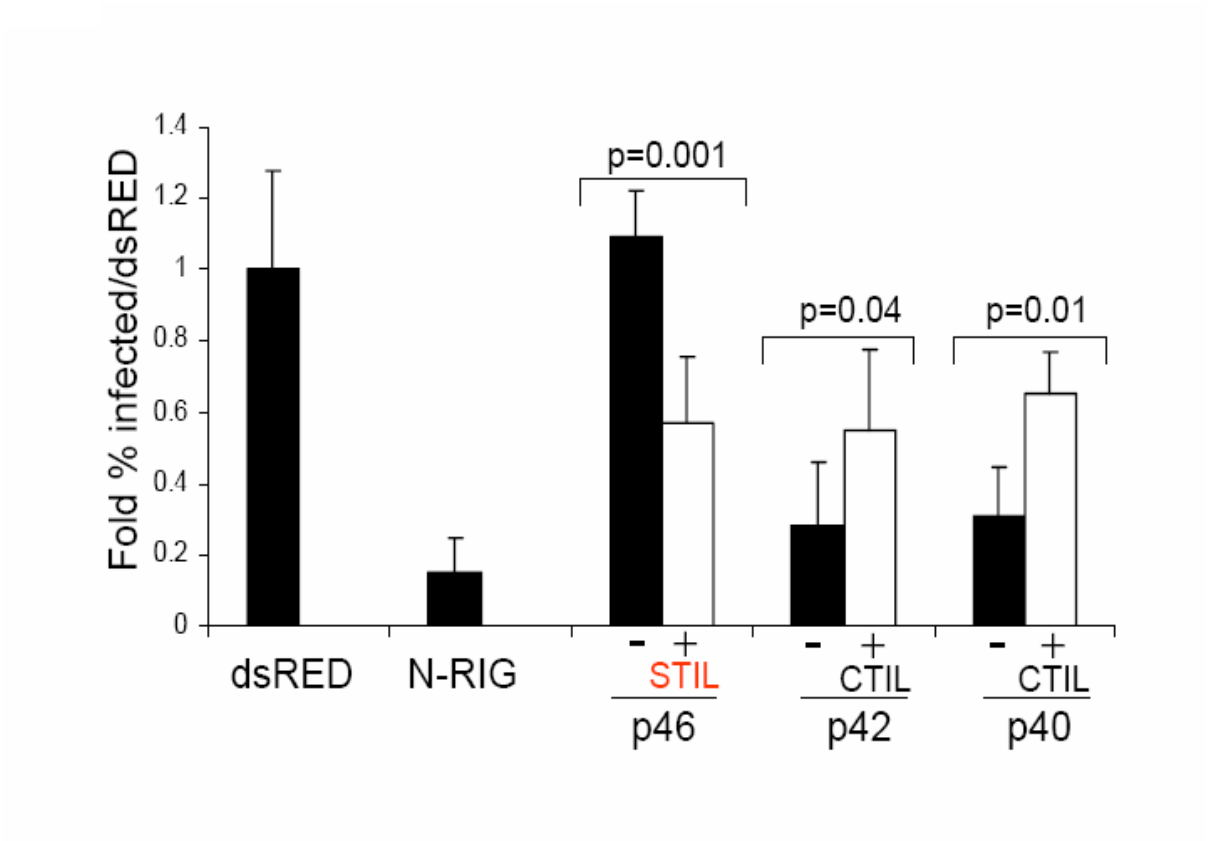

Figure 4-4. The absence of the geranylgeranylation sequence, CTIL, in p40 and p42 confers anti-HCV functions to the protein. Huh7.5 cells were transfected with the indicated plasmids for 24 h followed by mock **(a)** or HCV 2a virus infection **(b,c)**. 48 hours later cells were immunostained with HCV 2a patient serum (green) and anti-RIG-1 or OAS serum (red). Nuclei were visualized by staining the cells with DAPI (blue). **(a)** Arrows indicate punctate, perinuclear staining (a, top panel) or vacuole formation (a, bottom panel). **(b)** Representative images of transfected and HCV-infected Huh7.5 cells. **(c)** The graph represents the levels of HCV 2a infection in cells expressing the OAS1 isoforms. Results shown were determined by calculating the percentage of infected cells in 4 fields from each transfected well and are expressed in the bar graph as the average (n=4) fold decrease in the percentage of infected cells as compared to the percent infected in the dsRED transfected control wells. Black bars represent infection levels in cells expressing dsRED, N-RIG or the wild-type OAS variants. White bars are the respective OAS1 isoforms containing mutations to either change, p46 (CTIL/STIL) or add, the CTIL sequence to the protein. P values shown represent significant differences between the percent infected in cells transfected with the mutant versus wild-type OAS1 proteins (two-tailed, unpaired t-test). Error bars, s.d. Images were taken using a Zeiss Axiovert digital imaging microscope (Scale bars, 20μm).

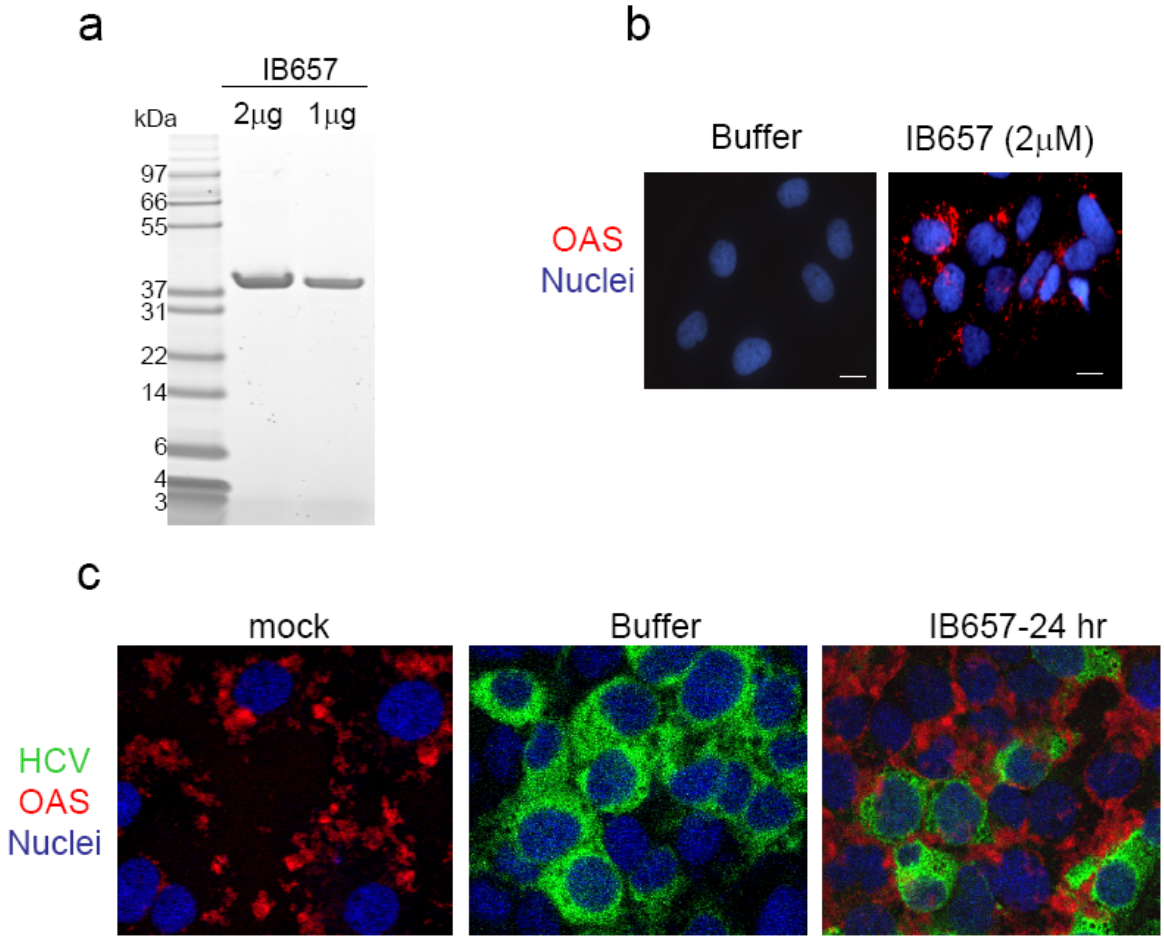

Figure 4-5. IB657 is a recombinant protein drug form of the endogenous p42 OAS1 isoform. **(a)** Coomassie staining of the indicated amounts of purified recombinant IB657 protein. **(b)** Huh7 cells treated with buffer or 2 μM IB657 were immunostained at 48 hours after treatment with anti-OAS for intracellular IB657 expression (red). The nuclei were visualized by DAPI staining (blue). Images were taken with a Zeiss Axiovert digital imaging microscope (Scale bars, 20μm). **(c)** Huh7 and HCV 2a infected-Huh7 cells were cultured for 24 hours with buffer or 2μM IB657, and immunostained for HCV (green), OAS (red), and DAPI (blue). Images were taken using a Zeiss laser scanning confocal microscope.

TABLE 4-2. IB657 CYTOTOXICITY AND APOPTOSIS ANALYSIS

	Cell Line	Description	Drug Treatment Period (hour)	Initial Drug Concentration (μM)	Apoptosis Testing Method	Cytotoxicity Testing Method	Apoptosis	Cytotoxicity
1	A3	T Lymphocyte	24	0 - 15	Fluor. Caspase 3/7 Assay	MTS	Neg.	Neg.
2	DU145	Prostate Epithelial	24	0 - 15	Fluor. Caspase 3/7 Assay	MTS	Neg.	Neg.
3	HeLa	Cervical Carcinoma	20 - 24	0 - 10	Not Done	MTS	ND	Neg.
4	MCF7	Mammary Epithelial	4 - 24	0 - 10	Fluor. Caspase 3/7 Assay; WB w/ PARP & Casp. 3 Ab	MTS	Neg.	Neg.
5	PC3	Prostate Epithelial	24	0 - 10	Fluor. Caspase 3/7 Assay	MTS	Neg.	Neg.
6	Huh7	Hepatocyte	20 - 24	0 - 15	Fluor. Caspase 3/7 Assay	MTS	Neg.	Neg.
7	T47D	Mammary Epithelial	4 - 24	0 - 10	Fluor. Caspase 3/7 Assay; WB w/ PARP & Casp. 3 Ab	MTS	Neg.	Neg.
8	MRC5	Lung Fibroblast	24 - 96	0 - 10	Not Done	MTS; resazurin reduction; LDH release	ND	Neg.

MTS, (3-(4,5-dimethylthiazol-2-yl)-5- (3-carboxymethoxyphenyl) 2-(4-sulfophenyl)-2H-tetrazolium). Fluor. Caspase, fluorescent caspase 3/7 activation assay.

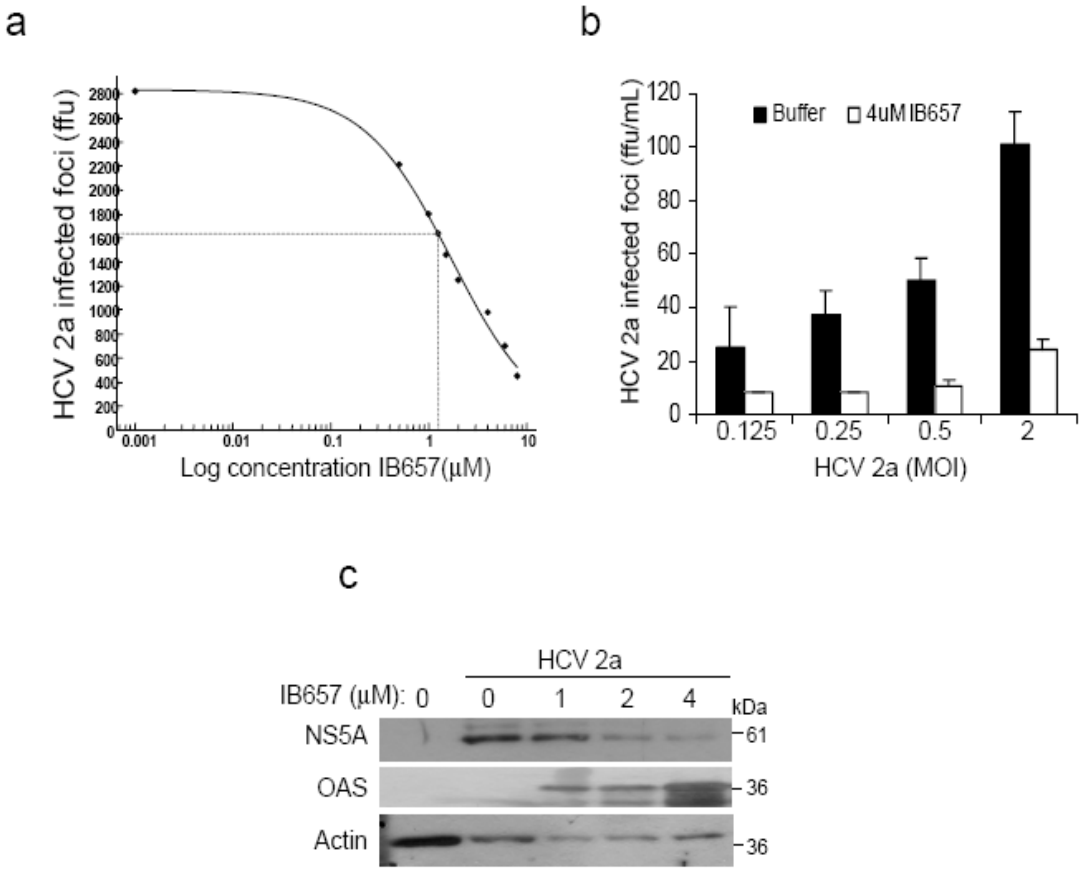

Figure 4-6. Anti-HCV activity of IB657. (a) The antiviral potency of IB657 in HCV 2a-infected Huh7 cells. Results are expressed as the mean number of infected foci (ffu) after treatment. The IC_{50} of IB657 on HCV 2a was calculated to be 1.25 µM. **(b)** HCV 2a-infected Huh7.5 cells were treated for 24 hours with buffer (black bars) or IB657 (white bars), the cells were washed and fresh drug-free media added for an additional 24 hours. The HCV 2a viral titer was then determined using the drug-free cell supernatant. Results are displayed as the mean number of infected foci/mL (ffu/mL) ± s.d. and are representative of two independent experiments performed in triplicate. **(c)** Immunoblot of HCV NS5A, OAS and actin levels in Huh7 cells mock infected (mock) or infected with HCV 2a and treated with the indicated concentrations of IB657 for 72 hours.

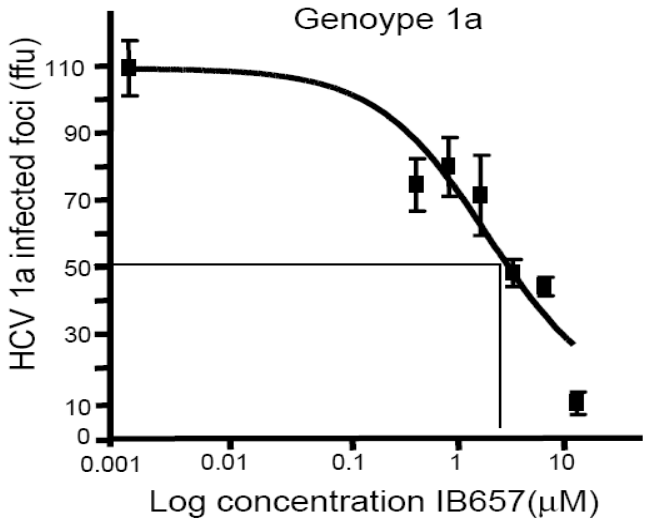

Figure 4-7. IB657 suppresses the IFN-resistant HCV genotype 1a virus. Huh7.5 cells were transfected with HCV 1a RNA for 48 hours, passaged, and cultured in media containing buffer or increasing concentrations of IB657. After 72 hours of IB657 treatment the number of HCV 1a infected cells quantified by FFA. The graph shows the mean number of infected foci (n=3) ±s.d., with a calculated IC_{50} value of 2.6 μM.

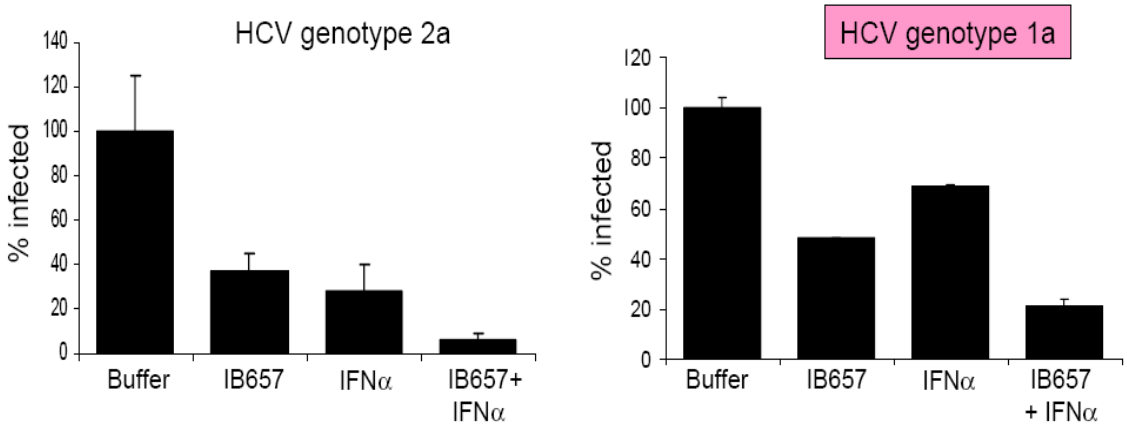

Figure 4-8. IB657 enhances the antiviral effects of IFN. HCV 2a-infected (left panel) and 1a RNA-transfected (right panel) hepatoma cells were treated with 2μM IB657, 25U/mL of IFNα-2a or both for 72 hours. Cells were fixed, stained, and the number of HCV infected cells determined. Results are reported as a percentage of the buffer treated control cells, which was set to 100%. Results are representative of three independent experiments. Error bars, s.d.

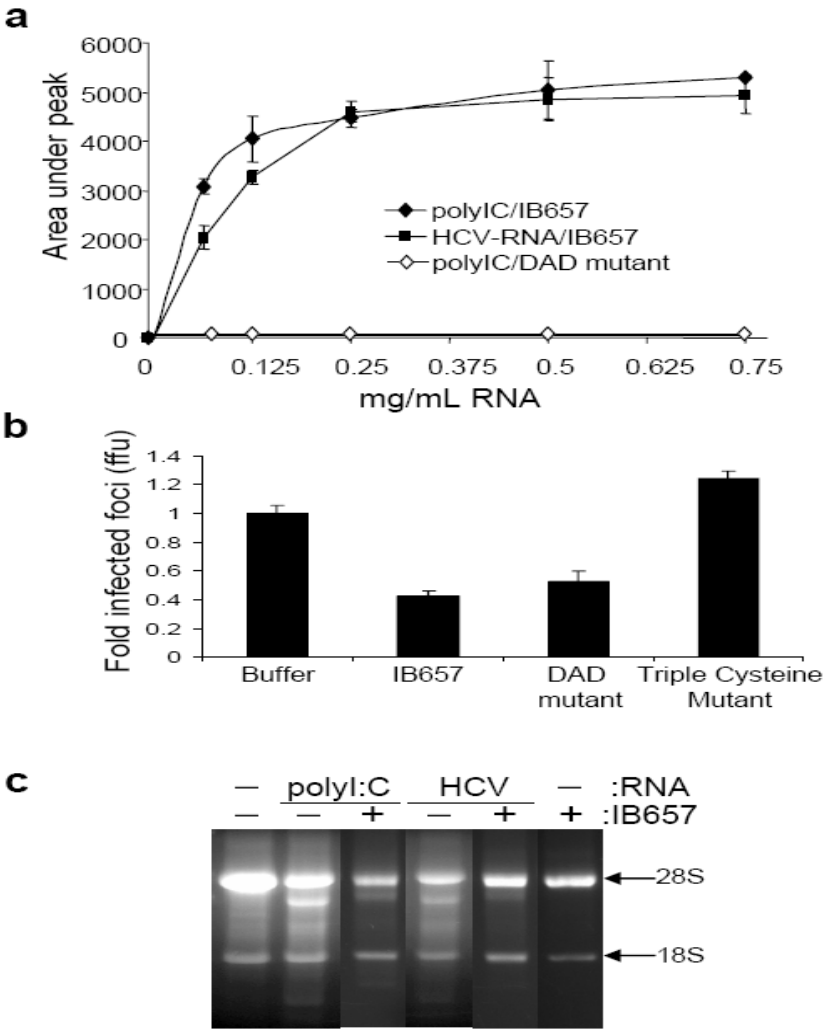

Figure 4-9. Suppression of HCV infection by IB657 is independent of OAS/RNase L activation. (a) Activation of IB657 OAS activity by polyIC (diamond) and HCV 2a RNA (squares). 50ng of IB657 (black) or the IB657-DAD mutant (white) was incubated with the OAS enzyme substrates, dATP and NAD and increasing amounts of polyIC or HCV RNA. The amount of product formation (dATP-NAD) was purified and quantitated using HPLC. Measurements are the mean product formation ± s.d. and are represented as the area under the peak. **(b)** HCV 2a-infected Huh7 cells were treated with 4 μM of the indicated drugs for 48 hrs and the number of infected cells determined by focus forming assay. Results are the mean (n=3) number of infected foci ± s.d. and are presented as the number of infected foci/number of infected foci in buffer treated control cells (fold infected foci). **(c)** HeLa cells were pretreated with buffer or 2 μM IB657 for 6 hrs at which time the cells were transfected with 4 μg/6-well of polyIC or in vitro transcribed HCV 2a RNA. After 4 hrs total RNA was isolated and run on a 1% agarose gel. Arrows denote the 28S and 18S ribosomal bands.

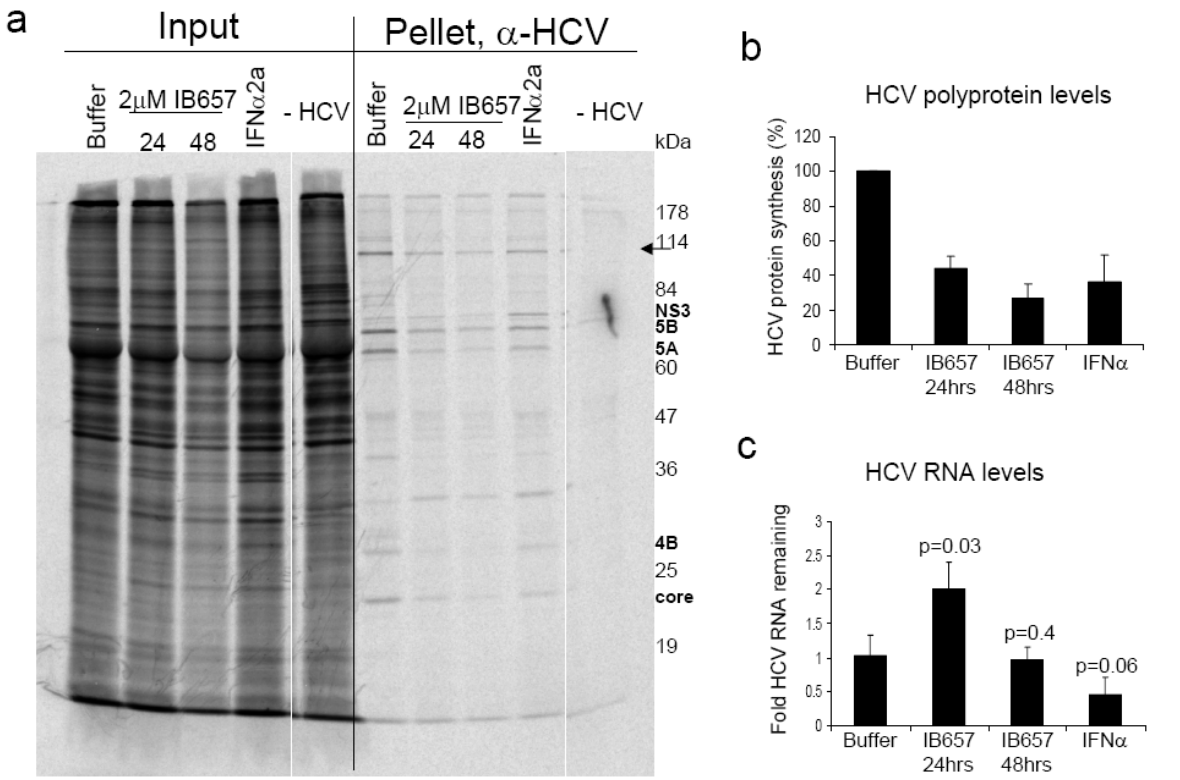

Figure 4-10. IB657 inhibits HCV protein synthesis. [^{35}S]methionine pulse-labelling of uninfected (-HCV) and HCV 2a-infected Huh7.5 cells cultured for 24 or 48 hours in the presence of buffer, 2μM IB657, or 50U/mL IFN-α2a. **(a)** Shown is the autoradiogram from SDS-PAGE analyses of the total cellular proteins (input) and HCV proteins (Pellet, α-HCV) recovered from cell extracts by immunoprecipitation. **(b)** Incorporation of radiolabel into the HCV polyprotein (arrow) was quantified by phosphorimager analysis and is reported as a percentage of the untreated sample, set to 100%. The error bars represent s.d. of the mean polyprotein band intensities from two independent experiments. Quantification of the other HCV proteins such as NS3, NS5B, NS5A, NS4B and core followed a similar trend **(see a)**. **(c)** Levels of HCV RNA present in each sample were determined by qRT-PCR and the amount remaining is presented as a fold of the untreated sample. Error bars represent the standard deviation of the means of HCV RNA levels performed in triplicate. No significant differences ($p<0.01$, two-tailed, unpaired t-test) were detected in HCV RNA levels as compared to buffer treated samples. Results are representative of at least two independent experiments.

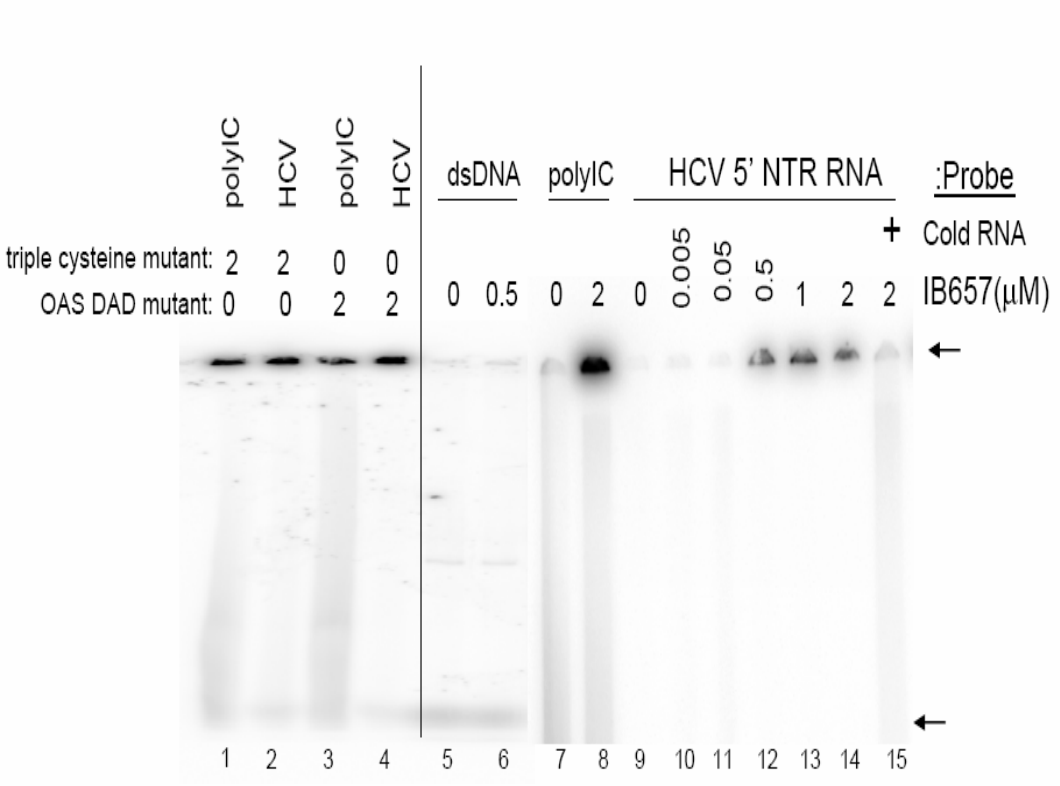

Figure 4-11. IB657 efficiently binds to the HCV 5′NTR. Electrophoretic mobility shift assay was performed with the indicated concentrations of recombinant purified IB657, IB657-triple cysteine or DAD mutants. Radiolabeled dsDNA (lanes 5 and 6), polyIC (lanes 1,3,7 and 8) or HCV 5'NTR RNA (lanes 2,4, 9-15) were used for binding with the indicated concentrations of IB657 or mutant proteins. Lanes 5, 7 and 9 are binding reactions without IB657. The top arrow denotes the IB657-specific shifted band that was competed out by 100-fold excess of unlabeled HCV RNA (lane 15) and the bottom arrow shows the unbound probe. Results are representative of three independent experiments.

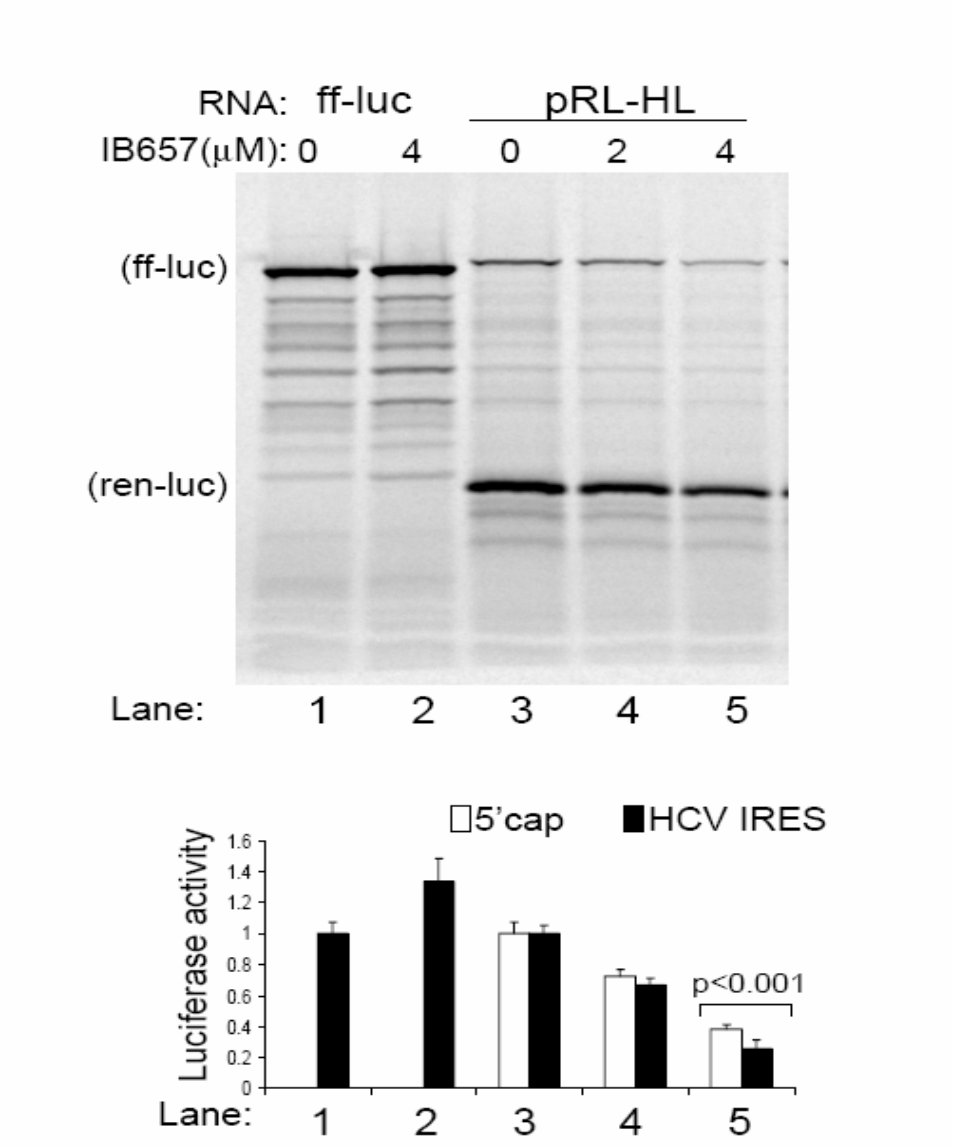

Figure 4-12. IB657 dominantly inhibits HCV IRES-directed translation. In vitro translation of pRL-HL RNA to simultaneously assess, 5'cap-dependent *Renilla* luciferase (ren-luc) and HCV IRES-directed firefly luciferase (ff-luc) translation, in the presence of IB657. The top panel shows an autoradiogram of the translation products resolved by SDS-PAGE. *Renilla* (shaded bars) and firefly luciferase translation products (white bars) were also analyzed using dual-luciferase assays. Results displayed are the mean (n=6) luciferase activities normalized to untreated samples (lanes 1 and 3) ± s.d. The p value shown denotes significance with comparison between firefly and *Renilla* luciferase levels in lane five, no other significant differences were found (two-tailed, unpaired Student's t-test).

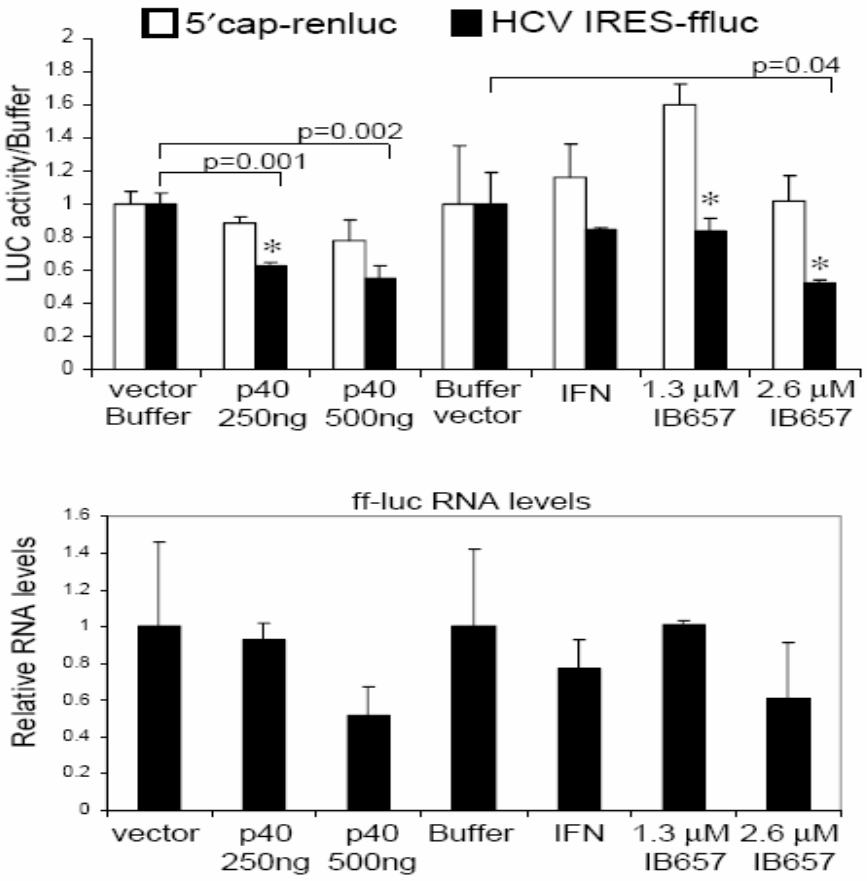

Figure 4-13. In vivo analysis of IB657 translation suppression. Cells were cotransfected with pRL-HL and the indicated concentrations of p40 or cultured with IB657. 48-72 h after transfection luciferase (luc) activity (top panel) and firefly luc (ff-luc) RNA levels (bottom panel) were assessed from cell extracts. Results shown are the mean *Renilla* (white bars) and ff-luc (black bars) activity values (n=4) or ff-luc RNA levels (n=3) normalized to buffer treated control cells, transfected with pRL-HL and empty vector. P values shown denote significance as compared to control samples and asterisks represent significance ($p<0.05$, two-tailed, unpaired t-test) when compared to the ren-luc values in the same sample.

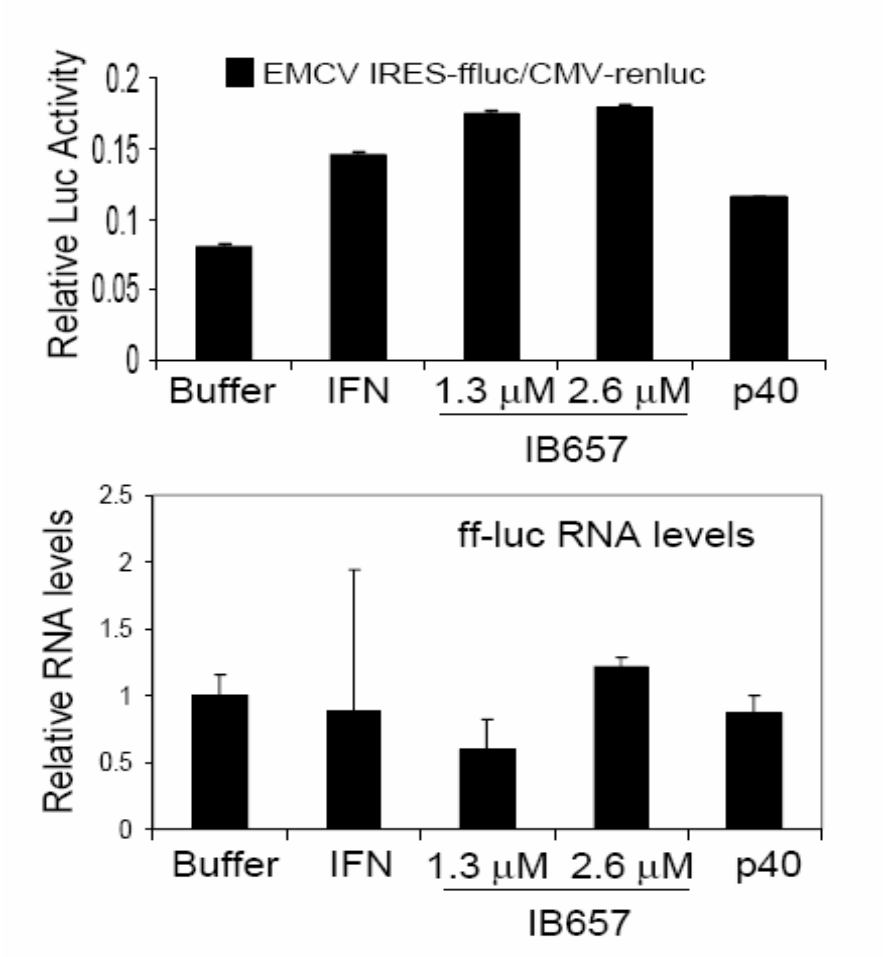

Figure 4-14. IB657 does not suppress EMCV IRES-directed translation.
Using dual-luciferase assay we simultaneously assessed CMV-directed *Renilla* luciferase (renluc) translation and EMCV IRES-directed firefly luciferase (ff-luc) translation in p40 transfected or IB657-treated Huh7 cells, similar to Figure 4-12 with the HCV IRES-directed ff-luc construct. Results shown are the mean ± s.d. (n=3) relative luciferase activities, ff-luc/CMV-*Renilla*-luc (renluc) (upper panel), and ff-luc RNA levels (bottom panel) at 72 hours after transfection. Results are representative of at least two independent experiments. No significant differences ($p<0.01$, two-tailed, unpaired T-test) were found in ff-luc RNA levels.

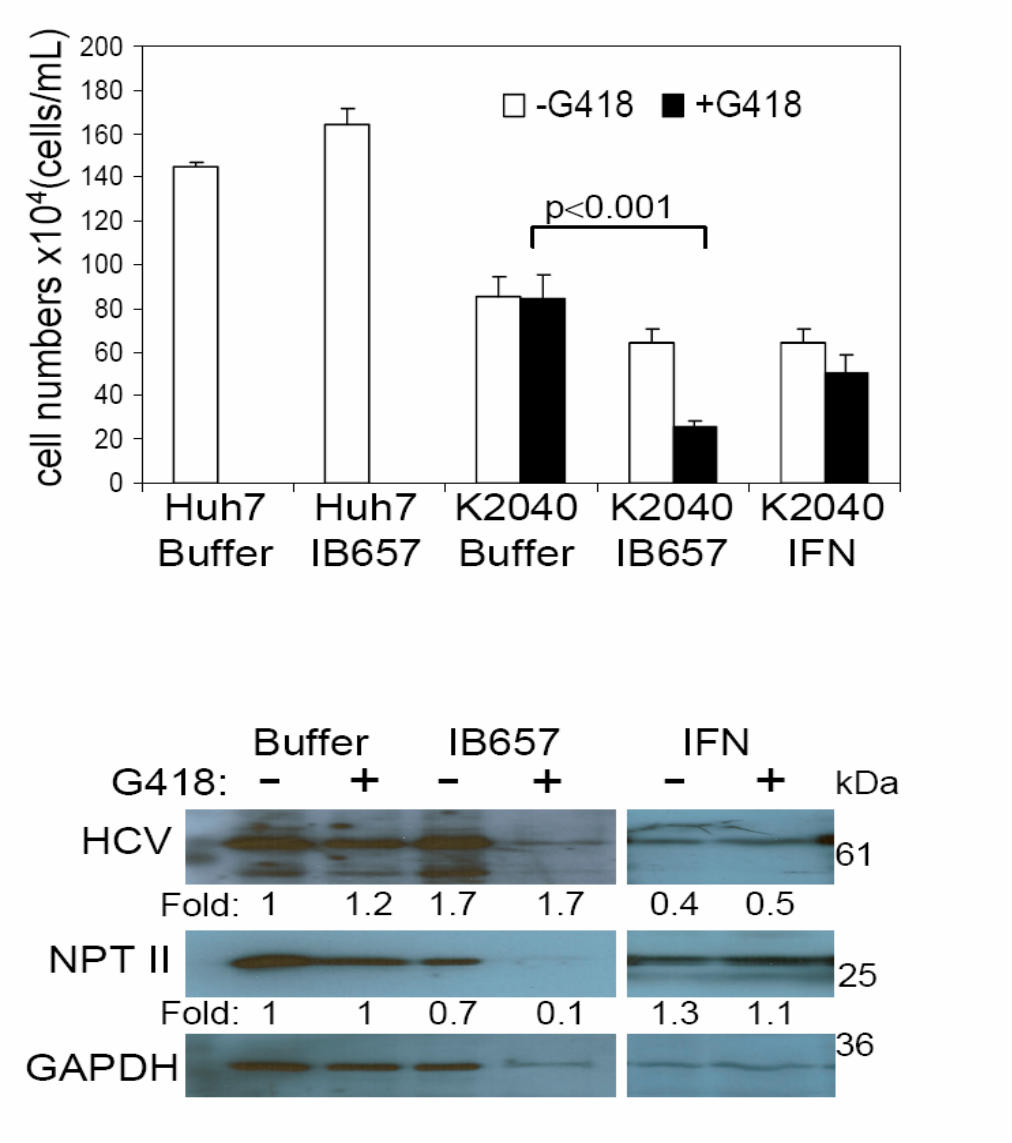

Figure 4-15. IB657 specifically suppresses HCV IRES-directed translation. Huh7 and Huh7-K2040 replicon cells were cultured for 72 hours in medium containing buffer, IB657 or IFNα with (black bars) or without (white bars) 5μg/mL G418. The top panel shows the number of cells/mL ± s.d. (n=4) remaining in each sample. The p value shown denotes a significant difference in IB657+G418 as compared to K2040+G418. No other significant differences in cell survival were found ($p<0.01$, two-tailed, unpaired students T-test). Parallel immunoblot analysis was performed on the samples to evaluate NPT II, HCV and GAPDH protein levels in equivalent cell numbers. The numbers under each blot represent the relative protein expression levels (NPT II or HCV band intensity/GAPDH band intensity) as a fold of the amount present in K2040 untreated control cells, set to 1. Band intensities were determined using densitometry. Results shown are one representative of at least three independent experiments.

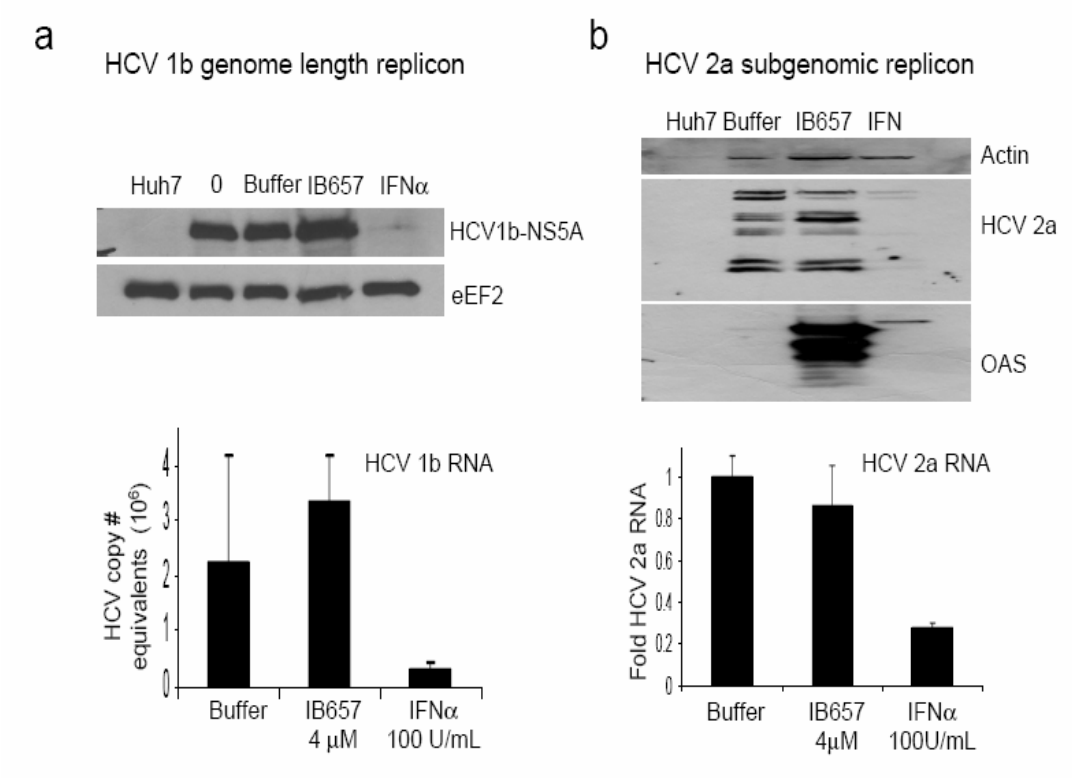

Figure 4-16. IB657 does not have an antiviral effect on the subgenomic or genome length HCV-RNA replicons. Huh7 and Huh7 cells harboring the genome-length genotype 1b HCV RNA, C5B2-3, as well as, the genotype 2a subgenomic replicon containing cells were treated with media alone (0), buffer (μL amounts equal to IB657), 4μM IB657 or 100 U/mL of IFNα-2a for 48 hours. Cells were trypsinized, pelleted, washed, and total RNA and proteins harvested. Viral protein levels were evaluated by immunoblot analysis using two well characterized patient serum to detect HCV 1b or HCV 2a proteins. Immunoblots were stripped and also probed for OAS1 and either actin or eEF2 for loading controls. Total RNA from treated cells was used for qRT-PCR analysis in order to quantitate the amount of HCV RNA remaining. Results shown were quantified using the standard curve method for RNA from the HCV-C5B2-3 full length replicon cells, with in vitro transcribed HCV 1a RNA as the standard, and presented above as HCV copy number equivalents. For the subgenomic 2a HCV replicons, relative HCV RNA levels were calculated with human GAPDH as the internal standard, and fold change values calculated using the $\Delta\Delta C_t$ ($2^{-\Delta\Delta Ct}$) method relative to the buffer treated control cells.

TABLE 4-3. IB657 HAS BROAD ANTIVIRAL ACTIVITY

Virus	Inhibits*
Hepatitis C Virus Genotype 1a and 2a	Viral replication and spread (IC_{50} 1.6 μM, 2.3 μM), infectious virus production
Encephalomyocarditis Virus	Infectious virus production (IC_{50} 0.78 μM) cellular CPE (100% cell rescue with 3 μM)
Respiratory Syncytial Virus (A-2)	Viral protein expression, infectious virus production(IC_{50} 1.01 μM), CPE
Influenza A Virus (A/WSN/33) H1N1	Viral nucleoprotein expression
West Nile Virus Madagascar-78 and Texas-02	Viral protein expression of IFN-resistant Texas-02 strain, infectious virus production (IC_{50} 1.66 μM)

*Detected using standard viral assays in appropriate cell lines.

$IC_{50,}$ 50% Inhibitory Concentration of IB657

CPE, cytopathic effects detected using MTS assay

CHAPTER FIVE
Conclusions and Recommendations

ANTIVIRAL EFFECTORS OF IFN ACTION AGAINST HCV: PAST, PRESENT AND FUTURE

The studies in Chapter 3 focused on a comparison analysis of the in vitro antiviral effects and signaling potency of CIFN, IFN-α2a and pegylated-IFN-α2b. The ability of CIFN to suppress HCV replication and spread to levels not achievable by the other IFNs even at very high concentrations, suggested that CIFN induces distinct IFN-receptor mediated signaling events and downstream effector molecules that act to limit HCV infection. These results were expected as CIFN contains a number of amino acid differences from IFN-α2a and IFN-α2b **(Appendix A-alignment of IFNs)**, and has higher homology to IFNβ, which has been shown to induce distinct biological actions when compared to IFNα subtypes (van Boxel-Dezaire et al., 2006). A functional genomics analysis of IFN treated primary hepatocytes was utilized to identify ISGs that were differentially induced by CIFN, thus indicating their involvement in suppressing HCV infection. 86 CIFN-induced genes were identified as being distinct from IFN-α2a or PEG-IFN induction, in either the kinetics and/or magnitude of expression **(Appendix B)**. A subset of seven of these genes was chosen for evaluation, based on antiviral actions against other viruses and/or the putative biological functions of the encoded proteins. The ISGs chosen include ISG15, Usp18 (ISG15 deconjugating enzyme), UbcH8 (ISG15 E2 ligase), viperin (RSAD2 or cig5), ISG20, IFI44, and NOD27. To note a few genes with unknown function were identified

that are potentially interesting, and would be relevant in characterizing further, including FLJ11286, which has a putative helicase domain. ISGs for which we have begun cloning but have no further data include ISG20, IFI44, and NOD27. ISG20 has just recently been shown to exhibit antiviral activity against HCV dependent on its 3'-5' exonuclease activity (Jiang et al., 2008a). NOD27, nucleotide-binding oligomerization domains 27, is thought to be involved in the immune response to pathogens based on its atypical CARD-domain. This molecule is of particular interest in that it is a potential component of the signaling pathways involved in the innate antiviral response, such as the CARD-containing proteins RIG-I and IPS-1, yet has only been evaluated in the immune response to Legionella pneumophila (Martinon and Tschopp, 2005). IFI44 was recently reported as associating with a successful response to IFN-based therapy in HCV-infected individuals, and has been shown to have antiproliferative actions (Hallen et al., 2007; Hwang et al., 2006). Described below are preliminary results from studies evaluating the roles of ISGylation and viperin in the innate IFN response to HCV infection. The importance of these types of studies in delineating the molecular mechanisms of IFN antiviral actions is demonstrated by the large number of recently published articles describing the antiviral actions of novel ISGs (discussed below).

ISGylation and HCV

Although ISG15 was cloned over 20 years ago, little was known about the cellular and antiviral functions of this protein when we initiated these studies (Blomstrom et al., 1986). ISG15 had been identified as a ubiquitin homologue, and like ubiquitin, it is covalently

attached to numerous cellular proteins. ISG15 conjugation is regulated by the IFN response, and is referred to as ISGylation. ISG15 uses an IFN-inducible conjugating cascade (Ube1L, UbcH8, Herc5) that is reversible by the IFN-induced deconjugating enzyme Usp18/Ubp43. ISGylation of proteins is observed by immunoblot analyses of IFN-treated cell lysates as a ladder of ISG-15 conjugated proteins **(Figure 5-1)** (Loeb and Haas, 1992). The identification of putative ISG15 target proteins was, and is, an area of intense research with now more than 158 proteins identified, many of which are involved in the type I IFN response (Giannakopoulos et al., 2005; Takeuchi and Yokosawa, 2008; Zhao et al., 2005). In 2005 the role of ISG15 in the innate antiviral response in vivo was controversial. In vitro studies had reported that overexpression of ISG15 enhanced IFN mediated suppression of HIV and Sindbis replication. However, initial evaluation of ISG15-deficient mice revealed normal IFN signaling and ISG induction, as well as normal resistance to vesicular stomatitis virus (VSV) and lymphocytic choriomeningitis virus (LCMV) infection (Osiak et al., 2005). These results were seemingly in conflict with previous studies demonstrating that Usp18/Ubp43-deficient mice are hypersensitive to IFN with prolonged Jak-STAT signaling, which was ascribed to enhanced ISGylation (Malakhova et al., 2003). Components of the ISGylation system were identified in our gene expression analysis as being highly induced by CIFN. Therefore, we examined the role of ISGylation in the antiviral response to HCV using the HCV RNA replicon system. We verified that CIFN treatment for 12 or 24 hours maximally induced ISG15 protein expression and ISGylation in Huh7 cells containing distinct HCV RNA replicons. We observed elevated levels of ISGylation in IFN treated cells containing the HCV-A7 replicon as compared to the IFN resistant HCV-HP replicon cells

(**Figure 5-1)**. At 24 hours after IFN treatment HCV-A7 protein levels were maximally decreased in CIFN treated cells, correlating with the greatest induction of ISGylation in these cells and demonstrating the sensitivity of this replicon to the antiviral actions of IFN (**Figure 5-1**). Consistent with previous studies, levels of the HCV-HP replicon proteins remained high after 24 hours of IFN treatment (**Figure 3-3)**. These results demonstrated that HCV replication induces high levels of unconjugated ISG15 protein (basal expression in untreated HCV-replicon containing cells), and a highly fit HCV variant (HCV-HP) suppresses IFN-induced ISGylation of cellular proteins (**Figure 5-1**).

To determine if ISG15 expression and/or ISGylation enhances the ability of IFN to suppress HCV replication and spread we examined viral protein levels in cells overexpressing different components of the ISGylation conjugating system. We found that overexpression of ISG15 alone did not enhance the anti-HCV actions of IFNα-2a **(Figure 5-2A).** However, expression of the conjugating enzymes with or without ISG15 resulted in decreased HCV-NS3 levels as compared to cells treated with a low dose (10U/mL) of IFNα-2a alone **(Figure 5-2A)**. Also, cells that were transfected with Usp18, the ISG15 deconjugating enzyme, had increased levels of viral proteins as compared to the IFN-treated, vector-transfected control cells **(Figure 5-2B, lanes 4 and 5)**. Experiments using siRNA silencing of Usp18 and UbcH8 (ISG15 E2 conjugating enzyme) confirmed and extended these overexpression analyses. We found that silencing of Usp18 led to increased ISGylation levels, correlating with decreased viral RNA and protein levels. However, siRNA silencing of UbcH8 (E2 ISG15 ligase) expression resulted in an increase in HCV replication, with higher viral RNA and protein levels than cells treated with a control siRNA. Importantly,

HCV protein and RNA levels in cells lacking both Usp18 and UbcH8 were similar to the levels in cells with only Usp18 levels reduced, suggesting that Usp18 inhibits the antiviral actions of IFNα independently of suppressing ISGylation **(Figure 5-2B)**.

Shortly after we performed these experiments Dr. Dhog-Er Zhang's group reported that Usp18 inhibits IFNα induced signaling separately from its ISG15 deconjugating activity. The authors found that Usp18 specifically binds to the IFNα receptor 2 (IFNAR2) blocking the interaction of Jak1 and the receptor, thus inhibiting IFNα activation of the Jak-STAT signaling pathway (Malakhova et al., 2006). A few months after these studies were published another group demonstrated that silencing of Usp18 enhanced the antiviral actions of IFN against HCV infection in vitro, performing very similar experiments to our Usp18 knockdown studies. However, these authors did not conclusively demonstrate that the Usp18 block in IFN signaling was independent of ISG15 deconjugation as our results suggested (Randall et al., 2006). Notably, recent in vivo studies using ISG15-/- mice demonstrated that ISG15 functions as a critical antiviral molecule against both RNA (influenza and Sindbis viruses) and DNA (herpes virus type-1) viruses (Lenschow et al., 2007). Together these findings and the previous report that ISG15-/- mice did not exhibit decreased resistance to VSV and LCMV (both RNA viruses) suggest that ISG15 exhibits antiviral activity against selective viruses (Osiak et al., 2005). Whether this is due to virally mediated resistance of ISG15 or inherent to the molecular mechanisms of its antiviral action requires further study. Nonetheless, the importance of ISG15 and Usp18 in modulating the IFN antiviral response is now realized. Further investigations into the functions of these proteins during IFN therapy and in response to different viral infections could provide new avenues for therapeutic

intervention to improve HCV therapies as well as therapies against other important human pathogens.

Viperin

Viperin (cig5 or radical S-adenosyl methionine domain containing 2) was previously identified in gene expression analyses as being highly induced in chronic HCV patients who had a sustained viral response after IFN therapy (Helbig et al., 2005). Viperin was also identified in our gene expression analysis of IFN treated primary hepatocytes, wherein viperin was induced by more than 200 fold in CIFN treated cells as compared to untreated cells, which was two fold higher than induction with IFNα-2a or PEG-IFN treatment **(RSAD2-Appendix B)**. These results suggested that viperin might play a role in controlling HCV replication and in mediating IFN-induced antiviral effects against chronic HCV infection. We examined the ability of viperin to suppress HCV replication in HCV replicon cells transfected with a full-length viperin expression plasmid in the presence or absence of IFN. We found that overexpression of viperin in Huh7-K2040, A7, or HP replicon containing cells for 72 hours did not result in a dramatic decrease of viral protein or RNA levels (unpublished observations). It is important to note that an inherent limitation to these experiments is the use of transient transfections, which does not routinely achieve optimal levels (100%) of transfection efficiency in Huh7-replicon containing cells, despite efforts to optimize the transfection conditions. Therefore, subtle antiviral effects of the proteins encoded by ISGs would be hard to detect by these analyses. However, these limitations could be overcome by reevaluating the antiviral actions of viperin in stably transfected cell

lines or in the context of the HCV cell culture infectious system. I have found that even small differences in viral titer and/or in the percentage of infected cells as compared to vector transfected control cells can be determined in the cell culture-infectious system. Also, the anti-HCV effects of expression of a particular protein can be evaluated on a cell by cell analysis using IFA. Revisiting viperin would be of interest as a number of recent reports have demonstrated that that this IFN-induced protein has potent antiviral activity against distinct viruses, yet the mechanism of antiviral action against HCV remains unknown (Jiang et al., 2008a; Wang et al., 2007; Zhang et al., 2007).

Discussion

Recent studies evaluating ISG expression in HCV-infected individuals before and after IFN treatment have reported very surprising results, suggesting that a failed response to IFN therapy might be acquired during the establishment of chronic HCV infection. It was found that HCV-infected individuals who do not respond to IFN therapy have a high baseline expression of ISGs, which does not increase above pretreatment levels after PEG-IFN administration. However, in patients with a rapid virological response to treatment, exogenous IFN induces a strong upregulation of STAT-1 phosphorylation and ISG induction. This phenotype did not correlate with the induction of specific ISGs that are involved in HCV clearance or to the pre-induction of suppressors of the IFN response in non-responders (SOCs, Usp18, etc). Importantly, the authors found a correlation between ISG expression in the liver and HCV genotype, in which the “difficult to treat” genotype 1 patients had slightly increased basal ISG expression as compared to genotypes 2 and 3 (Sarasin-Filipowicz et al.,

2008). A number of hypotheses have been proposed to explain this phenomenon but none have thus far been experimentally evaluated. It would be interesting to determine if this impairment of HCV clearance by preactivation of the endogenous IFN system could be overcome by treating patients with a different IFN, such as CIFN or IFNβ. It has been demonstrated that the type I IFN subtypes differentially activate the canonical and non-canonical IFN signaling pathways resulting in distinct biological responses. Therefore if the immune system has become refractory to endogenous IFNα signaling events then exogenous IFNα-2a is probably not going to add much, however treatment with a "stronger" IFN may overcome this refractory state, potentially enhancing the antiviral response. This phenomenon could provide an explanation as to why CIFN treatment of HCV 1a individuals who relapsed or did not respond to prior PEG-IFN therapy have increased rates of viral clearance than those retreated with PEG-IFN therapy (**Figure 1-1)**.

IFN modulates the expression of hundreds of ISGs, and it is unlikely that all these ISGs play a role in the antiviral response to different viruses. Therefore it is important that the biological function of the ISG effector proteins be associated with modulating disease outcome. For other viruses this can be achieved *in vivo* using mice deficient in the particular gene. However, for HCV, which does not infect mice, biological relevance can be achieved using integrated approaches as described in Chapter Four, where genetic polymorphisms in putative antiviral genes are correlated with resistance or susceptibility to virus infection. Although difficult, this is a powerful means of identifying or confirming gene function and measuring their contribution to disease.

OAS1/IB657 DISCUSSION

Host genetic determinants in the outcome of HCV infection

The studies in Chapter Four describe our efforts to characterize the antiviral actions of the ISG, OAS1 p42 isoform. Epidemiologic and molecular genetic studies led to the identification of a SNP in OAS1 that associated with resistance to HCV infection. Functional and molecular biology studies were used to evaluate the functional effects of this variant. Furthermore, an optimized recombinant drug form of the protein, termed IB657, possesses antiviral functions in the absence of exogenous IFN. In the following discussion IB657 will be used for consistency when discussing the truncated protein, and p42 or p46 used when discussing endogenous OAS1 isoforms. The study presented in Chapter Four is distinct from previous studies in that the goal was to identify "beneficial" mutations leading to resistance to HCV infection. In order to identify genetic determinants of resistance to HCV infection, two populations of IVDUs were compared, HCV-negative case subjects and HCV-positive control subjects. The case subjects were individuals who remain HCV-seronegative despite high-risk behaviors for acquiring HCV infection, characterized by intravenous drug use for ten or more years and an additional risk factor. Previous studies have identified genetic determinants that are involved in susceptibility to HCV infection by comparing individuals with self-limiting infections (anti-HCV antibody positive, HCV RNA negative) to individuals with chronic infection. Also, a number of studies have attempted to identify genes that associate with the outcome of response to IFN therapy, by comparing individuals with a sustained viral response and individuals with no response to therapy. From previous studies the most convincing host genetic determinant involved in the outcome

of HCV infection is the association of self-limiting HCV infection with major histocompatibility complex (MHC) class II genes. However, these associations are not consistently reproducible and the MHC alleles involved are highly variable depending on the ethnicity of the study participants (reviewed in (Ksiaa et al., 2007; Yee, 2004). While host antiviral fitness definitely benefits from increased diversity in immune gene families such as the MHC genes, studies of viral diseases such as hepatitis B, suggest that the MHC genes may contribute less than non-MHC genes to clinical outcome of infection (Hohler et al., 2002). Knapp, S et al. have reported that polymorphisms in the ISGs; MxA, OAS1 and PKR associate with the outcome of HCV infection. The authors found that heterozygosity for a single-nucleotide polymorphism in the promoter of PKR was associated with spontaneous clearance of HCV. Two genotypes were found in MxA that associated with self-limiting infection and the authors hypothesize that this is due to increased transcription of these variants. Further studies evaluating the biological effects of the proteins encoded by these polymorphisms and their influence on disease outcome, have not been reported. Important to our studies, it was found that the GG genotype at a locus in the 3' UTR of OAS1 associates with persistent HCV infection (Knapp et al., 2003). A separate group found that GG at this locus is in almost complete linkage disequilibrium with genotype GG at a splice-acceptor site in exon 7 of OAS1, resulting in production of the 'wild-type' p46 OAS1 isoform in these individuals who have persistent HCV infection. Furthermore, genotype GG or GA (encoding p46 or p46/48/52/40 variants respectively) at the splice-site polymorphism also associates with increased susceptibility to autoimmune type I diabetes, which is proposed to have a viral etiology (Field et al., 2005). Functional effects of the p46 variant include increased basal

OAS enzymatic activity in vivo as compared to other OAS1 variants (Bonnevie-Nielsen et al., 2005). However, the increased OAS enzymatic activity of p46 has not been directly correlated with the outcome of HCV infection or with the susceptibility to diabetes. Therefore functional effects of the polymorphisms in OAS1 that influence disease outcome may not be directly related to p46 expression, but rather due to decreased expression of other OAS1 variants, such as p42 and p48. We found that individuals having both the OAS1 1D1 and 1A1 alleles produced much lower levels of p42 than p46 **(Figure 4-1)**, and that resistance to HCV infection occurred in a homozygous (1D1/1D1) recessive genetic fashion. The OAS1 p48 isoform was previously shown to promote apoptosis through binding and inhibition of the antiapoptotic proteins of the Bcl-2 family (Ghosh et al., 2001). Therefore decreased or no expression of p42 and/or p48 in genotype GA and GG individuals could lead to an attenuated antiviral response. Notably, the proposed viral trigger for the autoimmune process in diabetic patients is Coxsackievirus (Field et al., 2005), a positive-sense RNA virus of the picornaviridae, and we found that IB657 has antiviral activity against a number of RNA viruses including the picornavirus EMCV, but not DNA viruses. Alternatively the increased OAS activity of p46 could result in increased virally-induced immunopathology that leads to destruction of insulin-producing cells in type I diabetics. Also, p46 could enhance HCV replication through a geranylgeranylation dependent process, as was previously demonstrated for the cellular protein FBL2 (Wang et al., 2005). However, we do not see evidence of this in our in vitro infection experiments, as p46 overexpression in human hepatoma cells did not significantly enhance HCV infection levels over vector transfected cells. Also, co-treatment of HCV-infected cells with IFNα, which induces p46 expression in

Huh7.5 cells (unpublished observations), and IB657 resulted in a decrease in HCV-infected cells as compared to treatment with IFNα or IB657 alone. As endogenous levels of IFN-induced p46 are not as high as exogenous IB657 in IB657+IFNα treated cells, analysis of HCV infection in cells overexpressing both p46 and IB657 would further define the roles of these proteins in HCV infection.

Future Studies

Studies in Chapter Four reveal functional effects of the OAS1 p42 variant, that result in altered subcellular localization of the protein, and subsequent suppression of HCV replication by targeting the HCV IRES and reducing viral protein synthesis. However, the biological effects of the p42 variant and IB657 are likely not limited to suppression of HCV IRES-directed translation, as antiviral activity of the protein against a number of other RNA viruses has been demonstrated. Therefore, more in depth studies aimed at elucidating the complete repertoire of the antiviral actions of this protein are of interest.

Translation suppression

Studies aimed at identifying IB657 binding sites in the HCV genome would definitively demonstrate that IB657 is binding directly to the HCV IRES and allow identification of the domain/s in the 5' NTR that are targeted. The roles of the different HCV IRES domains in viral translation are well characterized which would help predict the possibility of IB657-resistant viral variants emerging as well as in the development of improved drug specificity. It is also possible that IB657 is not binding directly to the IRES but to regulatory regions

outside the IRES, or to regions within the HCV genome which could block ribosome processivity. Although we did not detect induction of ISG56 or activation of PKR in IB657 treated cells, other mechanisms of translation suppression such as IB657 binding to a cellular factor specific for HCV IRES mediated translation have not been evaluated. Surprisingly, IB657 was not able to suppress EMCV IRES-directed translation, but does have antiviral activity against the virus. Therefore, EMCV infection assays similar to those performed for HCV would be useful in identifying additional antiviral strategies of IB657. Furthermore, mutational analyses aimed at identifying areas of IB657 critical for selectively targeting the HCV IRES would be of interest in defining how IB657 and other dsRNA binding proteins, such as PRRs and ISG20, discriminate self from non-self RNA.

Subcellular localization

Another important aim for future studies is to further characterize the cellular localization of OAS1 variants and IB657 in HCV-infected and non-infected cells. A recent study found that around 70% of the plus-strand HCV RNA in HCV-infected cells is cytoplasmic, while 100% of the negative-strand is membrane associated, presumably in the replication complex (Miyanari et al., 2007). Considering our data demonstrating that IB657 inhibits HCV IRES function and is distributed throughout the cytoplasm, it would be informative to look for co-localization of the HCV RNA positive-strand and IB657. These experiments would confirm and extend our results demonstrating that the absence of the C-terminal geranylgeranylation site in the OAS1 variants results in altered subcellular localization of the protein impacting its ability to interact with HCV RNA. The ability of IB657 to bind to the positive-sense

genome strand of HCV RNA could mediate dual antiviral functions, by decreasing viral protein synthesis as well as tethering the viral RNA within the cytoplasm, thus preventing its incorporation into newly formed virions. In support of this model, we have consistently demonstrated that IB657 treatment of HCV infected cells does not significantly impact HCV RNA levels, which remained stable at 48 and 72 hours after treatment (**Figure 4-10c** and unpublished observations). However, we observed reduced viral protein synthesis and a five-fold decrease in infectious virus production within 48 hours of IB657 treatment **(Figure 4-6)**.

Both inhibitor experiments and mutational analyses demonstrated that the when geranylgeranylation of the OAS1 isoforms is blocked the proteins primarily localize to cellular cytoplasmic fractions **(Figure 4-3)**. Furthermore, OAS1 variants lacking the C-terminal CTIL sequence did not co-localize with viral proteins and were often found surrounding vacuole like structures that contained viral proteins **(Figure 4-4)**. Identification of the origin of these vacuoles would further define the antiviral functions of IB657. For instance, identification of these vacuoles as secretory vesicles derived from the ER or Golgi, could suggest that IB657 is sequestering viral proteins and replication components to prevent the assembly and release of new viral particles. Also, these vacuoles could be degradation compartments, consistent with the dramatically reduced if any viral protein expression observed in cells expressing p40/IB657 or the mutant p46 (CTIL-STIL).

The potential for IB657 as an effective therapeutic for HCV infection is very promising. Therefore it would be of interest to evaluate the antiviral potency of IB657 using the chimeric-liver mouse model and chronically HCV-infected chimpanzees. Of course the final goal of these studies is to clinically evaluate IB657 in HCV-infected individuals, with

the hopes that this drug will provide enhanced viral clearance with minimal contraindications.

Evolution of OAS1 diversity

In order to determine the evolutionary basis of the OAS1 polymorphisms the OAS sequences of our closest relatives, the great apes, were analyzed. It was found that common chimpanzees (*Pan troglodytes*), western chimpanzees and gorillas all have polymorphisms in their OAS1 gene that results in the production of a truncated OAS1 protein. For chimpanzees there is a mutation resulting in a stop codon at amino acid 335 that is close to the splice site for the terminal exon 6. This premature stop codon in the chimpanzee OAS1 results in the expression of a 39kDa protein that is functionally similar to the truncated p42 OAS1 isoform in humans (Iadonato, SP unpublished observations). Furthermore, this mutation was found to be conserved in all available chimpanzee alleles, but not in the OAS1 alleles from bonobos, which express a protein of 46 kDA, and is very similar to the human p46 isoform **(Appendix C)**. It is estimated that western and common chimpanzees split from each other around 600,000 years ago and diverged from bonobos around 1.8 million years ago, thus the truncated OAS1 mutation must have become fixed in the great apes during this time (Beadle, 1981; Stone et al., 2002). The stable selection of a mutation that results in such a dramatic change in the protein produced suggests enormous evolutionary pressure, as could occur from a viral epidemic. These results are particularly interesting considering the outcome of HCV infection in the chimpanzee model. The majority of chimpanzees acutely infected with HCV clear the virus spontaneously, while only 15-30% of humans successfully

resolve acute HCV infection (Bassett et al., 1999). The studies described herein and the pure homozygosity of chimpanzees for the truncated OAS1 isoform, imply that chimpanzees are inherently resistant to HCV infection, and may only develop persistent infections when p39 (p42 in humans) expression/function is compromised, perhaps through advanced age of the animal. Sequencing of the OAS1 gene in the chimpanzees that do develop persistent HCV infection could potentially identify regions that are critical for the antiviral functions of the protein. To date there has been no compelling evidence of when HCV was first introduced in humans or where the virus came from. The identification and characterization of the p42 OAS1 isoform described herein may provide insight into the origin of HCV. One could envision a model in which chimpanzees are the natural reservoir for modern day HCV which may have evolved within resistant animals from an ancient viral epidemic.

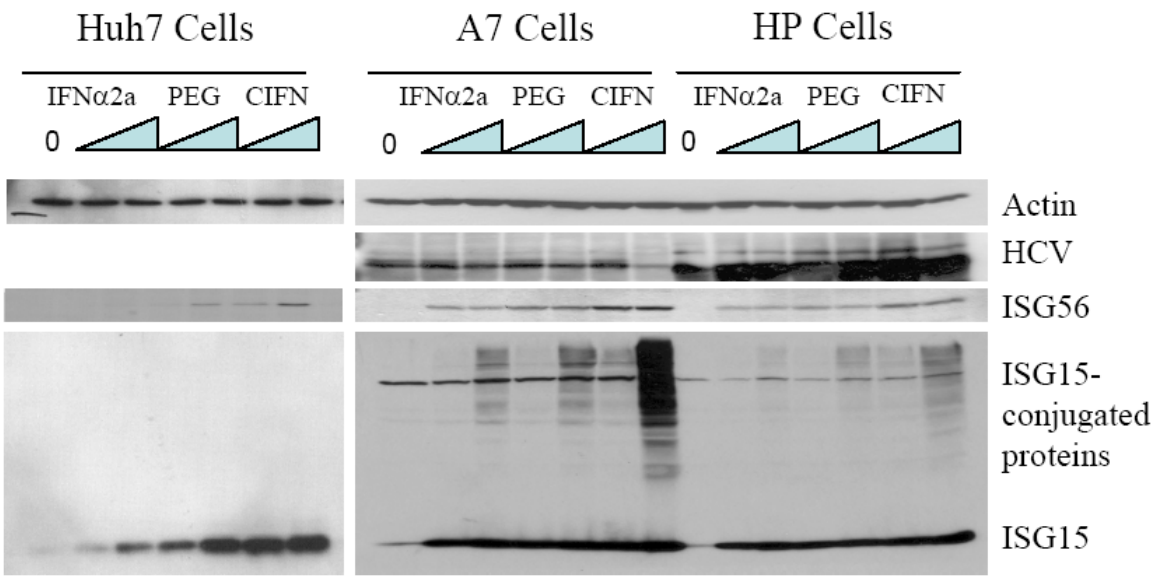

Figure 5-1. ISGylation in Huh7 cells and Huh7-HCV replicons. Cells were cultured for 12 or 24 hours (blue triangles) with media (0) or media containing 130 pg/mL IFNα2a, 360 pg/mL PEG-IFN or 80 pg/mL CIFN. Immunoblot analysis was performed with antiserum specific for ISG15, ISG56, HCV-NS5A or actin levels. A7 –IFN sensitive HCV RNA replicon containing Huh7 cells, HP -IFN resistant HCV RNA replicon containing Huh7 cells

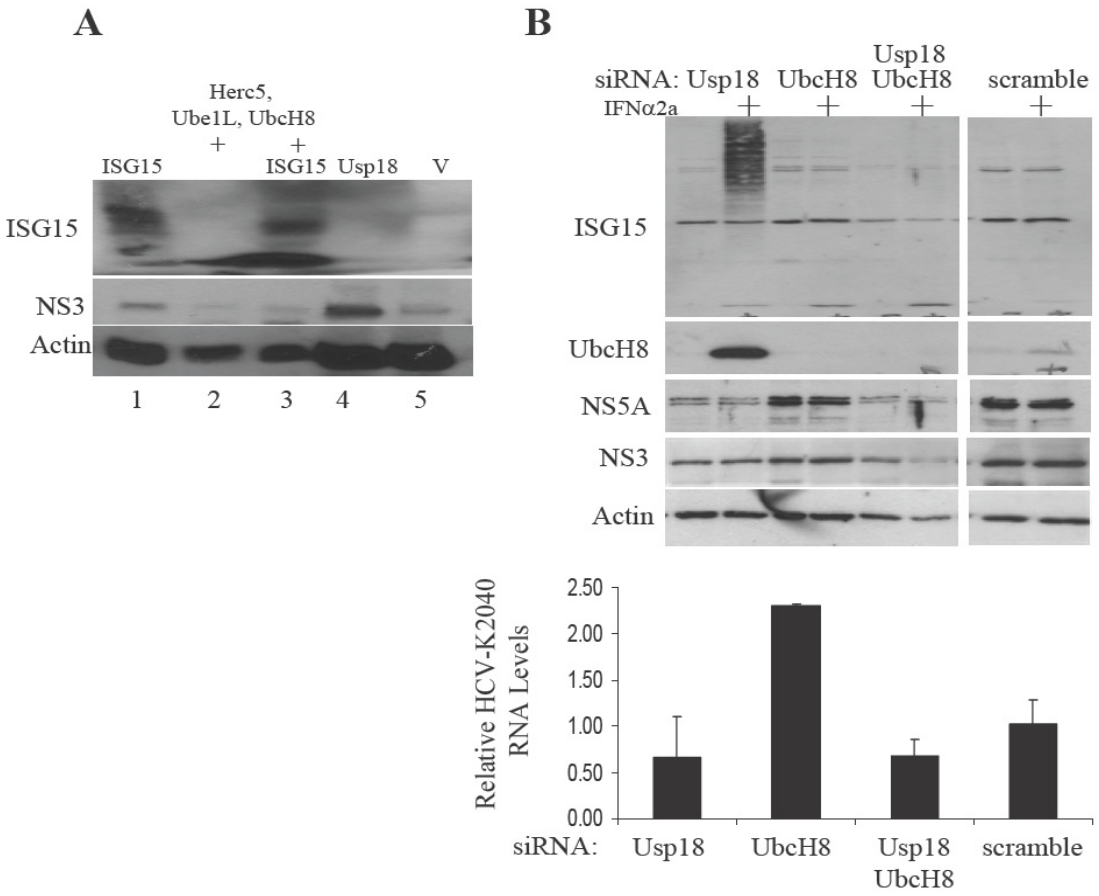

Figure 5-2. Effects of ISGylation on HCV replication. **(A)** Huh7-HCV K2040 replicon cells were transfected cells with the indicated plasmids for 24 hours when media was replaced with media containing 130 pg/mL of IFNα. Immunoblot analysis was performed 24 hours later. V, vector transfected; +, transfected with Herc5, Ube1L and UbcH8. **(B)** K2040 cells were transfected with the indicated siRNA(s) for 48 hours and 10U/mL of IFNα added to the cells a further 24 hours later. Protein and RNA was harvested from parallel transfected/treated cells for immunoblot analysis (top panel) or qRT-PCR for HCV-RNA levels (bottom panel) with GAPDH as the internal control. Bars represent the relative HCV RNA levels as compared to scramble which was set to 1. error bars, s.d.

APPENDIX A
Amino acid sequences of IFNα-2a, IFNα-2b and CIFN*

IFNα-2a	C D L P Q T HS L G S R R T L M L L A Q M R R I S L F S C L K D R H D F G F P Q
PEG-IFN α-2b	C D L P Q T HS L G S R R T L M L L A Q M R K I S L F S C L K D R H D F G F P Q
CIFN	C D L P Q T HS L G N R R A L I L L A Q M R R I S P F S C L K D R H D F G F P Q
IFNα-2a	E E F G N Q F Q K A E T I P V L H E M I Q Q I F N L F S T K D S S A A W D E T
PEG-IFN α-2b	E E F G N Q F Q K A E T I P V L H E M I Q Q I F N L F S T K D S S A A W D E T
CIFN	E E F D G N Q F Q K A Q A I S V L H E M I Q Q T F N L F S T K D S S A A W D E S
IFNα-2a	L L D K F Y T E L Y Q Q L N D L E A C V I Q G V G V T E T P L M K E D S I L A V
PEG-IFN α-2b	L L D K F Y T E L Y Q Q L N D L E A C V I Q G V G V T E T P L M K E D S I L A V
CIFN	L L E K F Y T E L Y Q Q L N D L E A C V I Q E V G V E E T P L M N V D S I L A V
IFNα-2a	R K Y F Q R I T L Y L K E K K Y S P C A W E V V R A E I M R S F S L S T N L Q E
PEG-IFN α-2b	R K Y F Q R I T L Y L K E K K Y S P C A W E V V R A E I M R S F S L S T N L Q E
CIFN	K K Y F Q R I T L Y L T E K K Y S P C A W E V V R A E I M R S F S L S T N L Q E
IFNα-2a	S L R S K E
PEG-IFN α-2b	S L R S K E
CIFN	R L R R K E

*Alignment of amino acid sequences of therapeutic IFNs. CIFN is a very different molecule having 18 or 19 amino acid changes (highlighted in green) from IFNα-2a and IFNα-2b, which have only one amino acid change (highlighted in blue and brown respectively). CIFN has 30% homology to IFNβ which is higher than any of the IFNα subtypes and has 60% sequence identity with IFN omega.

APPENDIX B
List of 86 genes differentially induced by CIFN

Expression data* of the 86 probe sets identified as having significant CIFN-dependent differences in primary hepatocytes.

Gene Symbol	Gene Title	CIFN (4hr)	IFN-α2a (4hr)	PEG – IFN (4hr)	CIFN (8hr)	IFN-α2a (8hr)	PEG – IFN (8hr)	CIFN (20hr)	IFN-α2a (20hr)	PEG – IFN (20hr)
---	Transcribed locus	9.84	7.99	6.69	8.13	5.46	5.80	4.45	4.29	3.76
APOL6	apolipoprotein L, 6	10.85	8.70	8.20	5.64	3.62	3.79	2.84	2.16	1.99
APOL6	apolipoprotein L, 6	5.71	4.92	4.02	4.10	3.03	2.56	2.15	2.09	1.97
BTC	betacellulin	8.22	6.10	6.20	15.18	9.48	8.51	6.52	3.64	3.30
C1orf38	chromosome 1 open reading frame 38	11.46	9.62	8.88	5.04	3.36	3.34	3.81	3.29	2.86
C7orf6	chromosome 7 open reading frame 6	46.05	34.99	32.32	31.28	21.10	20.72	11.49	7.44	6.32
C7orf6	chromosome 7 open reading frame 6	29.10	20.68	21.19	16.56	9.66	8.83	7.70	6.26	5.22
CASP1	caspase 1, apoptosis-related cysteine protease	6.36	4.59	4.28	8.22	5.56	5.91	3.16	2.72	2.60
CEACAM1	carcinoembryonic antigen-related cell adhesion molecule 1	4.48	2.51	2.92	4.50	2.39	2.24	0.85	0.47	0.41
CXCL10	chemokine (C-X-C motif) ligand 10	45.24	10.70	10.61	3.92	2.61	1.94	0.67	1.10	0.63
EPSTI1	epithelial stromal interaction 1 (breast)	18.99	17.13	15.37	21.53	17.13	16.52	11.09	8.77	8.61
EPSTI1	Epithelial stromal interaction 1 (breast)	18.07	15.39	14.13	20.53	15.74	15.85	9.87	7.11	7.11
FLJ11286	hypothetical protein FLJ11286	6.84	6.37	6.24	6.43	5.11	5.43	4.84	4.46	3.97
GCH1	GTP cyclohydrolase 1 (dopa-responsive dystonia)	3.95	2.99	2.91	1.15	0.93	0.93	0.97	0.93	0.93
GMPR	guanosine monophosphate reductase	8.16	5.46	5.03	9.76	5.50	5.86	2.83	2.12	2.16
HERC5	hect domain and RLD 5	243.23	181.98	131.93	298.85	171.13	159.55	66.21	37.15	27.70

Gene Symbol	Gene Title	CIFN (4hr)	IFN-α2a (4hr)	PEG – IFN (4hr)	CIFN (8hr)	IFN-α2a (8hr)	PEG – IFN (8hr)	CIFN (20hr)	IFN-α2a (20hr)	PEG – IFN (20hr)
HLA-B	major histocompatibility complex, class I, B	2.92	2.40	2.36	3.18	2.86	2.68	3.38	2.77	2.78
HLA-B/HLA-C	major histocompatibility complex, class I, B/C	2.79	2.25	2.20	2.90	2.65	2.47	3.24	2.68	2.66
HLA-C	major histocompatibility complex, class I, C	2.45	2.17	2.00	2.47	2.29	2.13	2.52	2.15	2.16
HLA-F	major histocompatibility complex, class I, F	2.49	2.15	2.15	2.78	2.52	2.39	2.61	2.15	2.19
HRASLS2	HRAS-like suppressor 2	4.27	2.94	2.90	4.79	3.51	3.22	2.13	1.55	1.43
HSXIAPAF1	XIAP associated factor-1	421.53	366.00	359.55	796.30	583.18	570.70	463.68	284.03	258.48
IFI44	interferon-induced protein 44	134.58	125.45	117.63	152.48	115.38	115.75	124.53	84.46	80.06
IFI44L	interferon-induced protein 44-like	69.79	68.83	64.61	99.28	77.13	74.57	131.93	86.40	84.38
IFIH1	interferon induced with helicase C domain 1	195.83	152.98	136.25	146.15	99.91	105.45	71.19	58.73	48.81
IFIT2	interferon-induced protein with tetratricopeptide repeats 2	176.15	100.19	97.92	32.51	12.74	11.51	4.78	3.58	3.68
IFIT3	interferon-induced protein with tetratricopeptide repeats 3	82.96	65.61	66.24	53.36	31.21	32.49	22.00	15.18	15.1
IFIT3	interferon-induced protein with tetratricopeptide repeats 3	78.40	59.40	58.73	48.31	33.13	36.53	34.01	26.94	24.08
IFITM1	interferon induced transmembrane protein 1 (9-27)	12.23	10.78	10.34	18.28	15.52	14.03	21.16	14.53	16.17
IFITM1	interferon induced transmembrane protein 1 (9-27)	13.95	13.28	11.81	23.21	18.23	17.18	29.05	20.38	20.98
IFITM2	interferon induced transmembrane protein 2 (1-8D)	2.49	2.07	2.02	2.63	2.34	2.18	2.49	2.17	2.26
IFRG28	28kD interferon responsive protein	27.71	21.30	21.06	18.31	8.63	8.99	10.85	5.83	6.06

Gene Symbol	Gene Title	CIFN (4hr)	IFN-α2a (4hr)	PEG – IFN (4hr)	CIFN (8hr)	IFN-α2a (8hr)	PEG – IFN (8hr)	CIFN (20hr)	IFN-α2a (20hr)	PEG – IFN (20hr)
IL15RA	interleukin 15 receptor, alpha	3.70	2.78	2.77	2.86	2.11	1.99	1.38	0.99	0.96
INDO	indoleamine-pyrrole 2,3 dioxygenase	30.58	15.61	11.78	26.85	14.25	10.36	4.15	2.89	2.99
IRF7	interferon regulatory factor 7	6.80	6.45	5.79	8.07	6.94	6.69	8.05	6.82	6.32
ISG20	interferon stimulated gene 20kDa	14.57	10.53	9.80	19.18	15.31	15.36	6.66	3.40	3.31
ISG20	interferon stimulated gene 20kDa	10.25	8.54	7.80	15.01	11.68	11.00	4.96	2.79	2.74
JAK2	Janus kinase 2 (a protein tyrosine kinase)	2.83	2.29	2.02	1.50	1.05	1.02	1.17	1.00	0.98
KIAA1404	KIAA1404 protein	6.40	5.65	5.48	3.53	2.50	2.61	1.74	1.45	1.33
LAMP3	lysosomal-associated membrane protein 3	16.41	11.96	11.52	18.45	13.15	12.89	10.99	6.82	5.75
LAP3	leucine aminopeptidase 3	3.30	2.88	2.87	4.51	3.69	3.87	3.31	2.90	2.90
LOC129607	hypothetical protein LOC129607	15.38	14.60	13.95	16.43	9.93	11.16	7.77	4.92	4.26
MGC20410	hypothetical protein BC012330	22.68	13.75	13.96	13.24	6.89	7.26	7.27	5.36	5.45
MLKL	mixed lineage kinase domain-like	3.76	3.30	2.88	3.35	2.57	2.74	1.46	1.20	1.21
MX1	myxovirus (influenza virus) resistance 1	78.26	69.05	64.98	91.85	80.99	76.41	69.91	54.44	56.34
MYD88	myeloid differentiation primary response gene (88)	5.51	4.89	4.57	4.05	2.95	3.15	1.92	1.65	1.62
NCOA7	nuclear receptor coactivator 7	4.98	4.16	4.12	2.09	1.51	1.34	1.49	1.23	1.23
NMI	N-myc (and STAT) interactor	5.08	4.57	4.66	6.75	5.59	5.55	4.25	3.37	3.24
NOD27	nucleotide-binding oligomerization domains 27	5.38	4.69	4.51	4.00	2.61	2.43	2.14	1.83	2.06
NT5C3	5'-nucleotidase, cytosolic III	3.67	2.99	2.96	2.42	1.85	1.79	1.21	0.96	0.97
OAS2	2'-5'-oligoadenylate synthetase 2, 69/71kDa	65.51	50.84	48.58	140.13	98.30	95.19	110.66	73.28	63.87
OAS2	2'-5'-oligoadenylate synthetase 2, 69/71kDa	134.58	129.90	119.60	154.98	125.63	125.93	68.68	54.59	50.88
OASL	2'-5'-oligoadenylate synthetase-like	38.07	31.29	30.21	33.54	21.93	21.63	8.43	4.80	4.75
OASL	2'-5'-oligoadenylate synthetase-like	56.19	45.35	45.79	53.41	33.34	33.54	12.47	8.50	7.77
PARP14	poly (ADP-ribose) polymerase family, member 14	16.53	12.76	12.71	14.39	11.49	11.21	6.76	5.50	5.90

Gene Symbol	Gene Title	CIFN (4hr)	IFN-α2a (4hr)	PEG – IFN (4hr)	CIFN (8hr)	IFN-α2a (8hr)	PEG – IFN (8hr)	CIFN (20hr)	IFN-α2a (20hr)	PEG – IFN (20hr)
PCGF5	polycomb group ring finger 5	4.42	3.42	3.39	5.14	4.16	3.82	2.17	1.58	1.70
PDZK3	PDZ domain containing 3	12.30	9.62	7.48	6.42	3.28	3.85	2.66	1.83	1.68
PIK3AP1	phosphoinositide-3-kinase adaptor protein 1	12.55	12.25	10.61	10.42	7.28	6.72	4.10	2.39	2.57
PSMB8	proteasome subunit, beta type, 8	2.70	2.61	2.55	3.83	3.27	3.12	3.10	2.56	2.65
RIG-I	DEAD (Asp-Glu-Ala-Asp) box polypeptide 58	43.83	34.67	34.07	25.06	17.52	18.62	13.48	11.24	10.55
RIG-I	DEAD (Asp-Glu-Ala-Asp) box polypeptide 58	31.74	26.57	24.92	14.89	10.58	10.24	5.68	4.64	4.48
RSAD2	radical S-adenosyl methionine domain containing 2	282.60	226.08	198.65	226.38	108.76	116.58	49.79	27.02	26.46
RSAD2	radical S-adenosyl methionine domain containing 2	235.98	186.23	153.60	168.25	83.23	86.81	41.45	22.45	19.00
SAMD9	sterile alpha motif domain containing 9	34.76	27.36	28.87	21.29	15.33	14.23	10.09	8.07	7.35
SAMHD1	SAM domain and HD domain 1	4.93	4.72	4.43	6.37	5.56	5.40	4.86	4.18	4.23
SCARB2	scavenger receptor class B, member 2	2.07	1.82	1.71	2.26	1.91	1.87	1.44	1.39	1.31
SLC25A28	solute carrier family 25, member 28	5.72	4.63	4.17	2.65	1.80	1.71	1.49	1.22	1.18
SLC25A28	solute carrier family 25, member 28	6.83	5.23	5.33	2.91	2.04	2.01	1.76	1.46	1.44
SP110	SP110 nuclear body protein	11.09	10.24	9.77	9.41	7.58	7.40	5.19	4.75	4.52
SPTLC2	serine palmitoyltransferase, long chain base subunit 2	1.64	1.42	1.37	1.26	1.10	1.08	0.86	0.78	0.83
TAP1	transporter 1, ATP-binding cassette, sub-family B	9.51	7.59	7.34	9.24	7.98	7.49	3.41	2.71	2.58
TAP2	transporter 2, ATP-binding cassette, sub-family B	3.25	2.90	2.79	3.49	3.13	3.03	1.50	1.18	1.19
TDRD7	tudor domain containing 7	6.60	5.86	5.57	4.15	3.43	3.49	2.82	2.36	2.28
TGM2	transglutaminase 2	1.65	1.37	1.25	2.19	1.72	1.69	0.37	0.28	0.26
TNFSF10	tumor necrosis factor (ligand) superfamily, member 10	92.17	47.60	45.64	24.53	9.28	9.01	16.06	13.20	13.37

Gene Symbol	Gene Title	CIFN (4hr)	IFN-α2a (4hr)	PEG – IFN (4hr)	CIFN (8hr)	IFN-α2a (8hr)	PEG – IFN (8hr)	CIFN (20hr)	IFN-α2a (20hr)	PEG – IFN (20hr)
TNFSF10	tumor necrosis factor (ligand) superfamily, member 10	247.60	124.02	119.93	57.32	22.39	19.75	32.87	26.64	28.19
TNFSF13B	tumor necrosis factor (ligand) superfamily, member 13b	38.98	20.13	18.73	35.89	17.39	16.48	3.06	1.96	1.93
TNFSF13B	tumor necrosis factor (ligand) superfamily, member 13b	17.66	11.17	9.68	17.51	7.93	8.85	2.18	0.89	0.86
TRIM22	tripartite motif-containing 22	19.19	16.04	15.61	38.21	25.78	26.86	13.37	8.19	6.62
TRIM38	tripartite motif-containing 38	6.47	5.18	4.77	4.42	2.88	2.75	2.89	2.57	2.78
TRIM38	tripartite motif-containing 38	6.18	5.36	5.13	3.99	2.72	2.53	2.57	2.38	2.40
TXNIP	thioredoxin interacting protein	2.74	1.89	1.84	1.92	1.75	1.69	2.43	2.11	1.92
WARS	tryptophanyl-tRNA synthetase	6.75	4.71	4.35	8.53	6.22	5.50	1.46	1.08	1.05
WARS	tryptophanyl-tRNA synthetase	6.45	4.81	4.50	7.64	5.59	5.37	1.80	1.36	1.31
ZBP1	Z-DNA binding protein 1	56.61	31.47	35.12	31.04	12.96	18.98	1.78	1.21	0.80
ZC3HDC1	zinc finger CCCH type domain containing 1	4.02	3.65	3.46	3.97	3.34	3.43	2.21	1.85	1.78

*Gene expression differences due to IFN treatment were identified by 2-way ANOVA and a Bonferonni, $p<0.05$ used as a multiple test correction. The mean fold induction of each probe set by each IFN treatment over untreated controls at every time point is listed.

APPENDIX C
Alignment of OAS1 sequences across primate species*

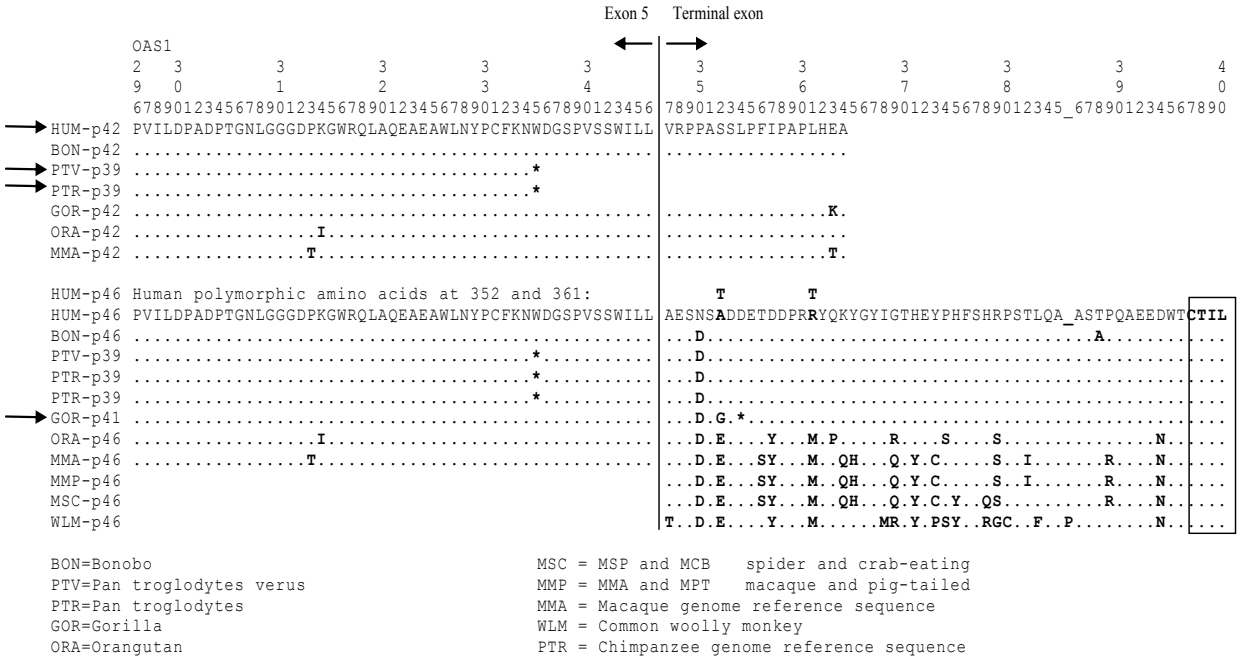

*Sequence alignment of predicted p42 and p46 primate amino acid sequences using splicing sites inferred from human sequences. Divergent amino acids are listed, with identical amino acids to the human sequence represented by dots. Box surrounds conserved CTIL motif and putative geranylgeranylation site. Arrows indicate primates having mutations resulting in the truncated OAS1 isoforms that are functionally similar to the human p42 variant.

BIBLIOGRAPHY

(2002). NIH Consensus Statement on Management of Hepatitis C: 2002. NIH Consens State Sci Statements *19*, 1-46.

(2004). Global burden of disease (GBD) for hepatitis C. J Clin Pharmacol *44*, 20-29.

Alexopoulou, L., Holt, A. C., Medzhitov, R., and Flavell, R. A. (2001). Recognition of double-stranded RNA and activation of NF-kappaB by Toll-like receptor 3. Nature *413*, 732-738.

Anonymous (1997, updated 2001). User Bulletin No. 2, Relative quantification of gene expression. ABI 7700 Sequence Detection System (Foster City, CA: Applied Biosystem, Applied Biosystem).

Appel, N., Zayas, M., Miller, S., Krijnse-Locker, J., Schaller, T., Friebe, P., Kallis, S., Engel, U., and Bartenschlager, R. (2008). Essential role of domain III of nonstructural protein 5A for hepatitis C virus infectious particle assembly. PLoS Pathog *4*, e1000035.

Barth, H., Liang, T. J., and Baumert, T. F. (2006). Hepatitis C virus entry: molecular biology and clinical implications. Hepatology *44*, 527-535.

Bartosch, B., and Cosset, F. L. (2006). Cell entry of hepatitis C virus. Virology *348*, 1-12.

Bassett, S. E., Brasky, K. M., and Lanford, R. E. (1998). Analysis of Hepatitis C Virus-Inoculated Chimpanzees Reveals Unexpected Clinical Profiles. J Virol *72*, 2589-2599.

Bassett, S. E., Thomas, D. L., Brasky, K. M., and Lanford, R. E. (1999). Viral Persistence, Antibody to E1 and E2, and Hypervariable Region 1 Sequence Stability in Hepatitis C Virus-Inoculated Chimpanzees. J Virol *73*, 1118-1126.

Beadle, L. C. (1981). The inland waters of tropical Africa: an introduction to tropical limnology (New York, Longman, London).

Bigger, C. B., Brasky, K. M., and Lanford, R. E. (2001). DNA microarray analysis of chimpanzee liver during acute resolving hepatitis C virus infection. J Virol *75*, 7059-7066.

Blanchard, E., Belouzard, S., Goueslain, L., Wakita, T., Dubuisson, J., Wychowski, C., and Rouille, Y. (2006). Hepatitis C virus entry depends on clathrin-mediated endocytosis. J Virol *80*, 6964-6972.

Blatt, L. M., Davis, J. M., Klein, S. B., and Taylor, M. W. (1996). The biologic activity and molecular characterization of a novel synthetic interferon-alpha species, consensus interferon. J Interferon Cytokine Res *16*, 489-499.

Blight, K. J., McKeating, J. A., and Rice, C. M. (2002). Highly permissive cell lines for subgenomic and genomic hepatitis C virus RNA replication. J Virol *76*, 13001-13014.

Blomstrom, D. C., Fahey, D., Kutny, R., Korant, B. D., and Knight, E., Jr. (1986). Molecular characterization of the interferon-induced 15-kDa protein. Molecular cloning and nucleotide and amino acid sequence. J Biol Chem *261*, 8811-8816.

Bode, J. G., Ludwig, S., Ehrhardt, C., Albrecht, U., Erhardt, A., Schaper, F., Heinrich, P. C., and Haussinger, D. (2003). IFN-alpha antagonistic activity of HCV core protein involves induction of suppressor of cytokine signaling-3. Faseb J *17*, 488-490.

Bonnevie-Nielsen, V., Field, L. L., Lu, S., Zheng, D. J., Li, M., Martensen, P. M., Nielsen, T. B., Beck-Nielsen, H., Lau, Y. L., and Pociot, F. (2005). Variation in antiviral 2',5'-oligoadenylate synthetase (2'5'AS) enzyme activity is controlled by a single-nucleotide polymorphism at a splice-acceptor site in the OAS1 gene. Am J Hum Genet *76*, 623-633.

Cai, Z., Zhang, C., Chang, K. S., Jiang, J., Ahn, B. C., Wakita, T., Liang, T. J., and Luo, G. (2005). Robust production of infectious hepatitis C virus (HCV) from stably HCV cDNA-transfected human hepatoma cells. J Virol *79*, 13963-13973.

Castelli, J. C., Hassel, B. A., Maran, A., Paranjape, J., Hewitt, J. A., Li, X. L., Hsu, Y. T., Silverman, R. H., and Youle, R. J. (1998). The role of 2'-5' oligoadenylate-activated ribonuclease L in apoptosis. Cell Death Differ *5*, 313-320.

Chebath, J., Benech, P., Hovanessian, A., Galabru, J., and Revel, M. (1987). Four different forms of interferon-induced 2',5'-oligo(A) synthetase identified by immunoblotting in human cells. J Biol Chem *262*, 3852-3857.

Chen, S. L., and Morgan, T. R. (2006). The natural history of hepatitis C virus (HCV) infection. Int J Med Sci *3*, 47-52.

Chin, K. C., and Cresswell, P. (2001). Viperin (cig5), an IFN-inducible antiviral protein directly induced by human cytomegalovirus. Proc Natl Acad Sci U S A *98*, 15125-15130.

Choo, Q. L., Kuo, G., Weiner, A. J., Overby, L. R., Bradley, D. W., and Houghton, M. (1989). Isolation of a cDNA clone derived from a blood-borne non-A, non-B viral hepatitis genome. Science *244*, 359-362.

Cocquerel, L., Voisset, C., and Dubuisson, J. (2006). Hepatitis C virus entry: potential receptors and their biological functions. J Gen Virol *87*, 1075-1084.

Colina, R., Costa-Mattioli, M., Dowling, R. J., Jaramillo, M., Tai, L. H., Breitbach, C. J., Martineau, Y., Larsson, O., Rong, L., Svitkin, Y. V.*, et al.* (2008). Translational control of the innate immune response through IRF-7. Nature *452*, 323-328.

D'Cunha, J., Ramanujam, S., Wagner, R. J., Witt, P. L., Knight, E., Jr., and Borden, E. C. (1996). In vitro and in vivo secretion of human ISG15, an IFN-induced immunomodulatory cytokine. J Immunol *157*, 4100-4108.

Darnell, J. E., Jr., Kerr, I. M., and Stark, G. R. (1994). Jak-STAT pathways and transcriptional activation in response to IFNs and other extracellular signaling proteins. Science *264*, 1415-1421.

Der, S. D., Zhou, A., Williams, B. R., and Silverman, R. H. (1998). Identification of genes differentially regulated by interferon alpha, beta, or gamma using oligonucleotide arrays. Proc Natl Acad Sci U S A *95*, 15623-15628.

Deutsch, M., and Hadziyannis, S. J. (2008). Old and emerging therapies in chronic hepatitis C: an update. J Viral Hepat *15*, 2-11.

Di Bisceglie, A. M., and Hoofnagle, J. H. (2002). Optimal therapy of hepatitis C. Hepatology *36*, S121-127.

Egger, D., Wolk, B., Gosert, R., Bianchi, L., Blum, H. E., Moradpour, D., and Bienz, K. (2002). Expression of hepatitis C virus proteins induces distinct membrane alterations including a candidate viral replication complex. J Virol *76*, 5974-5984.

El-Hage, N., and Luo, G. (2003). Replication of hepatitis C virus RNA occurs in a membrane-bound replication complex containing nonstructural viral proteins and RNA. J Gen Virol *84*, 2761-2769.

Espert, L., Degols, G., Gongora, C., Blondel, D., Williams, B. R., Silverman, R. H., and Mechti, N. (2003). ISG20, a new interferon-induced RNase specific for single-stranded RNA, defines an alternative antiviral pathway against RNA genomic viruses. J Biol Chem *278*, 16151-16158.

Espert, L., Eldin, P., Gongora, C., Bayard, B., Harper, F., Chelbi-Alix, M. K., Bertrand, E., Degols, G., and Mechti, N. (2006). The exonuclease ISG20 mainly localizes in the nucleolus and the Cajal (Coiled) bodies and is associated with nuclear SMN protein-containing complexes. J Cell Biochem *98*, 1320-1333.

Evans, M. J., von Hahn, T., Tscherne, D. M., Syder, A. J., Panis, M., Wolk, B., Hatziioannou, T., McKeating, J. A., Bieniasz, P. D., and Rice, C. M. (2007). Claudin-1 is a hepatitis C virus co-receptor required for a late step in entry. Nature *446*, 801-805.

Farci, P., Strazzera, R., Alter, H. J., Farci, S., Degioannis, D., Coiana, A., Peddis, G., Usai, F., Serra, G., Chessa, L.*, et al.* (2002). Early changes in hepatitis C viral quasispecies during interferon therapy predict the therapeutic outcome. Proc Natl Acad Sci U S A *99*, 3081-3086.

Fedetz, M., Matesanz, F., Caro-Maldonado, A., Fernandez, O., Tamayo, J. A., Guerrero, M., Delgado, C., Lopez-Guerrero, J. A., and Alcina, A. (2006). OAS1 gene haplotype confers susceptibility to multiple sclerosis. Tissue Antigens *68*, 446-449.

Feld, J. J., and Hoofnagle, J. H. (2005). Mechanism of action of interferon and ribavirin in treatment of hepatitis C. Nature *436*, 967-972.

Field, L. L., Bonnevie-Nielsen, V., Pociot, F., Lu, S., Nielsen, T. B., and Beck-Nielsen, H. (2005). OAS1 splice site polymorphism controlling antiviral enzyme activity influences susceptibility to type 1 diabetes. Diabetes *54*, 1588-1591.

Fink, J., Gu, F., Ling, L., Tolfvenstam, T., Olfat, F., Chin, K. C., Aw, P., George, J., Kuznetsov, V. A., Schreiber, M.*, et al.* (2007). Host Gene Expression Profiling of Dengue Virus Infection in Cell Lines and Patients. PLoS Neglected Tropical Diseases *1*, e86.

Floyd-Smith, G., Slattery, E., and Lengyel, P. (1981). Interferon action: RNA cleavage pattern of a (2'-5')oligoadenylate--dependent endonuclease. Science *212*, 1030-1032.

Foy, E., Li, K., Sumpter, R., Jr., Loo, Y. M., Johnson, C. L., Wang, C., Fish, P. M., Yoneyama, M., Fujita, T., Lemon, S. M., and Gale, M., Jr. (2005). Control of antiviral defenses through hepatitis C virus disruption of retinoic acid-inducible gene-I signaling. Proc Natl Acad Sci U S A *102*, 2986-2991.

Foy, E., Li, K., Wang, C., Sumpter, R., Jr., Ikeda, M., Lemon, S. M., and Gale, M., Jr. (2003). Regulation of interferon regulatory factor-3 by the hepatitis C virus serine protease. Science *300*, 1145-1148.

Fraser, C. S., and Doudna, J. A. (2007). Structural and mechanistic insights into hepatitis C viral translation initiation. Nat Rev Microbiol *5*, 29-38.

Fredericksen, B., Akkaraju, G. R., Foy, E., Wang, C., Pflugheber, J., Chen, Z. J., and Gale, M., Jr. (2002). Activation of the interferon-beta promoter during hepatitis C virus RNA replication. Viral Immunol *15*, 29-40.

Fried, M. W., Shiffman, M. L., Reddy, K. R., Smith, C., Marinos, G., Goncales, F. L., Jr., Haussinger, D., Diago, M., Carosi, G., Dhumeaux, D*., et al.* (2002). Peginterferon alfa-2a plus ribavirin for chronic hepatitis C virus infection. N Engl J Med *347*, 975-982.

Fujita, T., Reis, L. F., Watanabe, N., Kimura, Y., Taniguchi, T., and Vilcek, J. (1989). Induction of the transcription factor IRF-1 and interferon-beta mRNAs by cytokines and activators of second-messenger pathways. Proc Natl Acad Sci U S A *86*, 9936-9940.

Gale, M., Jr., Blakely, C. M., Kwieciszewski, B., Tan, S. L., Dossett, M., Tang, N. M., Korth, M. J., Polyak, S. J., Gretch, D. R., and Katze, M. G. (1998). Control of PKR protein kinase by hepatitis C virus nonstructural 5A protein: molecular mechanisms of kinase regulation. Mol Cell Biol *18*, 5208-5218.

Gale, M., Jr., and Foy, E. M. (2005). Evasion of intracellular host defence by hepatitis C virus. Nature *436*, 939-945.

Gale, M., Jr., and Katze, M. G. (1998). Molecular mechanisms of interferon resistance mediated by viral-directed inhibition of PKR, the interferon-induced protein kinase. Pharmacol Ther *78*, 29-46.

Gale, M. J., Jr., Korth, M. J., Tang, N. M., Tan, S. L., Hopkins, D. A., Dever, T. E., Polyak, S. J., Gretch, D. R., and Katze, M. G. (1997). Evidence that hepatitis C virus resistance to interferon is mediated through repression of the PKR protein kinase by the nonstructural 5A protein. Virology *230*, 217-227.

Garten, R. J., Lai, S., Zhang, J., Liu, W., Chen, J., Vlahov, D., and Yu, X. F. (2004). Rapid transmission of hepatitis C virus among young injecting heroin users in Southern China. Int J Epidemiol *33*, 182-188.

Ghosh, A., Sarkar, S. N., Rowe, T. M., and Sen, G. C. (2001). A specific isozyme of 2'-5' oligoadenylate synthetase is a dual function proapoptotic protein of the Bcl-2 family. J Biol Chem *276*, 25447-25455.

Giannakopoulos, N. V., Luo, J. K., Papov, V., Zou, W., Lenschow, D. J., Jacobs, B. S., Borden, E. C., Li, J., Virgin, H. W., and Zhang, D. E. (2005). Proteomic identification of proteins conjugated to ISG15 in mouse and human cells. Biochem Biophys Res Commun *336*, 496-506.

Goldstein, J. L., and Brown, M. S. (1990). Regulation of the mevalonate pathway. Nature *343*, 425-430.

Guo, J., Hui, D. J., Merrick, W. C., and Sen, G. C. (2000). A new pathway of translational regulation mediated by eukaryotic initiation factor 3. Embo J *19*, 6891-6899.

Guo, J. T., Bichko, V. V., and Seeger, C. (2001). Effect of alpha interferon on the hepatitis C virus replicon. J Virol *75*, 8516-8523.

Hagan, H., Thiede, H., and Des Jarlais, D. C. (2004). Hepatitis C virus infection among injection drug users: survival analysis of time to seroconversion. Epidemiology *15*, 543-549.

Hallen, L. C., Burki, Y., Ebeling, M., Broger, C., Siegrist, F., Oroszlan-Szovik, K., Bohrmann, B., Certa, U., and Foser, S. (2007). Antiproliferative activity of the human IFN-alpha-inducible protein IFI44. J Interferon Cytokine Res *27*, 675-680.

Han, J. Q., and Barton, D. J. (2002). Activation and evasion of the antiviral 2'-5' oligoadenylate synthetase/ribonuclease L pathway by hepatitis C virus mRNA. Rna *8*, 512-525.

Han, J. Q., Wroblewski, G., Xu, Z., Silverman, R. H., and Barton, D. J. (2004). Sensitivity of hepatitis C virus RNA to the antiviral enzyme ribonuclease L is determined by a subset of efficient cleavage sites. J Interferon Cytokine Res *24*, 664-676.

Hartmann, R., Justesen, J., Sarkar, S. N., Sen, G. C., and Yee, V. C. (2003). Crystal Structure of the 2'-Specific and Double-Stranded RNA-Activated Interferon-Induced Antiviral Protein 2'-5'-Oligoadenylate Synthetase. Molecular Cell *12*, 1173.

Hayashi, N., and Takehara, T. (2006). Antiviral therapy for chronic hepatitis C: past, present, and future. J Gastroenterol *41*, 17-27.

Heim, M. H. (1999). The Jak-STAT pathway: cytokine signalling from the receptor to the nucleus. J Recept Signal Transduct Res *19*, 75-120.

Heim, M. H., Moradpour, D., and Blum, H. E. (1999). Expression of hepatitis C virus proteins inhibits signal transduction through the Jak-STAT pathway. J Virol *73*, 8469-8475.

Helbig, K. J., Lau, D. T., Semendric, L., Harley, H. A., and Beard, M. R. (2005). Analysis of ISG expression in chronic hepatitis C identifies viperin as a potential antiviral effector. Hepatology *42*, 702-710.

Hohler, T., Reuss, E., Evers, N., Dietrich, E., Rittner, C., Freitag, C. M., Vollmar, J., Schneider, P. M., and Fimmers, R. (2002). Differential genetic determination of immune responsiveness to hepatitis B surface antigen and to hepatitis A virus: a vaccination study in twins. Lancet *360*, 991-995.

Honda, K., Takaoka, A., and Taniguchi, T. (2006). Type I interferon [corrected] gene induction by the interferon regulatory factor family of transcription factors. Immunity *25*, 349-360.

Honda, M., Beard, M. R., Ping, L. H., and Lemon, S. M. (1999). A phylogenetically conserved stem-loop structure at the 5' border of the internal ribosome entry site of hepatitis C virus is required for cap-independent viral translation. J Virol *73*, 1165-1174.

Honda, M., Brown, E. A., and Lemon, S. M. (1996). Stability of a stem-loop involving the initiator AUG controls the efficiency of internal initiation of translation on hepatitis C virus RNA. RNA *2*, 955-968.

Honda, M., Kaneko, S., Matsushita, E., Kobayashi, K., Abell, G. A., and Lemon, S. M. (2000). Cell cycle regulation of hepatitis C virus internal ribosomal entry site-directed translation. Gastroenterology *118*, 152-162.

Hoofnagle, J. H., Mullen, K. D., Jones, D. B., Rustgi, V., Di Bisceglie, A., Peters, M., Waggoner, J. G., Park, Y., and Jones, E. A. (1986). Treatment of chronic non-A,non-B hepatitis with recombinant human alpha interferon. A preliminary report. N Engl J Med *315*, 1575-1578.

Hovnanian, A., Rebouillat, D., Mattei, M. G., Levy, E. R., Marie, I., Monaco, A. P., and Hovanessian, A. G. (1998). The human 2',5'-oligoadenylate synthetase locus is composed of three distinct genes clustered on chromosome 12q24.2 encoding the 100-, 69-, and 40-kDa forms. Genomics *52*, 267-277.

Howell, C., Jeffers, L., and Hoofnagle, J. H. (2000). Hepatitis C in African Americans: summary of a workshop. Gastroenterology *119*, 1385-1396.

Hwang, Y., Chen, E. Y., Gu, Z. J., Chuang, W.-L., Yu, M.-L., Lai, M.-Y., Chao, Y.-C., Lee, C.-M., Wang, J.-H., Dai, C.-Y.*, et al.* (2006). Genetic predisposition of responsiveness to therapy for chronic hepatitis C. Pharmacogenomics *7*, 697-709.

Ikeda, M., Sugiyama, K., Mizutani, T., Tanaka, T., Tanaka, K., Sekihara, H., Shimotohno, K., and Kato, N. (1998). Human hepatocyte clonal cell lines that support persistent replication of hepatitis C virus. Virus Res *56*, 157-167.

Irshad, M., and Dhar, I. (2006). Hepatitis C virus core protein: an update on its molecular biology, cellular functions and clinical implications. Med Princ Pract *15*, 405-416.

Isaacs, A., and Lindenmann, J. (1957). Virus interference. I. The interferon. Proc R Soc Lond B Biol Sci *147*, 258-267.

Ishida, H., Ohkawa, K., Hosui, A., Hiramatsu, N., Kanto, T., Ueda, K., Takehara, T., and Hayashi, N. (2004). Involvement of p38 signaling pathway in interferon-alpha-mediated antiviral activity toward hepatitis C virus. Biochem Biophys Res Commun *321*, 722-727.

Jaeckel, E., Cornberg, M., Wedemeyer, H., Santantonio, T., Mayer, J., Zankel, M., Pastore, G., Dietrich, M., Trautwein, C., and Manns, M. P. (2001). Treatment of acute hepatitis C with interferon alfa-2b. N Engl J Med *345*, 1452-1457.

Jiang, D., Guo, H., Xu, C., Chang, J., Gu, B., Wang, L., Block, T. M., and Guo, J.-T. (2008a). Identification of Three Interferon-Inducible Cellular Enzymes That Inhibit the Replication of Hepatitis C Virus. J Virol *82*, 1665-1678.

Jiang, D., Guo, H., Xu, C., Chang, J., Gu, B., Wang, L., Block, T. M., and Guo, J. T. (2008b). Identification of three interferon-inducible cellular enzymes that inhibit the replication of hepatitis C virus. J Virol *82*, 1665-1678.

Johnson, C. L., Owen, D. M., and Gale, M., Jr. (2007). Functional and therapeutic analysis of hepatitis C virus NS3.4A protease control of antiviral immune defense. J Biol Chem *282*, 10792-10803.

Johnson, G. L., and Lapadat, R. (2002). Mitogen-activated protein kinase pathways mediated by ERK, JNK, and p38 protein kinases. Science *298*, 1911-1912.

Jones, C. T., Murray, C. L., Eastman, D. K., Tassello, J., and Rice, C. M. (2007). Hepatitis C Virus p7 and NS2 Proteins Are Essential for Production of Infectious Virus. J Virol *81*, 8374-8383.

Justesen, J., Hartmann, R., and Kjeldgaard, N. O. (2000). Gene structure and function of the 2'-5'-oligoadenylate synthetase family. Cell Mol Life Sci *57*, 1593-1612.

Kaiser S, H. H., Lutze B, Bissinger L, Gregor M (2006). Comparison of daily consensus interferon vs peginterferon alpha 2a extended therapy of 72 weeks for peginterferon/ribavirin relapse patients with chronic hepatitis C. Paper presented at: Digestive Disease Week (Los Angeles, CA).

Kapadia, S. B., and Chisari, F. V. (2005). Hepatitis C virus RNA replication is regulated by host geranylgeranylation and fatty acids. Proc Natl Acad Sci U S A *102*, 2561-2566.

Karla J. Helbig, D. T. Y. L. L. S. H. A. J. H. M. R. B. (2005). Analysis of ISG expression in chronic hepatitis C identifies viperin as a potential antiviral effector. Hepatology *42*, 702-710.

Katsoulidis, E., Li, Y., Mears, H., and Platanias, L. C. (2005). The p38 mitogen-activated protein kinase pathway in interferon signal transduction. J Interferon Cytokine Res *25*, 749-756.

Katze, M. G., He, Y., and Gale, M., Jr. (2002). Viruses and interferon: a fight for supremacy. Nat Rev Immunol *2*, 675-687.

Kaur, S., Uddin, S., and Platanias, L. C. (2005). The PI3' kinase pathway in interferon signaling. J Interferon Cytokine Res *25*, 780-787.

Kawai, T., Takahashi, K., Sato, S., Coban, C., Kumar, H., Kato, H., Ishii, K. J., Takeuchi, O., and Akira, S. (2005). IPS-1, an adaptor triggering RIG-I- and Mda5-mediated type I interferon induction. Nat Immunol *6*, 981-988.

Keller, B. C., Fredericksen, B. L., Samuel, M. A., Mock, R. E., Mason, P. W., Diamond, M. S., and Gale, M., Jr. (2006). Resistance to Alpha/Beta Interferon Is a Determinant of West Nile Virus Replication Fitness and Virulence. J Virol *80*, 9424-9434.

Kerr, I. M., and Brown, R. E. (1978). pppA2'p5'A2'p5'A: an inhibitor of protein synthesis synthesized with an enzyme fraction from interferon-treated cells. Proc Natl Acad Sci U S A *75*, 256-260.

Kim, K. I., Giannakopoulos, N. V., Virgin, H. W., and Zhang, D. E. (2004). Interferon-inducible ubiquitin E2, Ubc8, is a conjugating enzyme for protein ISGylation. Mol Cell Biol *24*, 9592-9600.

Knapp, S., Yee, L. J., Frodsham, A. J., Hennig, B. J., Hellier, S., Zhang, L., Wright, M., Chiaramonte, M., Graves, M., Thomas, H. C.*, et al.* (2003). Polymorphisms in interferon-induced genes and the outcome of hepatitis C virus infection: roles of MxA, OAS-1 and PKR. Genes Immun *4*, 411-419.

Kolumam, G. A., Thomas, S., Thompson, L. J., Sprent, J., and Murali-Krishna, K. (2005). Type I interferons act directly on CD8 T cells to allow clonal expansion and memory formation in response to viral infection. J Exp Med *202*, 637-650.

Kolykhalov, A. A., Mihalik, K., Feinstone, S. M., and Rice, C. M. (2000). Hepatitis C virus-encoded enzymatic activities and conserved RNA elements in the 3' nontranslated region are essential for virus replication in vivo. J Virol *74*, 2046-2051.

Kotenko, S. V., Gallagher, G., Baurin, V. V., Lewis-Antes, A., Shen, M., Shah, N. K., Langer, J. A., Sheikh, F., Dickensheets, H., and Donnelly, R. P. (2003). IFN-lambdas mediate antiviral protection through a distinct class II cytokine receptor complex. Nat Immunol *4*, 69-77.

Krieger, N., Lohmann, V., and Bartenschlager, R. (2001). Enhancement of hepatitis C virus RNA replication by cell culture-adaptive mutations. J Virol *75*, 4614-4624.

Ksiaa, L., Ayed-Jendoubi, S., Sfar, I., Gorgi, Y., Najjar, H. A., Abdallah, T. B., and Ayed, K. (2007). Clearance and persistence of hepatitis C virus in a Tunisian population: association with HLA class I and class II. Viral Immunol *20*, 312-319.

Kumar, A., Yang, Y. L., Flati, V., Der, S., Kadereit, S., Deb, A., Haque, J., Reis, L., Weissmann, C., and Williams, B. R. (1997). Deficient cytokine signaling in mouse embryo fibroblasts with a targeted deletion in the PKR gene: role of IRF-1 and NF-kappaB. Embo J *16*, 406-416.

Laporte, J., Malet, I., Andrieu, T., Thibault, V., Toulme, J. J., Wychowski, C., Pawlotsky, J. M., Huraux, J. M., Agut, H., and Cahour, A. (2000). Comparative analysis of translation efficiencies of hepatitis C virus 5' untranslated regions among intraindividual quasispecies present in chronic infection: opposite behaviors depending on cell type. J Virol *74*, 10827-10833.

Lau, D. T., Fish, P. M., Sinha, M., Owen, D. M., Lemon, S. M., and Gale, M., Jr. (2008). Interferon regulatory factor-3 activation, hepatic interferon-stimulated gene expression, and immune cell infiltration in hepatitis C virus patients. Hepatology *47*, 799-809.

Lenschow, D. J., Lai, C., Frias-Staheli, N., Giannakopoulos, N. V., Lutz, A., Wolff, T., Osiak, A., Levine, B., Schmidt, R. E., Garcia-Sastre, A.*, et al.* (2007). IFN-stimulated gene 15 functions as a critical antiviral molecule against influenza, herpes, and Sindbis viruses. Proc Natl Acad Sci U S A *104*, 1371-1376.

Lerner, E. C., Qian, Y., Hamilton, A. D., and Sebti, S. M. (1995). Disruption of oncogenic K-Ras4B processing and signaling by a potent geranylgeranyltransferase I inhibitor. J Biol Chem *270*, 26770-26773.

Li, K., Chen, Z., Kato, N., Gale, M., Jr., and Lemon, S. M. (2005a). Distinct poly(I-C) and virus-activated signaling pathways leading to interferon-beta production in hepatocytes. J Biol Chem *280*, 16739-16747.

Li, K., Foy, E., Ferreon, J. C., Nakamura, M., Ferreon, A. C., Ikeda, M., Ray, S. C., Gale, M., Jr., and Lemon, S. M. (2005b). Immune evasion by hepatitis C virus NS3/4A protease-mediated cleavage of the Toll-like receptor 3 adaptor protein TRIF. Proc Natl Acad Sci U S A *102*, 2992-2997.

Li, X. D., Sun, L., Seth, R. B., Pineda, G., and Chen, Z. J. (2005c). Hepatitis C virus protease NS3/4A cleaves mitochondrial antiviral signaling protein off the mitochondria to evade innate immunity. Proc Natl Acad Sci U S A *102*, 17717-17722.

Lindenbach, B. D., Evans, M. J., Syder, A. J., Wolk, B., Tellinghuisen, T. L., Liu, C. C., Maruyama, T., Hynes, R. O., Burton, D. R., McKeating, J. A., and Rice, C. M. (2005). Complete replication of hepatitis C virus in cell culture. Science *309*, 623-626.

Loeb, K. R., and Haas, A. L. (1992). The interferon-inducible 15-kDa ubiquitin homolog conjugates to intracellular proteins. J Biol Chem *267*, 7806-7813.

Lohmann, V., Korner, F., Koch, J., Herian, U., Theilmann, L., and Bartenschlager, R. (1999). Replication of subgenomic hepatitis C virus RNAs in a hepatoma cell line. Science *285*, 110-113.

Loo, Y. M., Owen, D. M., Li, K., Erickson, A. K., Johnson, C. L., Fish, P. M., Carney, D. S., Wang, T., Ishida, H., Yoneyama, M.*, et al.* (2006). Viral and therapeutic control of IFN-beta promoter stimulator 1 during hepatitis C virus infection. Proc Natl Acad Sci U S A *103*, 6001-6006.

Lu, G., Reinert, J. T., Pitha-Rowe, I., Okumura, A., Kellum, M., Knobeloch, K. P., Hassel, B., and Pitha, P. M. (2006). ISG15 enhances the innate antiviral response by inhibition of IRF-3 degradation. Cell Mol Biol (Noisy-le-grand) *52*, 29-41.

Majetschak, M., Krehmeier, U., Bardenheuer, M., Denz, C., Quintel, M., Voggenreiter, G., and Obertacke, U. (2003). Extracellular ubiquitin inhibits the TNF-alpha response to endotoxin in peripheral blood mononuclear cells and regulates endotoxin hyporesponsiveness in critical illness. Blood *101*, 1882-1890.

Malakhova, O. A., Kim, K. I., Luo, J. K., Zou, W., Kumar, K. G., Fuchs, S. Y., Shuai, K., and Zhang, D. E. (2006). UBP43 is a novel regulator of interferon signaling independent of its ISG15 isopeptidase activity. Embo J *25*, 2358-2367.

Malakhova, O. A., Yan, M., Malakhov, M. P., Yuan, Y., Ritchie, K. J., Kim, K. I., Peterson, L. F., Shuai, K., and Zhang, D. E. (2003). Protein ISGylation modulates the JAK-STAT signaling pathway. Genes Dev *17*, 455-460.

Malathi, K., Dong, B., Gale, M., Jr., and Silverman, R. H. (2007). Small self-RNA generated by RNase L amplifies antiviral innate immunity. Nature *448*, 816-819.

Malmgaard, L. (2004). Induction and regulation of IFNs during viral infections. J Interferon Cytokine Res *24*, 439-454.

Mannova, P., and Beretta, L. (2005). Activation of the N-Ras-PI3K-Akt-mTOR pathway by hepatitis C virus: control of cell survival and viral replication. J Virol *79*, 8742-8749.

Martell, M., Esteban, J. I., Quer, J., Genesca, J., Weiner, A., Esteban, R., Guardia, J., and Gomez, J. (1992). Hepatitis C virus (HCV) circulates as a population of different but closely related genomes: quasispecies nature of HCV genome distribution. J Virol *66*, 3225-3229.

Martinon, F., and Tschopp, J. (2005). NLRs join TLRs as innate sensors of pathogens. Trends in Immunology *26*, 447.

McHutchison, J. G. (2004). Understanding hepatitis C. Am J Manag Care *10*, S21-29.

McHutchison, J. G., and Bacon, B. R. (2005). Chronic hepatitis C: an age wave of disease burden. Am J Manag Care *11*, S286-295; quiz S307-211.

McHutchison, J. G., Bacon, B. R., Gordon, S. C., Lawitz, E., Shiffman, M., Afdhal, N. H., Jacobson, I. M., Muir, A., Al-Adhami, M., Morris, M. L.*, et al.* (2007). Phase 1B, randomized, double-blind, dose-escalation trial of CPG 10101 in patients with chronic hepatitis C virus. Hepatology *46*, 1341-1349.

McHutchison, J. G., Gordon, S. C., Schiff, E. R., Shiffman, M. L., Lee, W. M., Rustgi, V. K., Goodman, Z. D., Ling, M. H., Cort, S., and Albrecht, J. K. (1998). Interferon alfa-2b alone or in combination with ribavirin as initial treatment for chronic hepatitis C. Hepatitis Interventional Therapy Group. N Engl J Med *339*, 1485-1492.

Mercer, D. F., Schiller, D. E., Elliott, J. F., Douglas, D. N., Hao, C., Rinfret, A., Addison, W. R., Fischer, K. P., Churchill, T. A., Lakey, J. R.*, et al.* (2001). Hepatitis C virus replication in mice with chimeric human livers. Nat Med *7*, 927-933.

Meurs, E., Chong, K., Galabru, J., Thomas, N. S., Kerr, I. M., Williams, B. R., and Hovanessian, A. G. (1990). Molecular cloning and characterization of the human double-stranded RNA-activated protein kinase induced by interferon. Cell *62*, 379-390.

Meylan, E., Curran, J., Hofmann, K., Moradpour, D., Binder, M., Bartenschlager, R., and Tschopp, J. (2005). Cardif is an adaptor protein in the RIG-I antiviral pathway and is targeted by hepatitis C virus. Nature *437*, 1167-1172.

Meylan, E., Tschopp, J., and Karin, M. (2006). Intracellular pattern recognition receptors in the host response. Nature *442*, 39-44.

Miglioresi, L., Bacosi, M., Russo, F., Patrizi, F., Saccenti, P., Ursitti, A., Angelis, A. D., and Ricci, G. L. (2003). Consensus interferon versus interferon-alpha 2b plus ribavirin in patients with relapsing HCV infection. Hepatol Res *27*, 253-259.

Miyanari, Y., Atsuzawa, K., Usuda, N., Watashi, K., Hishiki, T., Zayas, M., Bartenschlager, R., Wakita, T., Hijikata, M., and Shimotohno, K. (2007). The lipid droplet is an important organelle for hepatitis C virus production. Nat Cell Biol *9*, 1089-1097.

Muir, A. J., Bornstein, J. D., and Killenberg, P. G. (2004). Peginterferon alfa-2b and ribavirin for the treatment of chronic hepatitis C in blacks and non-Hispanic whites. N Engl J Med *350*, 2265-2271.

Murashima, S., Kumashiro, R., Ide, T., Miyajima, I., Hino, T., Koga, Y., Ishii, K., Ueno, T., Sakisaka, S., and Sata, M. (2000). Effect of interferon treatment on serum 2',5'-oligoadenylate synthetase levels in hepatitis C-infected patients. J Med Virol *62*, 185-190.

Neumann, A. U., Lam, N. P., Dahari, H., Gretch, D. R., Wiley, T. E., Layden, T. J., and Perelson, A. S. (1998). Hepatitis C viral dynamics in vivo and the antiviral efficacy of interferon-alpha therapy. Science *282*, 103-107.

Osborn, B. L., Olsen, H. S., Nardelli, B., Murray, J. H., Zhou, J. X., Garcia, A., Moody, G., Zaritskaya, L. S., and Sung, C. (2002). Pharmacokinetic and pharmacodynamic studies of a human serum albumin-interferon-alpha fusion protein in cynomolgus monkeys. J Pharmacol Exp Ther *303*, 540-548.

Osiak, A., Utermohlen, O., Niendorf, S., Horak, I., and Knobeloch, K. P. (2005). ISG15, an interferon-stimulated ubiquitin-like protein, is not essential for STAT1 signaling and responses against vesicular stomatitis and lymphocytic choriomeningitis virus. Mol Cell Biol *25*, 6338-6345.

Ozes, O. N., Reiter, Z., Klein, S., Blatt, L. M., and Taylor, M. W. (1992). A comparison of interferon-Con1 with natural recombinant interferons-alpha: antiviral, antiproliferative, and natural killer-inducing activities. J Interferon Res *12*, 55-59.

Pawlotsky, J.-M., Chevaliez, S., and McHutchison, J. G. (2007). The Hepatitis C Virus Life Cycle as a Target for New Antiviral Therapies. Gastroenterology *132*, 1979.

Penin, F., Dubuisson, J., Rey, F. A., Moradpour, D., and Pawlotsky, J. M. (2004). Structural biology of hepatitis C virus. Hepatology *39*, 5-19.

Pfeifer, U., Thomssen, R., Legler, K., Bottcher, U., Gerlich, W., Weinmann, E., and Klinge, O. (1980). Experimental non-A, non-B hepatitis: four types of cytoplasmic alteration in hepatocytes of infected chimpanzees. Virchows Arch B Cell Pathol Incl Mol Pathol *33*, 233-243.

Pflugheber, J., Fredericksen, B., Sumpter, R., Jr., Wang, C., Ware, F., Sodora, D. L., and Gale, M., Jr. (2002). Regulation of PKR and IRF-1 during hepatitis C virus RNA replication. Proc Natl Acad Sci U S A *99*, 4650-4655.

Platanias, L. C., Uddin, S., and Colamonici, O. R. (1994). Tyrosine phosphorylation of the alpha and beta subunits of the type I interferon receptor. Interferon-beta selectively induces tyrosine phosphorylation of an alpha subunit-associated protein. J Biol Chem *269*, 17761-17764.

Platis, D., and Foster, G. R. (2003). Activity of hybrid type I interferons in cells lacking Tyk2: a common region of IFN-alpha 8 induces a response, but IFN-alpha2/8 hybrids can behave like IFN-beta. J Interferon Cytokine Res *23*, 655-666.

Prabhu, R., Joshi, V., Garry, R. F., Bastian, F., Haque, S., Regenstein, F., Thung, S., and Dash, S. (2004). Interferon alpha-2b inhibits negative-strand RNA and protein expression from full-length HCV1a infectious clone. Exp Mol Pathol *76*, 242-252.

Randall, G., Chen, L., Panis, M., Fischer, A. K., Lindenbach, B. D., Sun, J., Heathcote, J., Rice, C. M., Edwards, A. M., and McGilvray, I. D. (2006). Silencing of USP18 potentiates the antiviral activity of interferon against hepatitis C virus infection. Gastroenterology *131*, 1584-1591.

Rebouillat, D., and Hovanessian, A. G. (1999). The human 2',5'-oligoadenylate synthetase family: interferon-induced proteins with unique enzymatic properties. J Interferon Cytokine Res *19*, 295-308.

Rebouillat, D., Marie, I., and Hovanessian, A. G. (1998). Molecular cloning and characterization of two related and interferon-induced 56-kDa and 30-kDa proteins highly similar to 2'-5' oligoadenylate synthetase. Eur J Biochem *257*, 319-330.

Reid, T. S., Terry, K. L., Casey, P. J., and Beese, L. S. (2004). Crystallographic analysis of CaaX prenyltransferases complexed with substrates defines rules of protein substrate selectivity. J Mol Biol *343*, 417-433.

Robertson, B., Myers, G., Howard, C., Brettin, T., Bukh, J., Gaschen, B., Gojobori, T., Maertens, G., Mizokami, M., Nainan, O.*, et al.* (1998). Classification, nomenclature, and database development for hepatitis C virus (HCV) and related viruses: proposals for standardization. International Committee on Virus Taxonomy. Arch Virol *143*, 2493-2503.

Ruuth, K., Carlsson, L., Hallberg, B., and Lundgren, E. (2001). Interferon-[alpha] Promotes Survival of Human Primary B-Lymphocytes via Phosphatidylinositol 3-Kinase. Biochemical and Biophysical Research Communications *284*, 583.

Sadler, A. J., and Williams, B. R. (2008). Interferon-inducible antiviral effectors. Nat Rev Immunol *8*, 559-568.

Saito, T., and Gale, M., Jr. (2007). Principles of intracellular viral recognition. Curr Opin Immunol *19*, 17-23.

Saito, T., Hirai, R., Loo, Y. M., Owen, D., Johnson, C. L., Sinha, S. C., Akira, S., Fujita, T., and Gale, M., Jr. (2007). Regulation of innate antiviral defenses through a shared repressor domain in RIG-I and LGP2. Proc Natl Acad Sci U S A *104*, 582-587.

Saito, T., Owen, D. M., Jiang, F., Marcotrigiano, J., and Gale Jr, M. (2008). Innate immunity induced by composition-dependent RIG-I recognition of hepatitis C virus RNA. Nature.

Sakai, A., Claire, M. S., Faulk, K., Govindarajan, S., Emerson, S. U., Purcell, R. H., and Bukh, J. (2003). The p7 polypeptide of hepatitis C virus is critical for infectivity and contains functionally important genotype-specific sequences. Proc Natl Acad Sci U S A *100*, 11646-11651.

Santantonio, T., Fasano, M., Sinisi, E., Guastadisegni, A., Casalino, C., Mazzola, M., Francavilla, R., and Pastore, G. (2005). Efficacy of a 24-week course of PEG-interferon alpha-2b monotherapy in patients with acute hepatitis C after failure of spontaneous clearance. J Hepatol *42*, 329-333.

Sarasin-Filipowicz, M., Oakeley, E. J., Duong, F. H. T., Christen, V., Terracciano, L., Filipowicz, W., and Heim, M. H. (2008). Interferon signaling and treatment outcome in chronic hepatitis C. Proceedings of the National Academy of Sciences *105*, 7034-7039.

Sarkar, S. N., and Sen, G. C. (1998). Production, purification, and characterization of recombinant 2', 5'-oligoadenylate synthetases. Methods *15*, 233-242.

Sato, M., Suemori, H., Hata, N., Asagiri, M., Ogasawara, K., Nakao, K., Nakaya, T., Katsuki, M., Noguchi, S., Tanaka, N., and Taniguchi, T. (2000). Distinct and essential roles of transcription factors IRF-3 and IRF-7 in response to viruses for IFN-alpha/beta gene induction. Immunity *13*, 539-548.

Scherbik, S. V., Paranjape, J. M., Stockman, B. M., Silverman, R. H., and Brinton, M. A. (2006). RNase L plays a role in the antiviral response to West Nile virus. J Virol *80*, 2987-2999.

Schwarze, S. R., Ho, A., Vocero-Akbani, A., and Dowdy, S. F. (1999). In vivo protein transduction: delivery of a biologically active protein into the mouse. Science *285*, 1569-1572.

Seeff, L. B. (2002). Natural history of chronic hepatitis C. Hepatology *36*, S35-46.

Sen, G. C. (2001). Viruses and interferons. Annu Rev Microbiol *55*, 255-281.

Servant, M. J., Tenoever, B., and Lin, R. (2002). Overlapping and distinct mechanisms regulating IRF-3 and IRF-7 function. J Interferon Cytokine Res *22*, 49-58.

Shepard, C. W., Finelli, L., and Alter, M. J. (2005). Global epidemiology of hepatitis C virus infection. The Lancet Infectious Diseases *5*, 558.

Shimazaki, T., Honda, M., Kaneko, S., and Kobayashi, K. (2002). Inhibition of internal ribosomal entry site-directed translation of HCV by recombinant IFN-alpha correlates with a reduced La protein. Hepatology *35*, 199-208.

Silverman, R. H. (2007). Viral encounters with 2',5'-oligoadenylate synthetase and RNase L during the interferon antiviral response. J Virol *81*, 12720-12729.

Simmonds, P. (1995). Variability of hepatitis C virus. Hepatology *21*, 570-583.

Sjogren, M. H., Sjogren, R., Jr., Lyons, M. F., Ryan, M., Santoro, J., Smith, C., Reddy, K. R., Bonkovsky, H., Huntley, B., and Faris-Young, S. (2007). Antiviral response of HCV genotype 1 to consensus interferon and ribavirin versus pegylated interferon and ribavirin. Dig Dis Sci *52*, 1540-1547.

Smith, M. W., Yue, Z. N., Korth, M. J., Do, H. A., Boix, L., Fausto, N., Bruix, J., Carithers, R. L., Jr., and Katze, M. G. (2003). Hepatitis C virus and liver disease: global transcriptional profiling and identification of potential markers. Hepatology *38*, 1458-1467.

Solinas, A., Cossu, P., Poddighe, P., Tocco, A., Deplano, A., Garrucciu, G., and Diana, M. S. (1993). Changes of serum 2',5'-oligoadenylate synthetase activity during interferon treatment of chronic hepatitis C. Liver *13*, 253-258.

Stark, G. R., Kerr, I. M., Williams, B. R., Silverman, R. H., and Schreiber, R. D. (1998). How cells respond to interferons. Annu Rev Biochem *67*, 227-264.

Stone, A. C., Griffiths, R. C., Zegura, S. L., and Hammer, M. F. (2002). High levels of Y-chromosome nucleotide diversity in the genus Pan. Proc Natl Acad Sci U S A *99*, 43-48.

Sumpter, R., Jr., Loo, Y. M., Foy, E., Li, K., Yoneyama, M., Fujita, T., Lemon, S. M., and Gale, M., Jr. (2005). Regulating intracellular antiviral defense and permissiveness to hepatitis C virus RNA replication through a cellular RNA helicase, RIG-I. J Virol *79*, 2689-2699.

Sumpter, R., Jr., Wang, C., Foy, E., Loo, Y. M., and Gale, M., Jr. (2004). Viral evolution and interferon resistance of hepatitis C virus RNA replication in a cell culture model. J Virol *78*, 11591-11604.

Taguchi, T., Nagano-Fujii, M., Akutsu, M., Kadoya, H., Ohgimoto, S., Ishido, S., and Hotta, H. (2004). Hepatitis C virus NS5A protein interacts with 2',5'-oligoadenylate synthetase and inhibits antiviral activity of IFN in an IFN sensitivity-determining region-independent manner. J Gen Virol *85*, 959-969.

Takeuchi, T., and Yokosawa, H. (2008). Detection and analysis of protein ISGylation. Methods Mol Biol *446*, 139-149.

Tan, H., Derrick, J., Hong, J., Sanda, C., Grosse, W. M., Edenberg, H. J., Taylor, M., Seiwert, S., and Blatt, L. M. (2005). Global transcriptional profiling demonstrates the combination of type I and type II interferon enhances antiviral and immune responses at clinically relevant doses. J Interferon Cytokine Res *25*, 632-649.

Taniguchi, T., Ogasawara, K., Takaoka, A., and Tanaka, N. (2001). IRF family of transcription factors as regulators of host defense. Annu Rev Immunol *19*, 623-655.

Taylor, D. R., Shi, S. T., Romano, P. R., Barber, G. N., and Lai, M. M. (1999). Inhibition of the interferon-inducible protein kinase PKR by HCV E2 protein. Science *285*, 107-110.

Ting Zhang, Y. L. W.-Z. H. (2006). Drug abuse, innate immunity and hepatitis C virus. Reviews in Medical Virology *16*, 311-327.

Tong, M. J., Reddy, K. R., Lee, W. M., Pockros, P. J., Hoefs, J. C., Keeffe, E. B., Hollinger, F. B., Hathcote, E. J., White, H., Foust, R. T.*, et al.* (1997). Treatment of chronic hepatitis C with consensus interferon: a multicenter, randomized, controlled trial. Consensus Interferon Study Group. Hepatology *26*, 747-754.

Tscherne, D. M., Jones, C. T., Evans, M. J., Lindenbach, B. D., McKeating, J. A., and Rice, C. M. (2006). Time- and temperature-dependent activation of hepatitis C virus for low-pH-triggered entry. J Virol *80*, 1734-1741.

Tsukiyama-Kohara, K., Iizuka, N., Kohara, M., and Nomoto, A. (1992). Internal ribosome entry site within hepatitis C virus RNA. J Virol *66*, 1476-1483.

van Boxel-Dezaire, A. H., Rani, M. R., and Stark, G. R. (2006). Complex modulation of cell type-specific signaling in response to type I interferons. Immunity *25*, 361-372.

Vanwolleghem, T., Meuleman, P., Libbrecht, L., Roskams, T., De Vos, R., and Leroux-Roels, G. (2007). Ultra-rapid cardiotoxicity of the hepatitis C virus protease inhibitor BILN 2061 in the urokinase-type plasminogen activator mouse. Gastroenterology *133*, 1144-1155.

Wakita, T., Pietschmann, T., Kato, T., Date, T., Miyamoto, M., Zhao, Z., Murthy, K., Habermann, A., Krausslich, H. G., Mizokami, M.*, et al.* (2005). Production of infectious hepatitis C virus in tissue culture from a cloned viral genome. Nat Med *11*, 791-796.

Walters, K. A., Joyce, M. A., Thompson, J. C., Smith, M. W., Yeh, M. M., Proll, S., Zhu, L. F., Gao, T. J., Kneteman, N. M., Tyrrell, D. L., and Katze, M. G. (2006). Host-specific

response to HCV infection in the chimeric SCID-beige/Alb-uPA mouse model: role of the innate antiviral immune response. PLoS Pathog *2*, e59.

Wang, C., Gale, M., Jr., Keller, B. C., Huang, H., Brown, M. S., Goldstein, J. L., and Ye, J. (2005). Identification of FBL2 as a geranylgeranylated cellular protein required for hepatitis C virus RNA replication. Mol Cell *18*, 425-434.

Wang, C., Le, S. Y., Ali, N., and Siddiqui, A. (1995). An RNA pseudoknot is an essential structural element of the internal ribosome entry site located within the hepatitis C virus 5' noncoding region. Rna *1*, 526-537.

Wang, C., Pflugheber, J., Sumpter, R., Jr., Sodora, D. L., Hui, D., Sen, G. C., and Gale, M., Jr. (2003). Alpha interferon induces distinct translational control programs to suppress hepatitis C virus RNA replication. J Virol *77*, 3898-3912.

Wang, X., Hinson, E. R., and Cresswell, P. (2007). The interferon-inducible protein viperin inhibits influenza virus release by perturbing lipid rafts. Cell Host Microbe *2*, 96-105.

Wathelet, M. G., Lin, C. H., Parekh, B. S., Ronco, L. V., Howley, P. M., and Maniatis, T. (1998). Virus infection induces the assembly of coordinately activated transcription factors on the IFN-beta enhancer in vivo. Mol Cell *1*, 507-518.

Wen, Z., Zhong, Z., and Darnell, J. E., Jr. (1995). Maximal activation of transcription by Stat1 and Stat3 requires both tyrosine and serine phosphorylation. Cell *82*, 241-250.

Witthoeft, T., Fuchs, M., and Ludwig, D. (2007). Recent i.v.-drug users with chronic hepatitis C can be efficiently treated with daily high dose induction therapy using consensus interferon: an open-label pilot study. World J Gastroenterol *13*, 579-584.

Wong, J. J., Pung, Y. F., Sze, N. S., and Chin, K. C. (2006). HERC5 is an IFN-induced HECT-type E3 protein ligase that mediates type I IFN-induced ISGylation of protein targets. Proc Natl Acad Sci U S A *103*, 10735-10740.

Wreschner, D. H., McCauley, J. W., Skehel, J. J., and Kerr, I. M. (1981). Interferon action--sequence specificity of the ppp(A2'p)nA-dependent ribonuclease. Nature *289*, 414-417.

Yanagi, M., St Claire, M., Emerson, S. U., Purcell, R. H., and Bukh, J. (1999). In vivo analysis of the 3' untranslated region of the hepatitis C virus after in vitro mutagenesis of an infectious cDNA clone. Proc Natl Acad Sci U S A *96*, 2291-2295.

Yasuda, S., and Miyata, K. (2002). [Interferon alfacon-1 (Advaferon): a novel synthetic interferon for the treatment of hepatitis C, its pharmacological and clinical profile]. Nippon Yakurigaku Zasshi *120*, 421-426.

Ye, J., Wang, C., Sumpter, R., Jr., Brown, M. S., Goldstein, J. L., and Gale, M., Jr. (2003). Disruption of hepatitis C virus RNA replication through inhibition of host protein geranylgeranylation. Proc Natl Acad Sci U S A *100*, 15865-15870.

Yee, L. J. (2004). Host genetic determinants in hepatitis C virus infection. Genes Immun *5*, 237-245.

Yi, M., Villanueva, R. A., Thomas, D. L., Wakita, T., and Lemon, S. M. (2006). Production of infectious genotype 1a hepatitis C virus (Hutchinson strain) in cultured human hepatoma cells. Proc Natl Acad Sci U S A *103*, 2310-2315.

Yoneyama, M., Kikuchi, M., Natsukawa, T., Shinobu, N., Imaizumi, T., Miyagishi, M., Taira, K., Akira, S., and Fujita, T. (2004). The RNA helicase RIG-I has an essential function in double-stranded RNA-induced innate antiviral responses. Nat Immunol *5*, 730-737.

Yuan, W., and Krug, R. M. (2001). Influenza B virus NS1 protein inhibits conjugation of the interferon (IFN)-induced ubiquitin-like ISG15 protein. Embo J *20*, 362-371.

Zhang, F. L., and Casey, P. J. (1996). Protein prenylation: molecular mechanisms and functional consequences. Annu Rev Biochem *65*, 241-269.

Zhang, Y., Burke, C. W., Ryman, K. D., and Klimstra, W. B. (2007). Identification and Characterization of Interferon-Induced Proteins That Inhibit Alphavirus Replication. J Virol *81*, 11246-11255.

Zhao, C., Beaudenon, S. L., Kelley, M. L., Waddell, M. B., Yuan, W., Schulman, B. A., Huibregtse, J. M., and Krug, R. M. (2004). The UbcH8 ubiquitin E2 enzyme is also the E2 enzyme for ISG15, an IFN-alpha/beta-induced ubiquitin-like protein. Proc Natl Acad Sci U S A *101*, 7578-7582.

Zhao, C., Denison, C., Huibregtse, J. M., Gygi, S., and Krug, R. M. (2005). Human ISG15 conjugation targets both IFN-induced and constitutively expressed proteins functioning in diverse cellular pathways. Proc Natl Acad Sci U S A *102*, 10200-10205.

Zhong, J., Gastaminza, P., Cheng, G., Kapadia, S., Kato, T., Burton, D. R., Wieland, S. F., Uprichard, S. L., Wakita, T., and Chisari, F. V. (2005). Robust hepatitis C virus infection in vitro. Proc Natl Acad Sci U S A *102*, 9294-9299.